

University of 20 August 1955 – Skikda
Faculty of Technology
Department of Civil Engineering
Ref: D012125028D



جامعة 20 أوت 1955 – سكيكدة
كلية التكنولوجيا
قسم الهندسة المدنية
المرجع: D012125028D

Thesis presented for obtaining
The degree of
Doctorate of the 3rd cycle (LMD)

Department / Specialization

Civil engineering

Option

Materials in civil engineering

Presented by

MARROK Sara

Title

Study of concretes reinforced by hybrid fibers

Publicly defended on : 07/07/2025

Supervised by

PhD supervisor	Mr Belachia Mouloud	Pr	University of Guelma
PhD co-supervisor	Ms Kherraf Leila	MCA	University of Skikda

Jury composed by:

President	Ms Hebhouh Houria	Pr	University of Skikda
Examiner	Mr Achoura Djamel	Pr	University of Annaba
Examiner	Mr Mezhoud Sami	Pr	University of Setif 1
Examiner	Mr Merdas Abdelghani	Pr	University of Constantine 3

2024 / 2025

Université 20 Aout 1955- Skikda
Faculté de Technologie
Département de Génie Civil
Ref:



جامعة 20 أوت 1955 – سكيكدة
كلية التكنولوجيا
قسم الهندسة المدنية
المرجع:

Thèse présentée en vue de l'obtention
Du Diplôme de

Doctorat de 3^{ème} cycle (LMD)

Spécialité

Génie civil

Option

Materials en génie civil

Présentée par

MARROK Sara

Thème

Etude des bétons renforcés par un fibrage mixte

Soutenue publiquement le : 07/07/2025

Dirigée par :

Directeur de thèse	Mr Belachia Mouloud	Pr	Université de Guelma
Co-Directeur de thèse	Mme Kherraf Leila	MCA	Université de Skikda

Devant le jury compose de:

Présidente	Ms Hebhouh Houria	Pr	Université de Skikda
Examineur	Mr Achoura Djamel	Pr	Université de Annaba
Examineur	Mr Mezhoud Sami	Pr	Université de Sétif 1
Examineur	Mr Merdas Abdelghani	Pr	Université de Constantine 3

2024 / 2025



Acknowledgements

I would like to sincerely thank my PhD supervisor, Mr. Mouloud Belachia, for his guidance, patience, and continuous support throughout my scientific research.

I am also very grateful to my PhD co-supervisor, Mrs. Leila Kharref, for her helpful advice and valuable guidance.

I am profoundly grateful to the members of the jury for granting me the honor of having my thesis examined and for their time and effort in reviewing my thesis.

I would also like to express my gratitude to the staff and engineers at the LMGHU Laboratory, the LNHC Laboratory in Skikda, and the LEPN Laboratory at the University of Blida for their support and assistance during my research.



إهداء

بِسْمِ اللَّهِ الرَّحْمَنِ الرَّحِيمِ

أهدي هذا العمل المتواضع لي من كانوا دائماً مصدر قوتي وإلهامي
لي والديَّ العزيزين، اللذين وعماني طوال سنوات دراستي، وأسأل الله أن يجزئهما كل الخير، وأن يجردوا في هذا العمل تعبيراً عن
امتناني العميق

لي زوجي المحترم "بلال"، وابنتي الغالية "نسيم"، اللذان كانا منبع الحب والدعم
لي أختي "مروة" وأخوتي الأعمام "سيف الدين" و"نور الإسلام"، الذين كانوا دائماً بجانبني، يدعموني كل منضم بطريقته الخاصة
لي عائلتي "مروك" و"بوقلوف"، الذين كانوا هم القوة التي جعلتني أستمري في هذا الطريق
وأخيراً، لي كل من أصحتم في حياتي، الذين وقفوا معي في كل لحظة، وعموني في كل خطوة، وساهموا بشكل أو بآخر في وصولي إلى هذه
المرحلة

أهدي هذا العمل إليكم جميعاً، من كل قلبي



Table of contents

Abstract	I
Résumé	II
ملخص	III
List of figures	IV
List of tables	VIII
General introduction	IX
Chapter I: Literature review on industrial waste reinforced HFSC	1
I.1. Introduction	1
I.2. Industrial waste	1
I.2.1. Definition	1
I.2.2 Industrial solid wastes used in civil engineering	3
I.2.3 Types of industrial metals wastes in civil engineering	3
I.2.3.1. Industrial steel waste.....	5
<i>I.2.3.1.1. Steel shavings</i>	5
<i>I.2.3.1.2. Steel powder</i>	5
<i>I.2.3.1.3. Steel scraps</i>	6
I.2.3.2. Industrial bronze waste	6
<i>I.2.3.2.1. Bronze shavings</i>	6
<i>I.2.3.2.2. Bronze powder</i>	7
<i>I.2.3.2.3. Bronze scraps</i>	7
I.2.3.3. Industrial copper / brass waste.....	8
I.2.3.4. The relationship between copper/brass and bronze.....	8
<i>I.2.3.4.1. Composition</i>	8
<i>I.2.3.4.2. Properties</i>	9
I.2.4. Types of synthetic textile wastes in civil engineering	9
I.2.4.1. Polyester fiber waste	11
<i>I.2.4.1.1. Benefits of polyester fibers in concrete</i>	11
<i>I.2.4.1.2. Applications</i>	12
<i>I.2.4.1.3. Considerations</i>	12
<i>I.2.4.1.4. Optimal fiber content</i>	12
I.2.4.2. Polypropylene fiber waste.....	12

<i>I.2.4.2.1. Benefits of polypropylene fibers in concrete</i>	13
<i>I.2.4.2.2. Applications</i>	13
<i>I.2.4.2.3. Optimal fiber content</i>	14
<i>I.2.4.2.4. Fiber length</i>	14
I.2.4.3. Carbon fiber waste	14
<i>I.2.4.3.1. Benefits of carbon fibers in concrete</i>	14
<i>I.2.4.3.2. Applications</i>	15
<i>I.2.4.3.1. Considerations</i>	15
<i>I.2.4.3.3. Optimal fiber content</i>	16
I.2.4.4. Aramid fiber waste	16
<i>I.2.4.4.1. Benefits of aramid fibers in concrete</i>	16
<i>I.2.4.4.2. Applications</i>	17
<i>I.2.4.4.3. Considerations</i>	17
<i>I.2.4.4.3. Optimal fiber content</i>	17
I.2.5. Hybrid fiber reinforced concrete	18
I.2.5.1. Types of hybrid fibers in concrete	19
<i>I.2.5.1.1. Dual fiber systems</i>	19
<i>I.2.5.1.2. Triple fiber systems</i>	21
I.2.5.2. Advantages of hybrid fiber reinforced concrete	22
<i>I.2.5.2.1. Enhanced mechanical properties</i>	22
<i>I.2.5.2.2. Synergistic effects</i>	22
<i>I.2.5.2.3. Improved durability</i>	22
<i>I.2.5.2.4. Versatility in applications</i>	22
I.2.5.3. Disadvantages of Hybrid Fiber Reinforced Concrete	22
<i>I.2.5.3.1. Cost implications</i>	22
<i>I.2.5.3.2. Workability issues</i>	23
<i>I.2.5.3.3. Complexity in mix design</i>	23
<i>I.2.5.3.4. Potential for fiber debonding</i>	23
I.3. Sand concrete	23
I.3.1. Definition	23
I.3.2. Specificity of sand concrete	23
I.3.3. Constituent materials	23
I.3.3.1. Sand	23
I.3.3.2. Fines of addition	24
<i>I.3.3.2.1. Limestone fillers</i>	25
<i>I.3.3.2.2. Silica fume</i>	25

<i>I.3.3.2.3. Slag</i>	25
<i>I.3.3.2.4. Fly ash</i>	26
<i>I.3.3.3. Cement</i>	26
<i>I.3.3.4. Water</i>	26
<i>I.3.3.5. Admixture</i>	26
<i>I.3.3.6. Other additions</i>	27
<i>I.3.3.7. Gravel</i>	27
<i>I.3.3.8. Pigments (colorants)</i>	27
I.3.4. Essential properties	27
<i>I.3.4.1. General properties</i>	27
<i>I.3.4.1.1. Particle size (granulometry) - workability</i>	27
<i>I.3.4.1.2. Particle size (granulometry) – strength</i>	28
<i>I.3.4.2. Specific properties</i>	30
<i>I.3.4.2.1. Adhesion of rebar</i>	30
<i>I.3.4.2.2. Shrinkage and creep (deformation)</i>	30
<i>I.3.4.2.3. Durability</i>	31
<i>I.3.4.2.4. Washout resistance</i>	32
<i>I.3.4.2.5. Segregation</i>	32
<i>I.3.4.2.6. Microstructure SEM of sand concrete</i>	32
I.3.5. High flow sand concrete	33
<i>I.3.5.1. Definition</i>	33
<i>I. 3.5.2. Key properties</i>	33
<i>I. 3.5.3. Applications of HFSC</i>	33
<i>I. 3.5.3.1. Complex architectural elements</i>	33
<i>I. 3.5.3.2. Structures with dense reinforcement</i>	33
<i>I. 3.5.3.3. Projects requiring precise surface finishing</i>	34
<i>I. 3.5.3.4. Shotcrete applications</i>	34
<i>I.3.5.4. Advantages and disadvantages of HFSC</i>	35
<i>I.3.5.4.1. Advantages</i>	35
<i>I.3.5.4.2. Disadvantages</i>	35
I.4. Conclusion	35
Chapter II: Methodology and experimental program for HFSC mix design	37
II.1. Introduction	37
II.2. Constituents of the mixes	37
I.2.1. Sand (S)	37
<i>I.2.1.1. Sand equivalent (cleanliness)</i>	38

I.2.1.2. Methylene blue value	39
I.2.1.3. Particle size (granulometric) analysis	39
I.2.1.4. Fineness modulus.....	40
I.2.1.5. Bulk density	40
I.2.1.5. Absolute density.....	41
I.2.2. Cement (C)	42
I.2.3. Limestone filler (LF).....	42
I.2.4. Silica fume (SF).....	42
I.2.5. Fibers:	44
I.2.5.1. Stainless steel fibers (SSF-316L).....	44
I.2.5.2. Bronze fibers (BF –UE7)	45
I.2.5.3. Waste polyester fibers (WPF).....	45
I.2.6. Water reducer (SP).....	47
I.2.7. Water (W).....	47
I.3. Mix design	47
I.3.1. Experimental program	47
I.3.2. Formwork.....	49
I.3.3. Mix procedure.....	51
I.4. Norms & specimen dimensions.....	52
I.4.1. Physical properties.....	52
I.4.1.1. Slump	52
I.4.1.2. Density	53
I.4.1.3. Air content	54
I.4.2. Mechanical properties	55
I.4.2.1. Compressive strength.....	55
I.4.2.2. Flexural tensile strength.....	55
I.4.2.3. Split tensile strength.....	56
I.4.3. Chemical properties.....	57
I.4.3.1. Weight loss in hydrochloric acid (HCL).....	57
I.4.3.2. Weight loss in sulfuric acid (H ₂ SO ₄).....	58
I.4.4. Physio-chemical properties	58
I.4.4.1. Absorption by immersion.....	58
I.4.4.2. Capillary absorption.....	59
I.4.4.3. Sorptivity	60
I.4.4.4. Shrinkage and swelling.....	60
I.4.5. SEM and EDS-cartography	62

I.1.5.1. Scanning electron microscope (SEM).....	62
I.1.5.2. SEM-EDS cartography	63
I.6. Conclusion	64
Chapter III : Results and analysis	65
III.1 Introduction	65
III.2. High flow sand concrete reinforced with SSF-316L	65
III.2.1. Physical properties	65
III.2.1.1 Slump	66
III.2.1.2. Relationship between density & air content.....	66
III.2.2. Mechanical properties	67
III.2.2.1. Compressive strength	67
III.2.2.2. Flexural tensile strength	68
III.2.2.3. Split tensile strength	69
III.2.3. Physio-chemical properties	69
III.2.3.1. Absorption by immersion.....	69
III.2.3.2. Capillary absorption	70
III.2.3.3. Sorptivity.....	71
III.2.3.4. Shrinkage.....	71
III.2.3.5. Swelling.....	72
III.2.4. Chemical properties	73
III.2.4.1. Weight loss in sulfuric acid (H ₂ SO ₄).....	73
III.1.4.2. Weight loss in hydrochloric acid (HCl).....	74
III.2.5. SEM	74
III.2.6. Evaluation and justification for the optimal performance of SSF-316L in HFSC.....	75
III.3. High flow sand concrete reinforced with bronze fiber	76
III.3.1. Physical properties	76
III.3.1.1. Slump	76
III.3.1.2. Density	77
III.3.1.3. Air content.....	78
III.3.2. Mechanical properties	79
III.3.2.1. Compressive strength	79
III.3.2.2. Flexural tensile strength	79
III.3.2.3. Split tensile strength	80
III.3.3. Physio-chemical properties	81
III.3.3.1. Absorption by immersion.....	81
III.3.3.2. Capillary absorption	82

III.3.3.3. Sorptivity.....	82
III.3.3.4. Shrinkage.....	83
III.3.3.5. Swelling.....	83
III.3.4. Chemical properties	84
III.3.4.1. Weight loss in sulfuric acid (H ₂ SO ₄).....	84
III.3.4.2. Weight loss in hydrochloric acid (HCl).....	85
III.3.5. SEM	86
III.3.6. Evaluation and justification for the optimal performance of BF-UE7 in HFSC	86
III.4. High flow sand concrete reinforced with waste polyester fiber (WPF)	87
III.4.1. Physical properties	87
III.4.1.1. Slump	87
III.4.1.2. Density	88
III.4.1.3. Air content.....	89
III.4.1.4. Relationship between density & air content.....	90
III.4.2. Mechanical properties	90
III.4.2.1. Compressive strength.....	90
III.4.2.2. Flexural tensile strength	91
III.4.2.3. Split tensile strength.....	92
III.4.4. Physio-chemical properties	93
III.4.4.1. Absorption by immersion.....	93
III.4.4.2. Capillary absorption	94
III.4.4.3. Sorptivity.....	94
III.4.4.4. Shrinkage.....	95
III.4.4.5. Swelling.....	95
III.4.4. Chemical properties	96
III.4.4.1. Weight loss in sulfuric acid (H ₂ SO ₄).....	96
III.4.4.2. Weight loss in hydrochloric acid (HCl).....	96
III.4.5. SEM	97
III.4.6. Evaluation and justification for the optimal performance of WPF in HFSC	98
III.5. High flow sand concrete reinforced with hybrid fibers.....	98
III.5.1. Hybrid fiber integration in high-flow sand concrete	99
III.5.2. Physical properties	100
III.5.2.1. Slump	101
III.5.2.2. Density	102
III.5.2.3. Air content.....	103
III.5.2.4. Relationship between density & air content.....	103

III.5.3. Mechanical properties	104
III.5.3.1. Compressive strength	104
III.5.3.2. Flexural tensile strength	105
III.5.3.3. Split tensile strength	106
III.5.4. Physio-chemical properties	106
III.5.4.1. Absorption by immersion.....	106
III.5.4.2. Capillary absorption	107
III.5.4.3. Sorptivity.....	108
III.5.4.4. Shrinkage.....	108
III.5.4.5. Swelling.....	109
III.5.5. Chemical properties	110
III.5.5.1. Weight loss in sulfuric acid (H ₂ SO ₄).....	110
III.5.5.2. Weight loss in hydrochloric acid (HCl).....	111
III.5.6. SEM	111
III.6. Conclusion	112
Bibliography	
Technical data sheet (TDS)	

Abstract

Industrial waste is one of the most significant environmental challenges facing the world today, contributing substantially to environmental pollution. To mitigate these negative impacts, recycling industrial waste and utilizing it in various fields, such as civil engineering, has become an essential option to achieve environmental sustainability. These wastes can be employed as cost-effective alternative materials to enhance the properties of concrete and reduce its overall cost. Recycled industrial fibers play a dual role in improving concrete performance while minimizing the environmental impact of industrial waste. These materials also contribute to lowering the cost of concrete, making them a viable option for use in complex engineering structures. In this study, **High-Flow Sand Concrete (HFSC)** was selected due to its lower cost compared to conventional concrete, its fine internal structure free from coarse aggregates, and its distinctive physical properties. Three types of industrial fibers were added, each with specific characteristics: **stainless steel shavings (316L-SSF)** as macro fibers, **bronze shavings (UE7-BF)** as micro fibers, and **wasted polyester fibers (WPF)** as macro synthetic fibers. After evaluating the initial performance of each fiber type individually, they were combined into hybrid systems (dual and triple fibers) to analyze their effects on the physical, mechanical, chemical, and physio-chemical properties of the concrete. Fiber proportions at 0.25% , 0.50%, 1.00%, 1.50%, and 2.00% were used to ensure diverse results and determine the optimal ratios. Microscopic analysis (SEM) confirmed that the fibers improved the matrix cohesion of the concrete and reduced pore size, which contributed to enhancing its overall performance. These findings indicate that industrial fibers, whether mono or hybrid, represent a sustainable and efficient solution for improving the quality of High-Flow Sand Concrete, with broad potential applications in complex engineering construction projects.

Key words: High Flow Sand Concrete, SSF-316L, BF-UE7, WPF, Properties of concrete, Mono fiber, Hybrid (dual and triple) fibers.

Résumé

Les déchets industriels constituent l'un des défis environnementaux les plus importants auxquels le monde est confronté aujourd'hui, contribuant de manière significative à la pollution de l'environnement. Afin d'atténuer ces impacts négatifs, le recyclage des déchets industriels et leurs utilisations dans divers domaines, tels que le génie civil, sont devenus une option essentielle pour atteindre la durabilité environnementale. Ces déchets peuvent être employés comme matériaux alternatifs économiques pour améliorer les propriétés du béton et réduire son coût global. Les fibres industrielles recyclées jouent un rôle double en améliorant les performances du béton tout en minimisant l'impact environnemental des déchets industriels. Ces matériaux contribuent également à réduire le coût du béton, ce qui en fait une option viable pour les structures d'ingénierie complexes. Dans cette étude, le **béton de sable à haute fluidité (HFSC)** a été choisi en raison de son coût inférieur par rapport au béton conventionnel, de sa structure interne fine dépourvue de granulats grossiers et de ses propriétés physiques distinctives. Trois types de fibres industrielles ont été ajoutés, chacune avec des caractéristiques spécifiques : **copeaux d'acier inoxydable (316L-SSF)** comme fibres macro, **copeaux de bronze (UE7-BF)** comme fibres micro, et **fibres de polyester usagées (WPF)** comme fibres macro. Après avoir évalué la performance initiale de chaque type de fibre individuellement, elles ont été combinées en fibrage mixtes (fibres binaires et ternaires) pour analyser leurs effets sur les propriétés physiques, mécaniques, chimiques et physico-chimiques du béton. Des proportions de fibres à 0.25%, 0.50%, 1.00%, 1.50%, et 2.00% ont été utilisées pour assurer des résultats variés et déterminer les ratios optimaux. L'analyse microscopique (SEM) a confirmé que les fibres amélioraient la cohésion de la matrice du béton et réduisaient la taille des pores, ce qui a contribué à améliorer ses performances globales. Ces résultats indiquent que les fibres industrielles, qu'elles soient uniques ou hybrides, représentent une solution durable et efficace pour améliorer la qualité du béton de sable à haute fluidité, avec de larges applications potentielles dans des projets de construction d'ingénierie complexes.

Mot clé : Béton de Sable à Haute Fluidité, SSF-316L, BF-UE7, WPF, Propriétés du béton, Fibres individuelles, Fibrages mixtes (Binaires et ternaires)

ملخص

تعد النفايات الصناعية من أبرز التحديات البيئية التي تواجه العالم اليوم، حيث تساهم بشكل كبير في تلوث البيئة. وللحد من هذه التأثيرات السلبية، أصبحت إعادة تدوير النفايات الصناعية واستخدامها في مجالات مختلفة، مثل الهندسة المدنية، خياراً مهماً لتحقيق الاستدامة البيئية. يمكن توظيف هذه النفايات كمواد اقتصادية بديلة لتحسين خصائص الخرسانة وتقليل تكلفتها. تلعب الألياف الصناعية المعاد تدويرها دوراً مزدوجاً في تعزيز خصائص الخرسانة، إلى جانب تقليل الأثر البيئي للنفايات الصناعية. كما تساهم هذه المواد في خفض تكلفة الخرسانة، مما يجعلها خياراً مناسباً للاستخدام في المباني الهندسية المعقدة. في هذا البحث، تم اختيار الخرسانة الرملية عالية التدفق (HFSC) نظراً لتكلفتها المنخفضة مقارنة بالخرسانة التقليدية، وبنيتها الداخلية الناعمة التي تخلو من الركام الخشن، بالإضافة إلى خصائصها الفيزيائية المميزة. تمت إضافة ثلاثة أنواع من الألياف الصناعية، لكل منها خصائص محددة: نشارة الفولاذ المقاوم للصدأ (SSF-316L) كألياف كبيرة، نشارة البرونز (UE7-BF) كألياف دقيقة، وألياف البوليستر المهذرة (WPF) كألياف كبيرة. بعد دراسة الأداء الأولي لكل نوع من الألياف على حدة، تم دمجها في أنظمة هجينة (ثنائية وثلاثية الألياف) لتحليل تأثيرها على الخصائص الفيزيائية، الميكانيكية، الكيميائية، والفيزيائية-الكيميائية للخرسانة. تم استخدام نسب متفاوتة من الألياف (0.25%، 0.50%، 1.00%، 1.50% و 2.00%) لضمان تنوع النتائج وتحديد النسب المثلى. أثبت التحليل المجهرى (SEM) أن استخدام الألياف، سواء الأحادية أو الهجينة، أدى إلى تحسين التماسك داخل مصفوفة الخرسانة وتقليل حجم المسام، مما ساهم في تعزيز الأداء العام. تشير هذه النتائج إلى أن الألياف الصناعية تمثل حلاً مستداماً وفعالاً لتحسين جودة الخرسانة الرملية عالية التدفق، مع إمكانيات واسعة لتطبيقها في مشاريع البناء الهندسية المعقدة.

كلمات مفتاحية: الخرسانة الرملية عالية التدفق، نشارة الفولاذ المقاوم للصدأ ، نشارة البرونز، ألياف البوليستر المهذرة ، خصائص الخرسانة ، الالياف الأحادية ، الالياف الهجينة (ثنائية وثلاثية)

List of figures

Figure I. 1. Different industrial solid waste.....	3
Figure I. 2. Types of steel, (a) carbon steel, (b) alloy steel, (c) stainless steel	4
Figure I. 3. Types of metals (a) iron, (b) zinc, (c) lead (d) copper, (e) brass, (f) bronze.....	4
Figure I. 4. (A)steel turning, (b) ss by gloves, (c) ss by hand, (d) steel shavings.....	5
Figure I. 5. Powder steel.....	6
Figure I. 6. (a) machining steel, (b) steel scraps.....	6
Figure I. 7. (A) vibration cutting, (b) bronze spare parts, (c) bronze shavings	7
Figure I. 8. Bronze powder.....	7
Figure I. 9. (a) machining bronze, (b) bronze scraps.....	8
Figure I. 10. (A) machining brass, (b) brass shavings, (c) brass powder and scraps.....	8
Figure I. 11. Synthetic textile waste (a) polyester, (b) polypropylene, (c) carbon, (d)aramid.	11
Figure I. 12. Micro and macro fibers.....	20
Figure I. 13. Flow time as a function of fineness modulus	28
Figure I. 14. Effect of dosage and fineness of addition on strength	28
Figure I. 15. Influence of the nature of the addition on the level of resistance	29
Figure I. 16. Effect of granularity on resistance	29
Figure I. 17. Shrinkage evolution in sand concrete	30
Figure I. 18. Evolution of sand concrete creep.....	31
Figure I. 19. SEM – BF-UE7 fiber reinforced sand concrete.....	32
Figure I. 20. Complex architectural elements	33
Figure I. 21. Structural elements with closely spaced rebar.....	34
Figure I. 22. Smooth concrete floors.....	34
Figure I. 23. Shotcrete applications.....	35
Figure II. 1. Sand classe 0/2 – oued z’hor	37
Figure II. 2. Sand equivalent piston PS	38
Figure II. 3. Methylene Blue Value.....	39
Figure II. 4. Particle size analysis.....	39
Figure II. 5. Bulk density of sand 0/2.....	41
Figure II. 6. Absolute density of sand 0/2	41
Figure II. 7. SRC cement.....	42
Figure II. 8. Limestone filler	42
Figure II. 9. Silica fume.....	42
Figure II. 10. SEM-EDS cartography of chemical properties of cement, limestone fillers and silica fume.....	43
Figure II. 11. Stainless steel fibers (SSF-316L)	44
Figure II. 12. Bronze fibers (BF-UE7)	45
Figure II. 13. Waste polystyrene fibers (WPF)	46
Figure II. 14. Mix procedure	51
Figure II. 15. The slump test	53
Figure II. 16. Density test.....	54
Figure II. 17. Air content test	54
Figure II. 18. Compressive test.....	55
Figure II. 19. Flexural tensile test.....	56
Figure II. 20. Split tensile test	57

Figure II. 21. Weight loss --- hydrochloric acid (hcl)	58
Figure II. 22. Weight loss --- sulfuric acid (h ₂ so ₄).....	58
Figure II. 23. Absorption by immersion test	59
Figure II. 24. Capillary absorption test.....	60
Figure II. 25. Shrinkage test	61
Figure II. 26. Swelling test	62
Figure II. 27. Scanning electron microscope.....	62
Figure II. 28. Fei quanta 650 feg – sem.....	63
Figure II. 30. SEM-EDS cartography.....	63
Figure III. 1. Relationship between density & air content of mixes with ssf-316.....	66
Figure III. 2. Compressive strength of mixes with ssf-316l	67
Figure III. 3. Flexural tensile strength of mixes with ssf-316l	68
Figure III. 4. Split tensile strength of mixes with ssf-316l	69
Figure III. 5. Absorption by immersion of mixes with SSF-316L	70
Figure III. 6. Capillary absorption of mixes with SSF-316L.....	70
Figure III. 7. Sorptivity of mixes with SSF-316L	71
Figure III. 8. Shrinkage strain of mixes with SSF-316L	72
Figure III. 9. Swelling of mixes with SSF-316L	72
Figure III. 10. Weight loss of mixes with SSF-316L Exposed in Sulfuric acid.....	73
Figure III. 11. Weight loss of mixes with ssf-316l exposed hydrochloric acid.....	74
Figure III. 12. SEM of M0 --- without fibers	74
Figure III. 13. SEM of mix M1	75
Figure III. 14. Slump of mixes with BF-UE7.....	76
Figure III. 15. Density of mixes with BF-UE7.....	77
Figure III. 16. Air content of mixes with BF-UE7	78
Figure III. 17. Compressive strength of mixes with BF-UE7	79
Figure III. 18. Flexural tensile strength of mixes with BF-UE7.....	80
Figure III. 19. Split tensile strength of mixes with BF-UE7	80
Figure III. 20. Absorption by immersion of mixes with BF-UE7	81
Figure III. 21. Capillary absorption of Mixes with BF-UE7	82
Figure III. 22. Sorptivity of mixes with BF-UE7	82
Figure III. 23. Shrinkage of mixes with BF-UE7	83
Figure III. 24. Swelling of mixes with BF-UE7	84
Figure III. 25. Weight loss of mixes with BF-UE7 exposed sulfuric acid	84
Figure III. 26. Weight loss of mixes with BF-UE7 exposed Hydrochloric acid	85
Figure III. 27. SEM of M10 reinforced with BF-UE7.....	86
Figure III. 28. Slump of mixes with WPF	88
Figure III. 29. Density of mixes with WPF	88
Figure III. 30. Air content of mixes with WPF	89
Figure III. 31. Relationship between density & air content of mixes with WPF	90
Figure III. 32. Compressive strength of mixes with WPF	91
Figure III. 33. Flexural tensile strength of mixes with WPF	92
Figure III. 34. Split tensile strength of mixes with WPF.....	92
Figure III. 35. Absorption by immersion of mixes with WPF	93
Figure III. 36. Capillary absorption of mixes with WPF	94
Figure III. 37. Sorptivity of mixes with WPF	94
Figure III. 38. Shrinkage of mixes with WPF	95

Figure III. 39. Swelling of mixes with WPF	95
Figure III. 40. Weight loss of mixes with WPF -- (H ₂ SO ₄).....	96
Figure III. 41. Weight loss of mixes with WPF – (HCl)	97
Figure III. 42. SEM of mixes with WPF	97
Figure III. 43. Slump of mixes with hybrid fibers.....	101
Figure III. 44. Density of mixes with hybrid fibers.....	102
Figure III. 45. Air content of mixes with hybrid fibers	103
Figure III. 46. Relationship between density & air content of mixes with hybrid fibers	104
Figure III. 47. Compressive strength of mixes with hybrid fibers	104
Figure III. 48. Flexural tensile strength of mixes with hybrid fibers.....	105
Figure III. 49. Split tensile strength of mixes with hybrid fibers	106
Figure III. 50. Absorption by immersion of mixes with hybrid fibers	106
Figure III. 51. Capillary absorption of mixes with hybrid fibers.....	107
Figure III. 52. Sorptivity of mixes with hybrid fibers	108
Figure III. 53. Shrinkage of mixes with hybrid fibers	109
Figure III. 54. Swelling of mixes with hybrid fibers	109
Figure III. 55. Weight loss of mixes with hybrid fibers exposed sulfuric acid	110
Figure III. 56. Weight loss of mixes with hybrid fibers exposed hydrochloric acid	111
Figure III. 57. SEM of mixes with hybrid fibers	111

List of tables

Table I. 1. Characteristic solid wastes produced from various industrial activities	1
Table I. 2. Properties of synthetic fibers	10
Table I. 3. Relation between granularity and cement dosage	24
Table II. 1. Physical properties of sand	38
Table II. 2. Particle size of sand 0/2 mm according to nf en 933-1	40
Table II. 3. Chemical properties of cement, limestone fillers and silica fume.	43
Table II. 4. The physical properties of fibers	46
Table II. 5. The chemical properties of fibers	46
Table II. 6. The properties of water reducer viscocrete665	47
Table II. 7. The properties of water	47
Table II. 8. Identification of the mixtures	48
Table II. 9. The mixtures formulation	50
Table II. 10. Norms, specimen dimensions of concrete	52
Table III. 1. Physical properties of the hfcs reinforced with ssf-3161	66
Table III. 2. Mix design from hybrid (dual and triple) fibers reinforced HFSC	99
Table III. 3. Formwork from hybrid (dual and triple) fibers reinforced HFSC	100
Table III. 4. Physical properties of mixes with hybrid fibers	100

General introduction

General introduction

The global environment today faces significant challenges posed by the accumulation of industrial waste, leading to severe environmental pollution. Addressing these issues requires innovative and sustainable solutions, particularly in the field of civil engineering. This thesis investigates the integration of industrial waste, specifically **metallic shavings fibers and waste synthetic fibers**, into concrete production. By incorporating these waste fibers, the study aims to enhance the **physical, mechanical, chemical, and physio-chemical properties** of concrete while contributing to environmental sustainability and economic efficiency.

The research focuses on **High-Flow Sand Concrete (HFSC)**, a unique material known for its **fine-grained structure, high workability, and cost-effectiveness**. Unlike traditional concrete, HFSC lacks coarse aggregates, making it a suitable matrix for fiber reinforcement. Three types of waste fibers were selected for this study:

1. **Stainless steel shavings (SSF-316L)**: Macro metallic fibers characterized by high tensile strength.
2. **Bronze shavings (BF-UE7)**: Micro metallic fibers providing fine-scale reinforcement.
3. **Waste polyester fibers (WPF)**: Macro synthetic fibers known for their exceptional tensile properties.

The research examines both **mono fibers** (individual fiber types) and **hybrid fiber systems** (dual and triple combinations) with varying fiber ratios ranging from **0.25% to 2.00%**. The study evaluates their impact on the **mechanical strength, durability, and microstructural** of HFSC. Advanced analytical tools, such as **Scanning Electron Microscopy (SEM)**, were employed to explore the microstructural changes and matrix-fiber interactions.

This study aims to answer the following key research questions:

- Can industrial waste fibers serve as viable substitutes for conventional fiber reinforcements in concrete?
- How do different types of waste fibers (mono and hybrid systems) influence the **physical, mechanical, chemical, and physio-chemical properties** of HFSC?

- What is the optimal fiber dosage to achieve a balance between **strength, durability, porosity and workability** in HFSC?
- How does the microstructural interaction between HFSC and fibers contribute to its overall performance and resistance to aggressive environments?
- Does incorporating industrial waste fibers provide a cost-effective and environmentally sustainable alternative for large-scale construction applications?

This thesis is organized in the following chapters:

In Chapter I, the literature review addresses the problems associated with industrial waste, such as metallic shavings and waste synthetic fibers. It also discusses the environmental and economic benefits of using these wastes in construction materials. High-flow sand concrete was adopted in this research as a material for incorporating these waste fibers.

Chapter II explains the methodology employed in the study, focusing on the selection of constituent materials for high-flow sand concrete, such as sand, cement, limestone filler, silica fume, stainless steel shavings (SSF-316L), bronze shavings (BF-UE7), and waste polyester fibers (WPF). A total of 24 concrete mix designs will be studied, with varying fiber ratios ranging from 0.25% to 2%.

Chapter III presents a detailed analysis of the results, showing the performance of high-flow sand concrete reinforced with mono fibers and hybrid (dual and triple) fiber systems. The impact of fibers on the physical, mechanical, chemical, and physio-chemical properties of the mixtures will be analyzed. The study also includes Scanning Electron Microscopy (SEM) to investigate the microstructural matrix.

This study aims to demonstrate that the integration of industrial waste fibers, whether mono or hybrid, offers a sustainable approach to enhancing the quality of HFSC. The findings provide a foundation for the development of high-performance, cost-effective, and environmentally friendly construction materials suitable for complex engineering applications.

Chapter I

**Literature review on industrial
waste reinforced HFSC**

Chapter I: Literature review on industrial waste reinforced HFSC

I.1. Introduction

One of the challenges that our world is grappling with is Industrial waste, which stands as a primary contributor, to environmental contamination (Aldaood, et al., 2022). In the years following advancements, from the Industrial Revolution there has been a significant rise, in the generation of industrial waste. It can exist in solid, liquid or gaseous form (James & Pandian, 2016).

This research holds scientific and practical value as it addresses several problem. One of these issues pertains to finding methods, for industrial waste disposal that minimize harm to the environment. The other goal is to use these wastes as economic alternative, building materials that increase the strength and quality of concrete.

I.2. Industrial waste

I.2.1. Definition

Modern industries produce a significant amount of solid waste, including wood remnants, ash, slag, sludge, metal scraps, glass, plastic, concrete, and bricks, as shown in Table I.1 Some of these wastes are non-biodegradable, and some are classified as hazardous waste due to their toxic, ignitable, corrosive, or reactive nature. Poor handling of this waste can pose threats to human health and the environment. Therefore, it is crucial to use waste treatment methods to reduce toxicity levels and meet environmental regulatory limits (Cherian, et al., 2022)

TABLE I. 1. CHARACTERISTIC SOLID WASTES PRODUCED FROM VARIOUS INDUSTRIAL ACTIVITIES

Industry	Description	Typical waste by-product
Manufacturing	<ul style="list-style-type: none"> • Cement • Glass • Automobile • Pulp and paper • Textile • Chemical • Wineries • Food (rice milling) 	<ul style="list-style-type: none"> • Kiln dust and fly ash • Glass waste • Waste rubber tires • Waste wood, fibrous sludge, lime mud, dregs • Waste fabric and sludge • Acid slag, alkali slag, salt mud, kettle mud • Spent bentonite and sludge • Rice husk ash
Energy/Power	<ul style="list-style-type: none"> • Coal power plants • Bioenergy plants 	<ul style="list-style-type: none"> • Coal fly ash, bottom ash, slag from boilers

		<ul style="list-style-type: none"> • Biomass-based fly ash and bottom ash, slag
Metallurgy	<ul style="list-style-type: none"> • Smelting of iron in blast furnaces • Steel/copper smelting in furnace • Aluminum extraction from bauxite • Production of elemental silicon or alloy in an electric arc furnace 	<ul style="list-style-type: none"> • Blast furnace slag • Steel and copper slag • Red mud • Silica fume
Mining and quarrying	<ul style="list-style-type: none"> • Mining of coal • Metals and non-metal mining • Distillation process in mine 	<ul style="list-style-type: none"> • Coal tailing • Waste stones, quarry dust, phosphogypsum • Tailings from gold, copper, zinc mines
Construction	<ul style="list-style-type: none"> • Construction and demolition activities 	<ul style="list-style-type: none"> • Concrete • Bricks and blocks • Tiles • Aggregates • Gypsum • Asphalt • Metals • Glass • Steel • Timber
Waste/water treatment	<ul style="list-style-type: none"> • Wastewater treatment/ disposal • Solid waste incineration 	<ul style="list-style-type: none"> • Sewage sludge, sludge ash from incinerator • Fly ash and bottom ash
Miscellaneous	<ul style="list-style-type: none"> • Wastes from recycling industries 	<ul style="list-style-type: none"> • Scrap tire • Crushed glass • Polymer, polypropylene • Plastic, synthetic • Textile waste

Table I. 1 and Figure I. 1 shows that due, to industrial activities huge quantities of solid waste are produced, encompassing items such, as bricks, blocks, tiles, gravel, concrete, gypsum, asphalt, metals and steel glass, wood, textiles, plastic, polymer and various other materials.

This solid waste characterized by a high value allowing for its reuse, in ways to minimize the need for disposal, despite facing several obstacles in the recycling process (Yeheyis , et al., 2012) (Rahman, et al., 2022). Challenges include the absence of technology for waste management, instability of the source and a lack of knowledge of waste characteristics. Past studies, shows that utilizing these solid waste materials as reinforcements in concrete, roads, pavements, composite building materials, etc.,

is a sustainable option for waste management and helps prevent solid waste accumulation (Rastogi & Sharma, 2012).

Based on the important role of recycled industrial solid waste, in eco-friendly building, this study highlights specific types of solid waste, that can serve as valuable sustainable resources for construction materials.



FIGURE I. 1. DIFFERENT INDUSTRIAL SOLID WASTE

1.2.2 Industrial solid wastes used in civil engineering

The growing need, for construction materials and their rising prices have sparked a surge of technological advancements in the quest, for eco sustainable building alternatives. In fields of civil engineering, like researchers have explored ways to recycle solid industrial waste and exploiting it or replacing it with concrete materials (Ex: cement, fly ash, Coarse or fine aggregates, adjuvants and fibers) different forms and types (Meddah & Bencheikh, 2009) (Kalpana & Tayu, 2020).

Among various types of industrial solid waste, that can serve as primary or secondary materials, this study specifically concentrates on utilizing waste derived from metals and synthetic textile waste to improve the properties of concrete (Dogruyol, et al., 2024) (Haigh, 2024) (Al-Alusi, et al., 2024) (Jayalath, et al., 2024).

1.2.3 Types of industrial metals wastes in civil engineering

There are thousands of different types of metals out there, and each has been developed for very specific applications. The properties of metals are crucial to understanding because they reveal which

metals offer which qualities. In general, metals have three different types of characteristics (Yousef, 2023):

- *Physical property*: include things like their appearance, color, luster, weight, and texture.
- *Mechanical property*: such as hardness, ductility, malleability, and so on, represent their inherent capacity.
- *Chemical property*: indicate how metals behave in different chemical processes.

Some of the most well-known types of metals include steel, carbon steel, alloy steel, stainless steel Figure I. 2, iron, zinc, lead, copper , brass (yellow copper) , bronze Figure I. 3, aluminum, tin, titanium, tungsten, silver and gold.



FIGURE I. 2. TYPES OF STEEL, (A) CARBON STEEL, (B) ALLOY STEEL, (C) STAINLESS STEEL

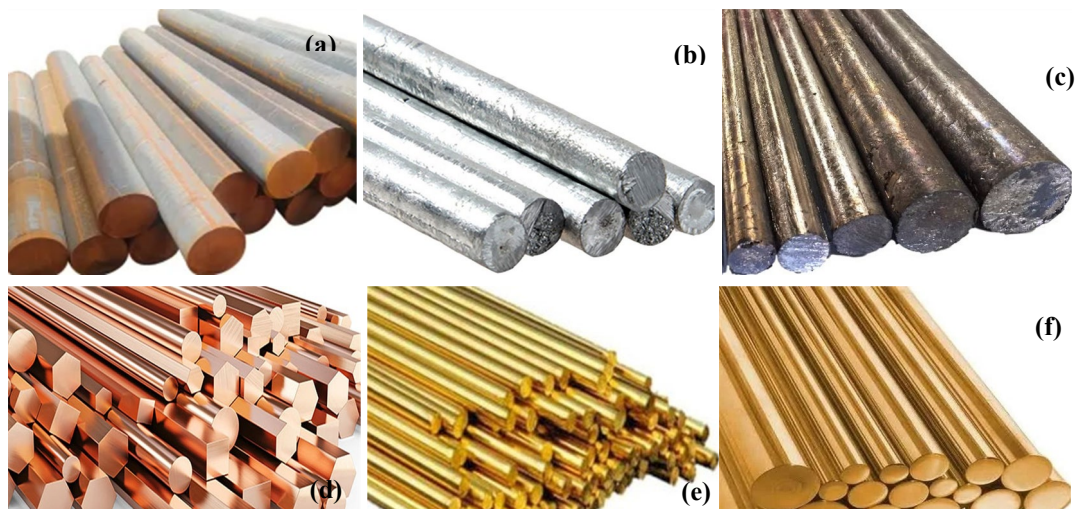


FIGURE I. 3. TYPES OF METALS (A) IRON, (B) ZINC, (C) LEAD (D) COPPER, (E) BRASS, (F) BRONZE

Machining of spare parts is taking a piece of metal or other material and removing some of it to create something of a particular shape, size, and functionality. This process is classified as "subtractive manufacturing" since it entails removing material to attain the desired form, size, or configuration of a part or finished product. The metal that's removed (filings, fines, shavings and turnings) is debris or waste known collectively as "chips" or "swarf." It usually winds up in a bin that's part of a machinist's workstation, and it's generally recyclable (COHEN, 2024).

In our research thesis we will concentrate on metals commonly disposed of as waste that're abundant, in the ALEMO (Algerian Equipment and Machine tools) society as they can be efficiently utilized in civil engineering at an economical price (ALEMO, 2024) :

I.2.3.1. Industrial steel waste

When the machining of spare parts, from steel three different types of swarf (turning) waste materials are produced: shavings, powder, and steel scraps. The swarf waste can be used in civil engineering applications such as concrete, mortar, plaster, and geotechnical studies. Some of these applications have been studied, while others remain to be explored. Three distinct types of swarf (turning) waste materials are:

I.2.3.1.1. Steel shavings

Steel Shavings (SS) are the most produced in steel turning. These sharp chips present a risk, if touched by hand directly .Therefore, the use of gloves is essential when dealing with them. Shavings come in sizes with thicknesses ranging from 0.1 mm, to 0.5 mm and widths varying between 1 mm and 10mm **Figure I. 4** Shavings measuring, between 1 mm and 3 mm, in width can serve as fibers to strengthen concrete, mortar and plaster. The assorted leftover shavings of varying sizes can be applied in research and other academic investigations



FIGURE I. 4. (A)STEEL TURNING, (B) SS BY GLOVES, (C) SS BY HAND, (D) STEEL SHAVINGS

I.2.3.1.2. Steel powder

Powder steel **Figure I. 5** is another byproduct produced when machining the spare parts of steel. This type of steel waste is very dangerous. Should not be touched directly. It's important to wear gloves and masks to prevent touching or breathing in the powder, which can be extremely harmful to the lungs. Despite its dangers, this fine material has potential applications in civil engineering, where it can be used as a substitute for cement, sand, or other construction materials.



FIGURE I. 5. POWDER STEEL

1.2.3.1.3. Steel scraps

Steel scraps [Figure I. 6,\(b\)](#) are irregularly sized and shaped pieces of waste produced during machining [Figure I. 6,\(a\)](#). Due to their irregularity, they are less frequently used as alternative building materials. However, ongoing research is exploring their potential uses. These steel scraps can be recycled and reshaped into usable forms for construction purposes, indicating a promising avenue for further utilization and sustainability, in material recycling.

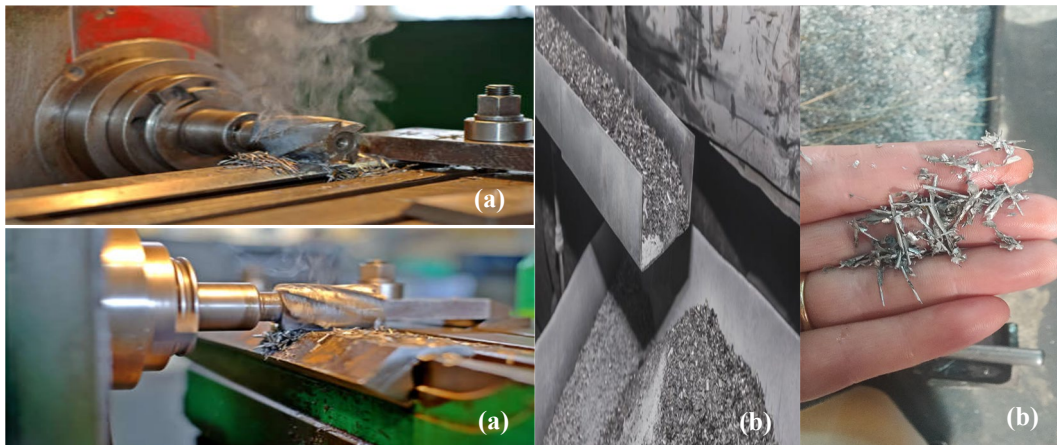


FIGURE I. 6. (A) MACHINING STEEL, (B) STEEL SCRAPS

1.2.3.2. Industrial bronze waste

When using vibration cutting [Figure I. 7,\(a\)](#) to manufacture spare parts [Figure I. 7,\(b\)](#), from bronze, the first type of swarf waste produced is shavings, which resemble microfibrs. During the machining of bronze spare parts, three different types of swarf waste materials are generated: shavings, scraps and bronze powder. These swarf wastes can be utilized in civil engineering applications.

1.2.3.2.1. Bronze shavings

Bronze shavings [Figure I. 7,\(c\)](#) are the least produced, as they only form during vibration cutting [Figure I. 7,\(a\)](#). These shavings are in the form of microfibrs and are very dangerous to handle without gloves because they are sharp and can penetrate the skin like needles. Their length does not exceed 10 mm, and their thickness does not exceed 1 mm. They can be used as fibers to reinforce concrete,

tiles, or plaster. In addition to their mechanical properties, which enhance construction materials, they also offer aesthetic advantages.

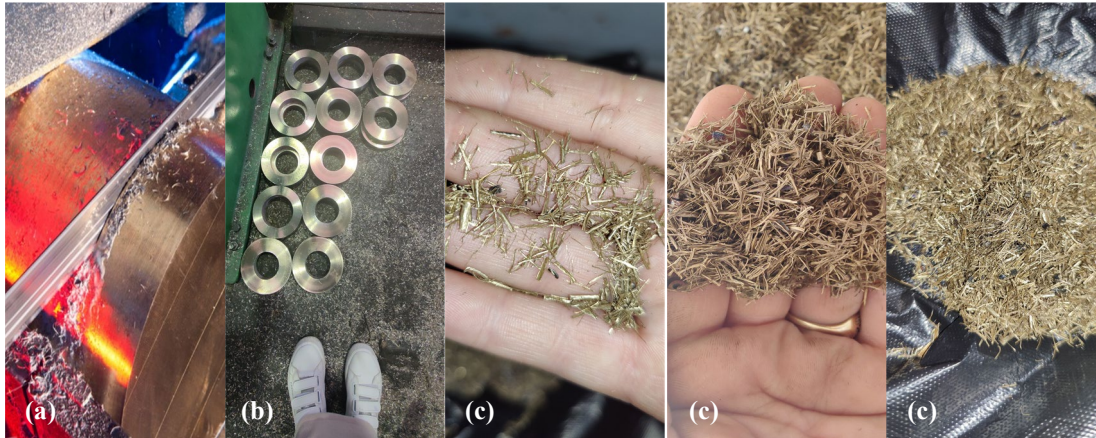


FIGURE I. 7. (A) VIBRATION CUTTING, (B) BRONZE SPARE PARTS, (C) BRONZE SHAVINGS

1.2.3.2.2. Bronze powder

Bronze powder [Figure I. 8](#) is the most byproduct produced when machining the spare parts of bronze. Using gloves and masks is crucial, for protecting against skin contact and inhaling the powder as it can have effects, on lung health. Despite the risks involved, this high quality material holds promise for uses, in civil engineering as a substitute for cement, sand, or other construction materials.



FIGURE I. 8. BRONZE POWDER

1.2.3.2.3. Bronze scraps

Bronze scraps in [Figure I. 9,\(b\)](#) are small-sized pieces produced during machining, as shown in [Figure I. 9,\(a\)](#). These scraps are generated in large quantities and have a density of 8.6 g/cm^3 , which is high compared to steel's density of 7.9 g/cm^3 . Additionally, bronze is a very durable material that does not form spiral shavings. Notably, these scraps can be used as alternative building materials.



FIGURE I. 9. (A) MACHINING BRONZE, (B) BRONZE SCRAPS

I.2.3.3. Industrial copper / brass waste

During the vibration cutting process shown in [Figure I. 10,\(a\)](#) to produce spare parts from copper or brass, as depicted in [Figure I. 10,\(b\)](#), the initial swarf waste generated consists of shavings that resemble microfibers. Throughout the machining of copper or brass parts, three main types of swarf waste are produced: shavings, scraps, and fine copper or brass powder [Figure I. 10,\(c\)](#).



FIGURE I. 10. (A) MACHINING BRASS, (B) BRASS SHAVINGS, (C) BRASS POWDER AND SCRAPS

I.2.3.4. The relationship between copper/brass and bronze

Copper and bronze are closely related metals, with distinct characteristics that influence their applications and properties.

I.2.3.4.1. Composition

- Copper

Copper is a pure elemental metal, represented by the symbol Cu on the periodic table. It is known for its excellent electrical and thermal conductivity, malleability, and ductility. Its natural reddish-brown color can develop a green patina over time due to oxidation.

- Bronze

Bronze is primarily an alloy of copper and tin, although it may also include other elements such as aluminum, manganese, or phosphorus to enhance specific properties. The addition of tin improves bronze's strength and corrosion resistance compared to pure copper.

I.2.3.4.2. Properties

- Corrosion resistance

Bronze exhibits superior corrosion resistance, particularly in marine environments, making it ideal for applications such as ship fittings and propellers. Copper also has good corrosion resistance but is more susceptible to acidic conditions.

- Mechanical strength

Bronze is generally harder and stronger than copper due to its alloying elements. This makes bronze suitable for heavy-duty applications like industrial machinery and tools, whereas copper is preferred for applications requiring high electrical conductivity.

- Density

Copper is denser than bronze. In terms of density, the order is as follows: copper > bronze > brass:

Copper: approximately 8.96 g/cm³

Bronze (copper-tin alloy): typically around 8.7 to 8.9 g/cm³, but it can vary slightly depending on the specific alloy composition.

Brass (copper-zinc alloy): ranges between 8.4 to 8.7 g/cm³, depending on the composition.

I.2.4. Types of synthetic textile wastes in civil engineering

Synthetic fibers play a crucial role in enhancing concrete performance, particularly in improving tensile strength, which is traditionally a weak point in concrete. These fibers are characterized by their long, slender form and are manufactured from natural or synthetic polymers. What makes synthetic fibers robust and durable is their carefully structured internal organization, achieved through a mechanical drawing process that stretches the fibers after production, increasing their strength and cohesion.

In concrete applications, synthetic fibers are added to address its weakness in resisting tensile forces. Typically, around 1% of the concrete mix is composed of fibers to strengthen it once cracks appear, helping to control their spread and prolong the concrete's lifespan. By increasing the fiber content to as much as 15%, the overall tensile strength of the concrete can be significantly improved even before cracks form. The fibers help distribute stress more evenly and reinforce weaker areas, leading to better overall performance (Surendra P, 1992).

In recent years, synthetic fibers have become more attractive as reinforcements for cementitious materials. These fibers provide effective and relatively low-cost reinforcement for concrete, and are alternatives to other fibers such as steel and glass. Types of fibers that have been incorporated into cement matrices include polyethylene (PE), polypropylene (PP), acrylics (PAN), poly(vinyl alcohol) (PVA), polyamides (PA), aramid, polyester (PES) and carbon. The properties of synthetic fibres vary widely, in particular with respect to the modulus of elasticity, an important property when fibres are

used for producing composites (Zheng & Feldman, 1995). Table I.2 provides a summary of the physical properties of various synthetic fibres, according to the study of Chandrathilaka et al (Chandrathilaka, et al., 2021):

TABLE I. 2. PROPERTIES OF SYNTHETIC FIBERS

Fibre type	Specific gravity	Tensile strength (MPa)	Elastic modulus (GPa)	Ultimate elongation (%) (max to min)
Asbestos	2.80	600-3600	69-150	0.3-0.1
Carbon	1.80	590-4800	28-520	2-1
Aramid	1.44	2700	62-130	4-3
Polypropylene (PP)	0.91	200-700	0.5-9.8	15-10
Polyamide	1.14	700-1000	3.9-6.0	15-10
Polyester	1.38	800-1300	up to 15	20-8
Rayon	1.50	450-1100	up to 11	15-7
Polyvinyl alcohol (PVA)	1.19	800-1500	29-40	10-6
Polyacrylonitrile	1.18	850-1000	17-18	9
Polyethylene (PE)	0.96	400	2-4	4-100
Highly oriented polyethylene (PE) (high molecular weight)	0.98	2585	117	2.2

The textile industry is expanding rapidly as the global population continues to demand more textiles, resulting in a significant increase in textile waste. The significant impact of this amount of accumulated waste leads to heightened environmental pollution. Conversely, this textile waste has huge potential for valorization in the field of construction and geotechnical engineering. This sector presents an opportunity, for the growth of the textile recycling industry. Table I. 2 displays the components and materials used in the textile industry, while Figure I. 11 illustrates some types of synthetic textile waste.

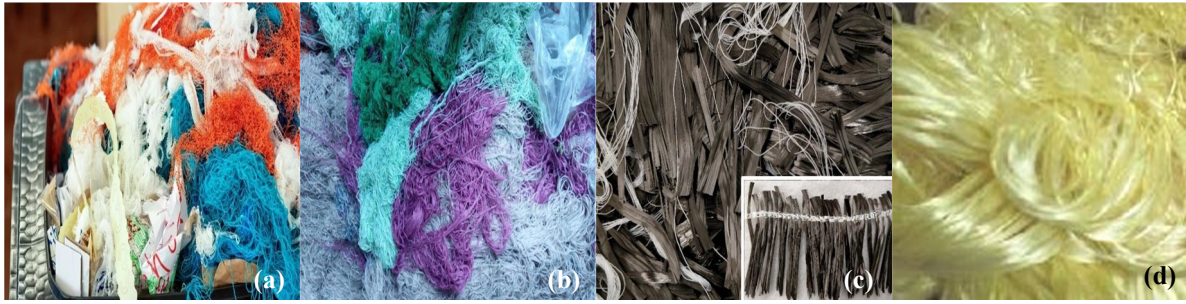


FIGURE I. 11. SYNTHETIC TEXTILE WASTE (A) POLYESTER, (B) POLYPROPYLENE, (C) CARBON, (D)ARAMID.

I.2.4.1. Polyester fiber waste

Polyester fiber waste presents a significant environmental challenge due to its widespread use in the textile industry and its resistance to biodegradation. Various methods and innovations are being explored to effectively recycle this waste, with chemical and mechanical recycling being the most notable options. However, both methods require substantial effort and energy, emphasizing the need for more efficient recycling strategies.

In civil engineering, polyester fibers can serve as an alternative material, especially given their distinctive properties such as high tensile strength, flexibility, and lightweight nature, which make them ideal for enhancing concrete performance.

Recycling polyester not only reduces textile waste but also mitigates the environmental impact associated with its production. Specifically, consumption-based recycling significantly lowers carbon emissions compared to the production of new polyester from petrochemical sources.

Polyester fibers are increasingly being utilized in concrete to enhance its mechanical properties, durability, and resistance to cracking. This innovative approach leverages the unique characteristics of polyester fibers, which contribute positively to various concrete formulations.

1.2.4.1.1. Benefits of polyester fibers in concrete

- Crack resistance

Polyester fibers help improve crack resistance by effectively bridging micro-cracks and preventing their propagation. This is particularly beneficial in cement matrices where tensile stresses can lead to cracking (Christopher, et al., 2023) (Malagavelli & Rao Patura, 2011).

- Mechanical strength

The incorporation of polyester fibers can enhance the compressive and flexural strength of concrete. Studies have shown that a combination of polyester and steel fibers can yield significant improvements in toughness and strength properties compared to plain concrete (Christopher, et al., 2023) (Wang, et al., 2023).

- Shrinkage control

Polyester fibers have been found to significantly reduce both drying and thermal shrinkage in cement-stabilized concrete. An optimal fiber content can improve shrinkage resistance, making it advantageous for applications where dimensional stability is critical (Wang, et al., 2023) (Ali, et al., 2020).

- Durability

The addition of polyester fibers contributes to the overall durability of concrete by improving its resistance to environmental factors such as moisture and temperature variations. This makes polyester fiber-reinforced concrete suitable for a variety of applications, including pavements and structural elements exposed to harsh conditions (Elite-indus, 2024) (Martinez-Berrera, et al., 2022).

1.2.4.1.2. Applications

- Hybrid fiber reinforcement

Combining polyester fibers with other types of fibers (e.g., steel) has shown synergistic effects, enhancing the overall performance of the concrete composite (Christopher, et al., 2023).

- High-tensile concrete projects

The fibers are particularly effective in high-tensile concrete projects, providing multi-functional reinforcement capabilities that are beneficial in heavy-load scenarios (Elite-indus, 2024).

1.2.4.1.3. Considerations

- Workability

While adding polyester fibers can improve certain mechanical properties, it may also reduce the workability of high-strength concrete mixtures. Adjustments in mix design may be necessary to maintain desired flow characteristics (Ali, et al., 2020) (Yeswanth & Praveenkumar, 2022).

1.2.4.1.4. Optimal fiber content

Research indicates that there is an optimal range for fiber content (typically between 0.1% and 1.0% by volume) beyond which the benefits may diminish or even reverse, particularly regarding shrinkage control (Wang, et al., 2023).

However, some studies by (Malagavelli & Rao Patura, 2011) have utilized polyester fiber content ranging from 0% to 6%.

1.2.4.2. Polypropylene fiber waste

Polypropylene fiber waste, particularly from recycled plastic packaging, is increasingly being utilized in concrete to enhance its properties while addressing environmental concerns. The incorporation of

recycled polypropylene fibers into concrete mixes has been shown to significantly improve mechanical properties, including compressive, flexural, and tensile strengths. For instance, studies indicate that adding approximately 1.0% of these fibers can lead to increases in compressive strength by nearly 70% and flexural strength by over 250% compared to unreinforced concrete. This not only enhances the durability and crack resistance of the concrete but also provides an eco-friendly solution by repurposing waste materials that would otherwise contribute to environmental pollution (Malek, et al., 2020).

Polypropylene fibers are synthetic fibers widely used in concrete to improve its mechanical properties, durability, and resistance to cracking. Their incorporation into concrete mixes offers several advantages, making them a valuable addition to construction materials.

1.2.4.2.1. Benefits of polypropylene fibers in concrete

- Crack control

Polypropylene fibers significantly reduce plastic shrinkage cracking by distributing tensile stresses more evenly throughout the concrete matrix. This helps maintain the integrity of the structure and prevents the formation of larger cracks (Bisley Company, 2021) (Bisley company, 2021).

- Enhanced durability

The fibers improve the overall durability of concrete by increasing its resistance to environmental factors such as moisture and freeze-thaw cycles. This leads to longer-lasting structures with reduced maintenance needs. (NBM&CW, 2022)

- Increased strength

Incorporating polypropylene fibers can enhance both tensile and flexural strength. Studies indicate that the addition of these fibers can increase splitting tensile strength by approximately 20% to 50% compared to plain concrete (KDO CHEMICAL, 2023).

- Cost-effectiveness

Using polypropylene fibers is a cost-effective method for achieving high-strength concrete without requiring significant modifications to traditional concrete mixes. They can be easily integrated into existing processes. (Bisley Company, 2021).

1.2.4.2.2. Applications

- Pavements and roads

Polypropylene fiber-reinforced concrete is commonly used in road construction due to its enhanced durability and crack resistance.

- Tunnels and underground structures

The fibers improve the cohesion and bonding of sprayed concrete in applications like shotcrete, making it suitable for tunnels and retaining walls. (KDO CHEMICAL, 2023)

- Precast elements

These fibers are also utilized in precast concrete products, where improved crack resistance and durability are essential.

1.2.4.2.3. Optimal fiber content

The effectiveness of polypropylene fibers depends on their volume fraction in the mix. Typically, a range of 0.25% to 1.25% by volume is recommended for optimal performance without adversely affecting compressive strength (Murthi, et al., 2023).

1.2.4.2.4. Fiber length

The length of the polypropylene fibers can impact their performance; longer fibers generally provide better reinforcement for larger projects, while shorter fibers may suffice for lighter applications (Bisley company, 2021) (NBM&CW, 2022).

1.2.4.3. Carbon fiber waste

Carbon fiber waste consists of remnants from the manufacturing of composite materials that rely on carbon fibers, known for their light weight and high strength. These waste fibers can be recycled and incorporated into concrete to enhance its tensile and flexural strength, significantly improving its overall durability (Bhandari & Nam, 2024).

Carbon fibers are increasingly being integrated into concrete to enhance its mechanical properties, durability, and overall performance. Their unique characteristics provide significant advantages over traditional reinforcement materials.

1.2.4.3.1. Benefits of carbon fibers in concrete

- High strength-to-weight ratio

Carbon fibers are known for their exceptional strength while being lightweight, making them an ideal choice for reinforcing concrete. They can significantly enhance the tensile strength of concrete without adding substantial weight, which is particularly beneficial in applications where structural weight is a concern. (Bisley Company, 2021)

- Improved ductility

The addition of carbon fibers increases the ductility of concrete, allowing it to deform under stress without fracturing. This property helps prevent sudden failures and improves the overall resilience of structures (Bisley Company, 2021)

- Crack resistance

Carbon fibers effectively control cracking by bridging micro-cracks that develop in the concrete matrix. This capability helps maintain the structural integrity and prolongs the lifespan of concrete elements (Bisley Company, 2021).

- Corrosion resistance

Unlike traditional steel reinforcement, carbon fibers do not corrode, which enhances the durability of concrete structures, especially in environments exposed to moisture or aggressive chemicals (Gao & Xia, 2023).

- Thermal stability

Carbon fibers can withstand high temperatures, making them suitable for applications where fire resistance is critical. This property ensures that structures remain stable and safe under extreme conditions.

1.2.4.3.2. Applications

- Structural reinforcement

Carbon fiber reinforced concrete (CFRC) is used in various structural applications, including bridges, parking garages, and high-rise buildings, where enhanced load-bearing capacity is required. (Bisley Company, 2021)

- Repair and strengthening

CFRC can be applied to existing structures to improve their load-carrying capacity without the need for extensive renovations or demolitions, offering a cost-effective solution for structural upgrades. (Bisley Company, 2021).

- Innovative designs

The flexibility and strength of carbon fibers allow for more creative architectural designs, enabling the construction of thinner and more complex structural elements (Bisley Company, 2021).

1.2.4.3.1. Considerations

- Cost

While carbon fibers offer numerous advantages, they are generally more expensive than traditional reinforcement materials like steel. This factor may limit their use in some projects unless the performance benefits justify the cost. (Gao & Xia, 2023)

- Mix design adjustments

The incorporation of carbon fibers may require adjustments in the concrete mix design to optimize performance and workability, ensuring that the fibers are evenly distributed throughout the matrix (Gao & Xia, 2023).

1.2.4.3.3. Optimal fiber content

The effectiveness of carbon fibers depends on their volume fraction in the mix. Typically, a range of 0.25% to 2.5% by volume is recommended for optimal performance without adversely affecting compressive strength. (Atiyeh & Aydin, 2020) (Li, et al., 2021)

1.2.4.4. Aramid fiber waste

Aramid fiber waste, particularly from the production and processing of aramid fibers like Kevlar, is increasingly being explored for its potential use in concrete. Utilizing aramid fiber waste in concrete not only addresses environmental concerns related to waste management but also enhances the mechanical properties of the concrete itself.

Aramid fibers, particularly para-aramid fibers, are increasingly being utilized in concrete to enhance its mechanical properties and durability. These synthetic fibers offer several advantages that make them suitable for various construction applications.

1.2.4.4.1. Benefits of aramid fibers in concrete

- High strength and toughness

Aramid fibers possess a high tensile strength, making them effective in reinforcing concrete structures. They can significantly improve the flexural and compressive strength of concrete, enhancing its overall load-bearing capacity. Studies have shown that concrete beams reinforced with para-aramid fiber sheets can exhibit an increase in ultimate load-carrying capacity by up to 23.9% compared to unreinforced specimens (Ruziev & Kim, 2023).

- Crack resistance

The incorporation of aramid fibers helps control cracking in concrete by bridging micro-cracks and preventing their propagation. This property is essential for maintaining the structural integrity of concrete elements under stress.

- Durability

Aramid fibers are resistant to environmental degradation, including moisture and chemical attacks. Research indicates that concrete wrapped with aramid fibers shows improved resistance to acid attacks and thermal effects, resulting in less weight loss and enhanced compressive strength over time (Talikota & Kandekar, 2019).

- Lightweight

Compared to traditional reinforcement materials like steel, aramid fibers are lighter, which can reduce the overall weight of concrete structures without compromising their strength.

- Fire resistance

Aramid fibers exhibit excellent fire resistance properties, making them suitable for applications where fire safety is a concern. This characteristic allows structures reinforced with aramid fibers to maintain their integrity under high temperatures (Talikota & Kandekar, 2019).

1.2.4.4.2. Applications

- Structural reinforcement

Aramid fiber-reinforced concrete (AFRC) is used in various structural applications, including beams, columns, and slabs, where enhanced mechanical properties are required.

- Repair and rehabilitation

The fibers are also employed in the repair of existing concrete structures, providing a cost-effective solution for strengthening elements that may have suffered damage or degradation.

- Hybrid fiber systems

Combining aramid fibers with other fiber types, such as carbon fibers, has shown to further enhance the mechanical properties of concrete. Hybrid systems can leverage the strengths of multiple fiber types to achieve superior performance (Li, et al., 2021).

1.2.4.4.3. Considerations

- Cost

While aramid fibers offer significant benefits, they tend to be more expensive than traditional reinforcement materials. This factor may influence their adoption in some projects unless justified by performance improvements.

- Mix design adjustments

The integration of aramid fibers may require modifications to the concrete mix design to optimize workability and ensure uniform distribution throughout the mix.

1.2.4.4.3. Optimal fiber content

The effectiveness of carbon fibers depends on their volume fraction in the mix. Typically, a range of 0.25% to 2.5% by volume is recommended for optimal performance without adversely affecting compressive strength. (Zheng & Feldman, 1995).

1.2.5. Hybrid fiber reinforced concrete

Hybrid fiber-reinforced concrete (HFRC) is an innovative composite material that combines two or more different types of fibers to enhance the mechanical properties of concrete. The primary goal of using hybrid fibers is to leverage the unique benefits of each fiber type, resulting in improved performance over conventional concrete.

Here are some notable previous studies and research findings on hybrid fiber-reinforced concrete (HyFRC), particularly focusing on the combination of different fibers such as steel (micro and macro fibers) and synthetic fibers (Bao.L et al, 2024) in an experimental investigation, focused on the axial compressive and splitting tensile behavior of reinforced concrete with a low content of hybrid steel fibers (both micro and macro steel fibers). The findings indicated that micro-straight steel fibers (mSF) had a more significant effect on retaining post-peak stress during the axial compression tests, while macro hooked-end steel fibers (MHF) positively contributed to the enhancement of peak strain. Furthermore, the average peak stress of the hybrid steel fiber-reinforced concrete (HSRC) was found to be 8.6% greater than that of H40 and 16.4% higher than that of S40. The study revealed that the incorporation of hybrid steel fibers significantly improved both the compressive and tensile strengths of the concrete. These fibers enhanced ductility and energy absorption capacity, leading to better performance under load. Additionally, the hybrid fibers facilitated a more uniform distribution of stress, reducing the likelihood of sudden failure. Overall, the research demonstrated that even a low content of hybrid steel fibers can substantially enhance the mechanical properties of reinforced concrete.

(Htet, et al., 2024) found in their study on hybrid fiber-reinforced recycled aggregate concrete (FRRAC) that to enhance the ductility of recycled aggregate concrete (RAC) for structural applications and mitigate the corrosion risks associated with steel fibers, they introduced a deflection-hardening hybrid fiber-reinforced recycled aggregate concrete (FRRAC). This was achieved by combining newly developed macro-basalt fibers (BF, 0.67% by volume) with recycled macro-polypropylene fibers (PF, 0.67% by volume). The fresh, static, and dynamic mechanical properties of this hybrid mix were examined and compared to a mix containing only macro-basalt fibers (1.34% by volume). A \varnothing 100 mm split Hopkinson pressure bar (SHPB) system was employed to evaluate the dynamic mechanical properties under both compression and tension. The hybrid FRRAC demonstrated the ability to retain up to 90% of its average initial peak load at a crack width of 3.5 mm. These results suggest that hybrid FRRAC is a promising material for structural applications, offering improved physical and mechanical properties as well as reduced corrosion risks compared to traditional steel fiber-reinforced concrete.

(Christopher, et al., 2023) investigated in steel and polyester fibers affect the mechanical and durability properties of steel-polymer hybrid fiber-reinforced concrete (HyFRC), specifically

focusing on toughness under indirect tensile loading conditions. The research utilizes steel and polyester fibers both individually (FRC) and in combination (HyFRC) within an M45 grade composite that includes fly ash and silica fume as supplementary cementitious materials. When steel fibers were used alone at a volume fraction of 0.75%, there was a 10% increase in compressive strength, and a maximum improvement of 14% was observed at a 0.5% volume fraction compared to plain concrete. The toughness under split tension was enhanced by 26% to 72% with hybrid fibers when compared to polyester fibers, and by 10% to 18% in comparison to steel fiber reinforcement. Additionally, water sorptivity results improved with the introduction of hybrid fibers.

The research conducted by (Aghaee & Khayat, 2024) investigates the use of hybrid fibers and shrinkage-mitigating materials in self-compacting concrete (SCC). This study specifically focuses on SCC incorporating hybrid synthetic polypropylene (PP) fibers and hybrid steel-synthetic (STPP) fibers. the incorporation of shrinkage-mitigating materials effectively reduces shrinkage strain, minimizing the risk of cracking. Test results show that the examined fiber-reinforced self-consolidating concrete (FRSCC) mixtures achieve adequate workability and maintain low shrinkage, limited to 600 μ strain after 224 days. However, a high content of expansive additive (EA), specifically at 10% by mass of the binder, can lead to excessive early-age expansion, resulting in microcracking and a decrease in mechanical properties. In contrast, the FRSCC mixture with 5% EA and 0.5% shrinkage-reducing admixture (SRA) by mass of binder, known as the 5EA0.5SRA mixture, exhibited superior mechanical properties, achieving a compressive strength of 50 MPa and a modulus of elasticity of 36 GPa.

I.2.5.1. Types of hybrid fibers in concrete

I.2.5.1.1. Dual fiber systems

- Micro and macro fibers:

Microfibers (diameter \leq 0.5mm): Primarily used to control plastic shrinkage cracking and improve density, porosity, and overall durability. They work from the moment of mixing to prevent microcracks during curing.

Macro Fibers (diameter $>$ 0.5mm): These fibers provide structural reinforcement after cracks have occurred, helping to prevent crack propagation. They are particularly effective in applications like pavements and slabs where load-bearing capacity is essential. The combination of these two types ensures both early-age crack control and post-cracking performance [Figure I. 12](#)

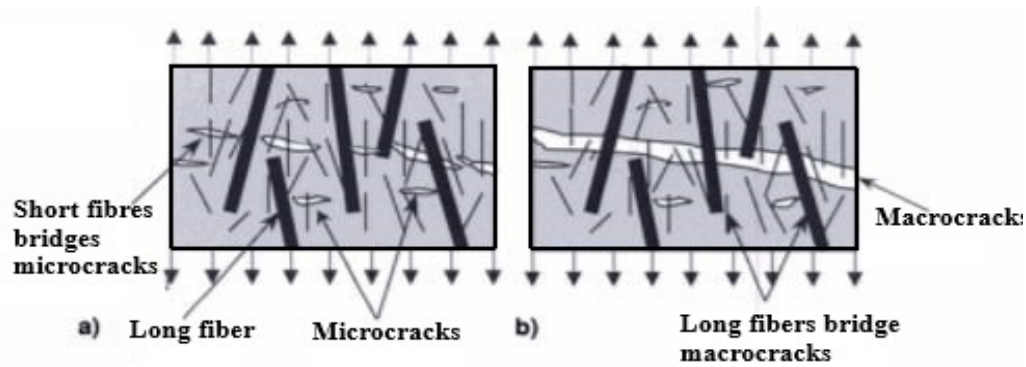


FIGURE I. 12. MICRO AND MACRO FIBERS

In the study conducted by (Bao,L et al, 2024), the mechanical properties of hybrid steel fiber-reinforced concrete (HSRC) with low fiber content were investigated, specifically focusing on both micro and macro fibers. The findings demonstrated that the inclusion of hybrid steel fibers led to enhancements in the performance and toughness of the concrete during the pre-peak phase. Additionally, measurements obtained through Digital Image Correlation (DIC) indicated that a higher replacement rate of short straight steel fibers (SSSF) was associated with a longer length of primary cracks for a given crack width.. Additionally, the results demonstrated that the inclusion of micro-straight steel fibers (mSF) and macro hooked-end steel fibers (MHF) significantly enhanced both the axial compressive strength and the splitting tensile strength of the concrete.

In the article by (Dong, et al., 2024), the authors investigated the self-heating curing process and its influence on the self-sensing properties of ultra-high performance concrete (UHPC) with hybrid stainless steel wires and steel fibers. They found that the self-heating curing method significantly improved the mechanical properties and durability of UHPC. Additionally, the study presents an innovative demonstration showing that the self-heating curing process can impart enhanced and consistent self-sensing sensitivity to hybrid stainless steel wire (SSW) and steel fiber-reinforced UHPC. This approach enables the rapid creation of multifunctional smart infrastructures with capabilities such as structural health monitoring, snow and ice melting, and indoor heating.

- Steel and synthetic fibers:

Steel Fibers: Known for their high tensile strength and ability to bridge cracks, steel fibers improve toughness and impact resistance.

Synthetic Fibers (like polyester): These fibers enhance ductility and reduce shrinkage cracking. The combination of steel and synthetic fibers can lead to significant improvements in both tensile strength and durability, making them suitable for various structural applications. In the study by (Patil & Prakash, 2024) the impact of adding macro-synthetic Polyolefin (PO) and hybrid steel-PO fibers on the behavior of square concrete columns reinforced with Glass Fiber Reinforced Polymer (GFRP) rebars under eccentric compression was investigated. The test results showed that specimens

reinforced with hybrid fibers exhibited better energy absorption and strength compared to those reinforced solely with macro-synthetic fibers. Moreover, they demonstrated improved post-peak performance under eccentric compression. The inclusion of fibers enhanced the load-carrying capacity of the GFRP-reinforced columns and effectively prevented full spalling of the concrete cover. Additionally, the fiber-reinforced specimens displayed increased deformability factors in comparison to control columns without fiber reinforcement.

In their study, (Guo, et al., 2021) examined the effects of combining steel and polypropylene fibers on high-strength concrete (HSC) through bending, quasi-static, and dynamic splitting tensile tests. The results indicated that the bending and quasi-static splitting tensile strengths of HSC reinforced with polypropylene fibers improved only when the fiber volume fraction reached 0.22%. Conversely, HSC reinforced with steel fibers showed higher bending strength, although a slight decrease in quasi-static splitting tensile strength was observed when the steel fiber volume exceeded 2.0%. However, the use of an optimal combination of steel and polypropylene fibers further improved both bending strength and quasi-static splitting tensile strength. The analysis of toughness factors, including the toughness ratio, toughness index, and energy dissipation, demonstrated that steel fibers significantly enhanced the toughness of HSC, while polypropylene fibers had a more modest effect. The most effective bending toughness was achieved when 0.12% polypropylene fibers were paired with 2.0% to 3.0% steel fibers. Specifically, a mix of 2.5% steel fibers and 0.12% polypropylene fibers produced the best dynamic and quasi-static splitting tensile toughness in HSC.

1.2.5.1.2. Triple fiber systems

- Hybrid steel and hybrid synthetic fibers:

This system integrates multiple fiber types, including steel fibers and various synthetic fibers such as polypropylene and polyester. The rationale for this combination is to leverage the unique advantages of each fiber: steel fibers contribute high tensile strength and effective crack bridging, while synthetic fibers enhance ductility, minimize shrinkage, and improve overall toughness. The study by (Kazemian & Shafei, 2022) investigates the formulation of hybrid fiber-reinforced concrete (FRC) mixtures that utilize low dosages of three synthetic fibers: polypropylene (PP), alkali-resistant (AR) glass, and polyvinyl alcohol (PVA) fibers. The results demonstrate that the incorporation of both micro and macro fibers significantly enhances the mechanical properties of the concrete, particularly in terms of compressive strength, splitting tensile strength, and flexural strength.

Research indicates that employing a combination of these fibers can result in superior mechanical properties, such as increased toughness and reduced crack propagation, compared to using single fiber types alone. The performance benefits of this hybrid approach are especially pronounced in applications that demand high durability and impact resistance.

I.2.5.2. Advantages of hybrid fiber reinforced concrete

I.2.5.2.1. Enhanced mechanical properties

- Strength and toughness

Hybrid fiber systems significantly improve the compressive strength, flexural strength, and toughness of concrete. For instance, the combination of steel fibers (providing tensile strength) with synthetic fibers (improving ductility) leads to superior energy absorption capabilities under load conditions .

- Crack resistance

The dual action of micro and macro fibers allows for effective crack bridging at different stages. Microfibers can control early-age shrinkage cracks, while macrofibers help manage larger cracks, thus providing a multi-level reinforcement approach .

I.2.5.2.2. Synergistic effects

The interaction between different types of fibers can produce a synergistic effect that enhances the overall performance beyond what each fiber could achieve individually. This phenomenon allows for optimized performance in terms of flexibility, ductility, and resistance to cracking.

I.2.5.2.3. Improved durability

Hybrid fiber systems can enhance the durability of concrete against environmental factors such as freeze-thaw cycles and chemical attacks. For example, synthetic fibers can provide resistance to water penetration, while steel fibers contribute to structural integrity.

I.2.5.2.4. Versatility in applications

HyFRC is suitable for various applications, including pavements, structural repairs, and precast elements due to its enhanced properties. The ability to tailor fiber combinations allows for specific performance characteristics needed for different environments .

I.2.5.3. Disadvantages of Hybrid Fiber Reinforced Concrete

I.2.5.3.1. Cost implications

The use of multiple types of fibers can increase material costs compared to traditional concrete mixes. Steel fibers, in particular, may contribute to a higher carbon footprint during production, which raises sustainability concerns .

1.2.5.3.2. Workability issues

Excessive amounts of steel fibers (beyond optimal dosages) can lead to workability challenges in the concrete mix. This can make the mixing process more difficult and may require adjustments in the formulation to maintain flowability .

1.2.5.3.3. Complexity in mix design

Designing a hybrid fiber mix requires careful consideration of the types and proportions of fibers used to achieve the desired mechanical properties without compromising workability or other performance metrics. This complexity can pose challenges during the mixing and application processes .

1.2.5.3.4. Potential for fiber debonding

In some cases, if not properly integrated into the matrix, there may be issues with fiber debonding or pull-out during loading conditions. Ensuring adequate bonding between fibers and the cement matrix is crucial for maximizing performance

I.3. Sand concrete

I.3.1. Definition

Sand concrete is composed of sand, fine additives, cement, and water. Based on this fundamental composition and to meet the needs of specific applications, other specific additives may be considered: gravel, fibers, admixtures, and so on. This definition is quoted from the book "Sand Concrete, Sablocrete" ([Sablocrete, 1994](#)).

I.3.2. Specificity of sand concrete

According to the NF P 18-500 standard ([AFNOR, 1995](#)), sand concrete differs from traditional concrete by a high dosage of sand(s), the absence or low dosage of gravel and the incorporation of addition(s). Sand concrete differs from mortar in its composition — the mortar is generally high in cement and does not systematically include an addition — and especially in its intended use: sand concretes are essentially intended for traditional concrete uses.

I.3.3. Constituent materials

I.3.3.1. Sand

The term "sand" refers to aggregates with dimensions ranging from 0 to 5 mm, excluding fillers. It can be natural alluvial or quarry sand derived from crushing massive or detrital rock. No specific granular criteria are inherently required to produce sand concrete: fine sand (like dune sand), medium

or coarse alluvial sand, or even crushed sand can all be used. The strength of sand concrete depends on the grain size of the sand and its fines. The higher the natural fines content in the sand, the more water it absorbs, resulting in an automatic reduction in concrete strength (Sablocrete, 1994) .

I.3.3.2. Fines of addition

Fine additives, also known as fillers, are mineral materials, natural or artificial, which act through their particle size ($D < 0.08$ mm) to enhance the compactness of sand concrete. They are used to fill voids and increase the density of the concrete, thereby reducing the demand for cement, which is costly. Depending on their nature and fineness, fillers improve the workability and strength of the concrete. The primary distinction between conventional concrete and sand concrete lies in the different particle size distributions of the aggregates used. In conventional concrete, the macro voids created by the largest elements, which are the gravel (10 to 20 mm), are filled with sand, and the voids within the sand are filled with fine cement particles to achieve the desired concrete density (Sablocrete, 1994) and (Guendouz, 2017).

This correlation (1) between the need for fillers and the dosage of cement is expressed by the well-known rule of:

$$C = 550/\sqrt[5]{D} \text{ OR } C = 700/\sqrt[5]{D} \text{ (ACCORDING TO THE USE OF CONCRETE)} \quad (1)$$

Table I. 3, providing the minimum cement dosage based on the diameter (D) of the aggregate used.

TABLE I. 3. RELATION BETWEEN GRANULARITY AND CEMENT DOSAGE.

Granularity	$\sqrt[5]{D}$	$550/\sqrt[5]{D}$	$700/\sqrt[5]{D}$	
0/25	1.904	290	370	Concrete
0/20	1.821	300	385	
0/16	1.741	315	400	
0/8	1.516	360	460	
-----0/6.3-----	-----1.445-----	-----380-----	-----480-----	
0/4	1.320	415	530	Mortar
0/2	1.149	480	610	
0/1	1.000	550	700	

The shape of the grains and the geological nature of the fillers affect the amount of water required to obtain a workable mix. Thus, fillers with spherical grains, such as limestone fillers, require less water than those with angular grains, such as silica fillers, and consequently, ensure better compactness in the hardened mix (Guendouz, 2017).

1.3.3.2.1. Limestone fillers

Limestone filler, a finely ground substance, is commonly added to concrete as a mineral supplement due to its distinct characteristics that greatly enhance the overall performance of the concrete. Its particles are less than 80 μm , and have a specific gravity of around 2750 kg/m^3 . This material helps improve the properties of sand concrete in both its fresh and hardened states. Adding limestone filler to concrete improves its workability, minimizes bleeding, and enhances the early strength of concrete. The presence of limestone filler leads to shrinkage in sand concrete if plasticizers are not included (Ladjel, et al., 2022). Studies conducted recently suggest that using limestone fillers, in concrete is both eco-friendly and cost effective (Hadjoudja, et al., 2021).

1.3.3.2.2. Silica fume

Silica fume is a byproduct generated during the production of silicon or silicon alloys, with a SiO_2 concentration and minimal carbon content. This material consists of spherical particles of amorphous silicon dioxide with an average diameter of about 0.1 μm and a specific surface area ranging from 20 to 25 m^2/g . It's characterized by its fine particle size and excellent bonding properties, which enhance the strength of concrete. Its application improves the connection between aggregate and cementitious matrix, resulting in decreased permeability (Alla, et al., 2021).

Silica fume is highly regarded as an effective material in enhancing the mechanical properties of concrete, such as increasing compressive and tensile strength (Hadjoudja, et al., 2021). Adding silica fume in amounts ranging from 7% to 15% relative to the cement mass enables concrete to achieve high physical and mechanical properties.

1.3.3.2.3. Slag

Slag is a mineral residue formed when slag from iron ore smelting in blast furnaces rapidly cools. These residues consist of a mix of calcium oxide (CaO), silicon dioxide (SiO_2), and magnesium oxide (MgO). Slag cements provide improved chemical resistance to aggressive environments such as sulfated water and marine environments, contributing to the durability of concrete (Guendouz, 2017). Slag can be used as a partial substitute for natural sand in concrete, enhancing its rheological and mechanical properties. Substituting natural sand with slag by up to 30% improves the ease of workability and mechanical characteristics of concrete. Incorporating slag into concrete presents an important economic and technical option that helps preserve natural resources and reduce environmental impact (Dask & Patro, 2018).

I.3.3.2.4. Fly ash

Fly ash, a fine powdery byproduct generated when pulverized coal is burned in power plants, is gathered from the flue gas through precipitators or bag filters. In the field of civil engineering, fly ash is commonly used as a supplementary cementitious material (SCM) in concrete production. It exhibits pozzolanic reactivity, meaning it reacts with calcium hydroxide ($\text{Ca}(\text{OH})_2$) in the presence of water to form additional cementitious compounds. This enhances the strength and durability of concrete. Incorporating fly ash reduces the permeability of concrete, making it less susceptible to water penetration and reducing its porosity (Liu, et al., 2023). This is crucial for long-term durability. A previous study indicated that concrete, with a fly ash content ranging from 30% to 75%, gains strength as time progresses (Zhao, et al., 2024).

I.3.3.3. Cement

Cement is a finely ground product obtained from cooling clinker, a blend of calcium silicates and aluminates heated to a fusion temperature between 1450 and 1550 °C. Cement has the property of hydrating and hardening in the presence of water. This hardening process is caused by the hydration of mineral compounds, such as calcium silicates and aluminates.

As with conventional concrete, the cement used for the production of sand concrete complies with the NF P 15-301 standard. The selection of cement is based on its strength class, hydration characteristics, environmental aggressiveness and more generally the composition of the concrete and its intended use (Sablocrete, 1994).

I.3.3.4. Water

The water used for the production of sand concrete complies with the NF P18-303 standard. Effective water includes, in addition to mixing water, a non-negligible amount of water brought in by additives, admixtures, and other additions, and especially by the sands (Sablocrete1994).

I.3.3.5. Admixture

Admixtures are chemical products used in concrete to modify the properties of concrete to which they are added in small proportions (about 5% of the cement weight). The different types of admixtures include:

- Water-reducing admixtures (Plasticizers).
- Super-plasticizing admixtures (high-range water reducers).
- Accelerating or retarding admixtures.
- Viscosity-modifying agents (water retainers).
- Air-entraining admixtures.

I.3.3.6. Other additions

I.3.3.6.1. The fibres

Fibers are primarily used to reduce early-age shrinkage: dosage and type are crucial parameters to ensure the effectiveness of this addition. In most cases, organic fibers such as polypropylene, polystyrene, etc., are used to counteract the effects of setting shrinkage and prevent resulting cracking. If enhanced ductility is desired, steel fibers or amorphous cast iron fibers can be used (Sablocrete, 1994).

I.3.3.7. Gravel

It is considered that a sand concrete can contain a certain percentage of gravel and still maintain its classification as sand concrete. Indeed, as long as the gravel is dispersed within the sand and does not form a structured framework, the behavior remains the same; adding gravel in small amounts can significantly improve certain characteristics such as creep, shrinkage, strength, and workability. In practical terms, sand concrete is typically recognized as long as the mass ratio G/S (gravel to sand) remains below 0.70 ($G/S < 0.70$) (Sablocrete, 1994).

I.3.3.8. Pigments (colorants)

The colorants typically used in traditional concretes can also be employed for certain applications of sand concretes. However, they require special care in homogenization and appropriate formulation of the sand concrete to maintain color stability over time (Sablocrete, 1994)

I.3.4. Essential properties

I.3.4.1. General properties

I.3.4.1.1. Particle size (granulometry) - workability

One of the particularities of sand concretes is the need for more water than traditional concretes: this is reflected in the values of the W/C (water/cement) ratio consistently above 0.5, this ratio generally being between 0.6 and 0.7. This particularity is due to a larger specific surface area of the mixture: moreover, if we consider not only the W/C ratio but the W/C + A ratio (A = Addition of fines), we obtain values similar to traditional concretes. The Particle size (granulometry) of the sand will also affect the water requirement: the richer the sand is in coarse elements, the better the workability improves. This is reflected in a relationship between ‘fineness modulus’ and workability.” Figure I.13 (Sablocrete, 1994)

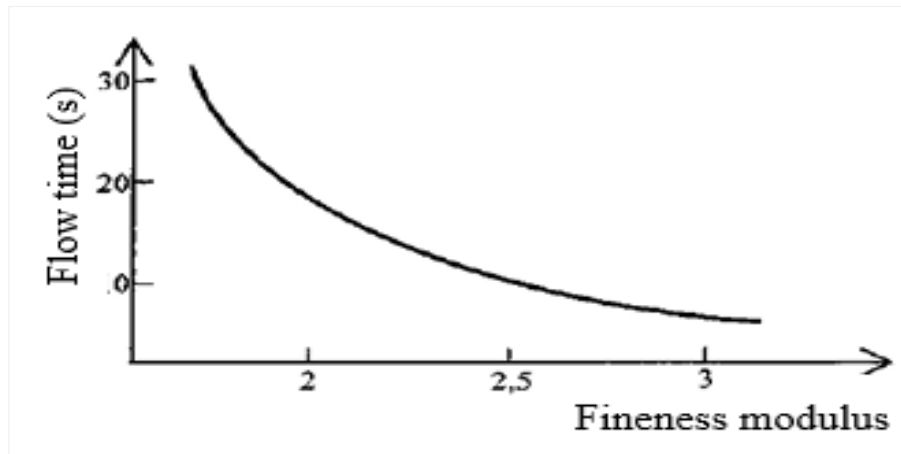


FIGURE I. 13. FLOW TIME AS A FUNCTION OF FINENESS MODULUS

1.3.4.1.2. Particle size (granulometry) – strength

At a constant cement dosage, the resistance can vary depending on several parameters, particularly:

- Fineness of the addition

The finer the addition, the more effective it is in terms of increasing compactness (and thus increasing resistance); this result is valid regardless of the sand's grain size. It is observed with fine limestones on both alluvial sand and dune sand [Figure I. 14 \(Sablocrete, 1994\)](#)

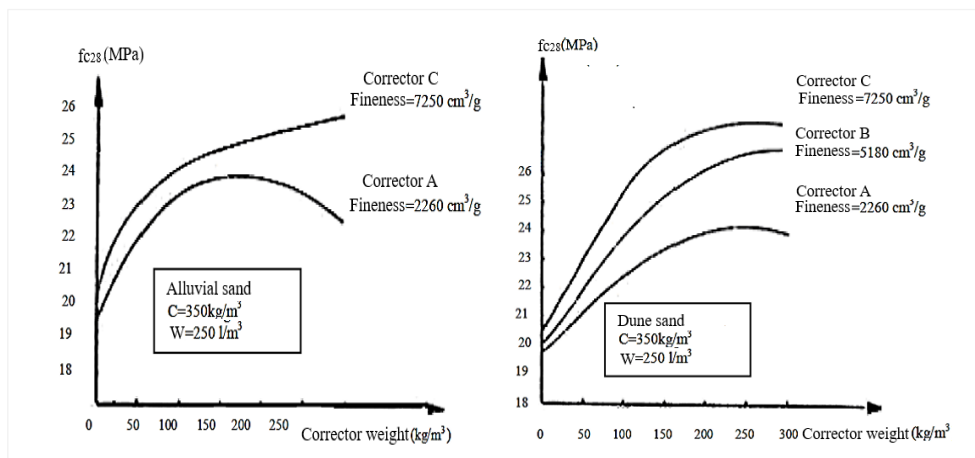


FIGURE I. 14. EFFECT OF DOSAGE AND FINENESS OF ADDITION ON STRENGTH

- Nature of the addition

At the same dosage, [Figure I. 15](#) shows the extreme diversity in the level of performance achieved depending on the type of filler: while the addition of fines systematically improves resistance, this gain is indeed very variable. For example, with a water-to-cement ratio (W/C) of 0.82 for a control sample (without fines) at 32 MPa, the resistance varies, with the addition of fines, from 34 to 53 MPa, depending on the type of fines added.

The difference is even more considerable when maintaining constant workability. The most effective fillers are those that are hydraulically active and also result in a reduction in water demand. It should

be noted that these results were obtained without any additives, and the use of a plasticizer would further enhance the effectiveness of certain hydraulically active fillers that require a significant amount of water. (Sablocrete, 1994)

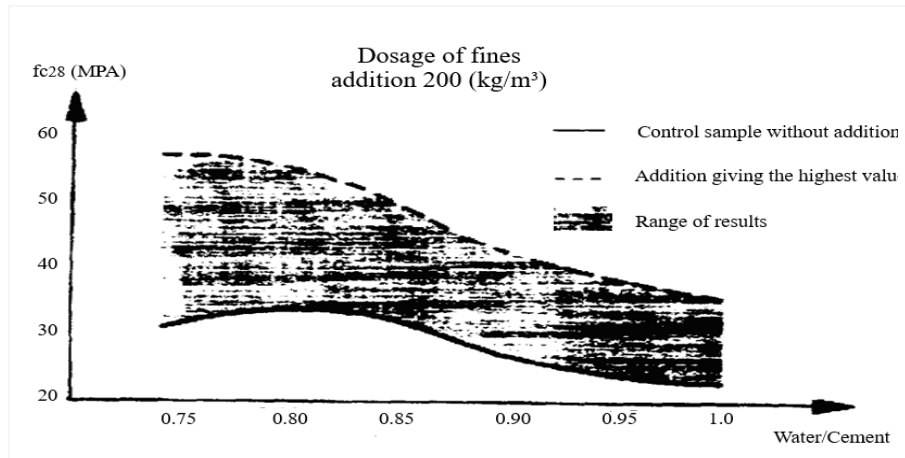


FIGURE I. 15. INFLUENCE OF THE NATURE OF THE ADDITION ON THE LEVEL OF RESISTANCE

- Maximum aggregate size D_{max} (0/D)

For the same water-to-cement ratio (W/C), it can be observed Figure I. 16 that the effect of the maximum aggregate diameter (D_{max}) is relatively minor and, in any case, not unfavorable to sands. The only issue lies in the significantly different workability of the concretes: highly workable in the case of 0/20, whereas it will be of prefabrication type in the case of sand.

At the same cement dosage Figure I. 16, but with different W/C ratios, the differences become much more significant. With identical workability, much more water will be required in the case of sands, which will result in a decrease in resistance. Again, this decrease can be minimized by using a water-reducing plasticizer (Sablocrete, 1994)

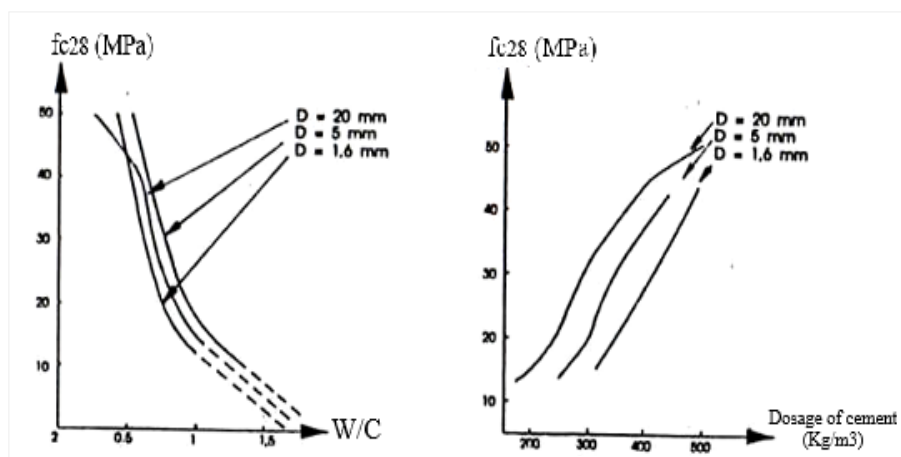


FIGURE I. 16. EFFECT OF GRANULARITY ON RESISTANCE

I.3.4.2. Specific properties

I.3.4.2.1. Adhesion of rebar

Sand concrete offers good adhesion with rebar, similar to traditional concrete, regardless of its granularity. Sablocrete (1994) found that adhesion with dune sand is superior to that with coarse sand. This makes it suitable for use as structural concrete, competing with traditional concrete (Rihia, 2020).

I.3.4.2.2. Shrinkage and creep (deformation)

Shrinkage and creep tests were conducted on sand concrete in comparison with traditional concrete.

▪ Shrinkage

As for shrinkage, the tests Figure I. 17 showed that when the material was isolated from the external environment (sealed conditions), the autogenous shrinkage of sand concrete was similar to that of traditional concrete. However, when the concrete was allowed to dry (unsealed conditions), the shrinkage of sand concrete could reach values twice that of traditional concrete Figure I. 17. This phenomenon was explained and is likely related to the different distribution and size of voids between the two materials.

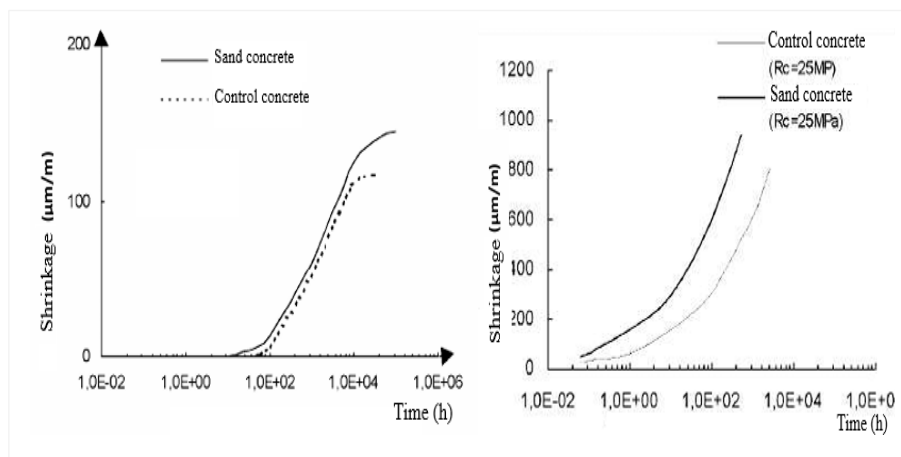


FIGURE I. 17. SHRINKAGE EVOLUTION IN SAND CONCRETE

▪ Creep (deformation)

In terms of creep, a similar phenomenon is observed Figure I. 18, likely related to the structure of the material, which is further confirmed by the significantly different values of the modulus of elasticity between sand concrete and traditional concrete (the modulus of sand concrete being lower).

It should be noted, however, that these comparative results were obtained at a compressive strength level of 25 MPa, and specifically for creep, a more resistant sand concrete does not exhibit the same behavior: it has lower creep, similar to that of traditional concrete.

Tests have confirmed this hypothesis [Figure I. 18](#), as increasing the compressive strength from 25 to 50 MPa reduces the creep by a factor of 5. At the same level of resistance, in this case 50 MPa, the creep of sand concrete is only 20% higher than that of traditional concrete of the same strength level.

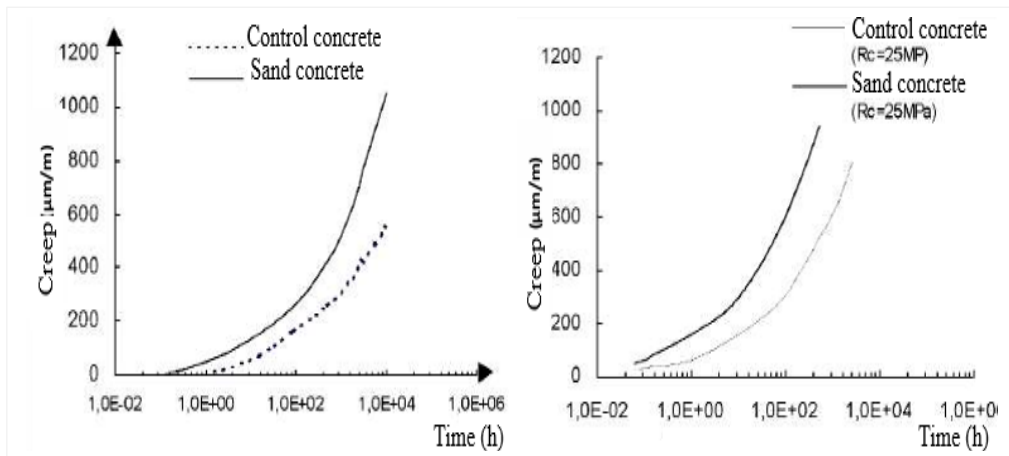


FIGURE I. 18. EVOLUTION OF SAND CONCRETE CREEP

1.3.4.2.3. Durability

Conventionally, the durability of concrete is linked to its capacity to interact with the external environment. Hence, parameters such as porosity, geometric arrangement of pores, and permeability are primary physical parameters affecting durability. Similarly, internal phenomena like alkali-silica reaction or delayed sulfate attack are deterioration processes accelerated by hydraulic exchanges with the external environment.

The resistance of concrete to these exchange phenomena also depends on its environmental exposure. Therefore, the estimation of durability generally involves one or more of the following tests, depending on the anticipated environmental conditions (urban, mountainous regions, marine environments, aggressive atmospheres):

- Air and water permeability
- Freeze - thaw resistance
- Carbonation
- Chloride ion penetration

These durability tests, aimed at qualifying concrete against exogenous or internal physicochemical attacks, are generally accelerated tests that quickly provide comparative information.

In general, sand concretes are more porous than traditional concretes. While they have more voids, the size and number of these voids differ from those in traditional concrete; they are more numerous, smaller, and more mono-dimensional ([Sablocrete, 1994](#)).

1.3.4.2.4. Washout resistance

Washout occurs in fresh concrete that is submerged and results in a loss of cohesion between the coarser and finer elements of the concrete, with the latter being carried away by water. To mitigate this phenomenon, which tends to produce concrete with no cohesion or compactness and thus unsuitable for its intended use in underwater placements, anti-washout admixtures can be used.

However, it is also possible to refine the composition, particularly the granulometry. Specifically, sand concretes, due to their fineness and better homogeneity, appear to resist washout effectively. This capability has indeed been observed in underwater sand concrete pouring projects (such as filling cavities under bridge piers), and it has also been demonstrated in laboratory tests (Sablocrete, 1994).

1.3.4.2.5. Segregation

The cohesion, homogeneity, and good workability of sand concrete provide a smooth surface finish by eliminating the problem of segregation (Rihia2020 ◌).

1.3.4.2.6. Microstructure SEM of sand concrete

Observation of hardened sand concrete fragments using a scanning electron microscope (SEM) allows for a description of the material as being free of significant cracks, with good overall homogeneity and strong adhesion between the cement paste and sand grains Figure I. 19.

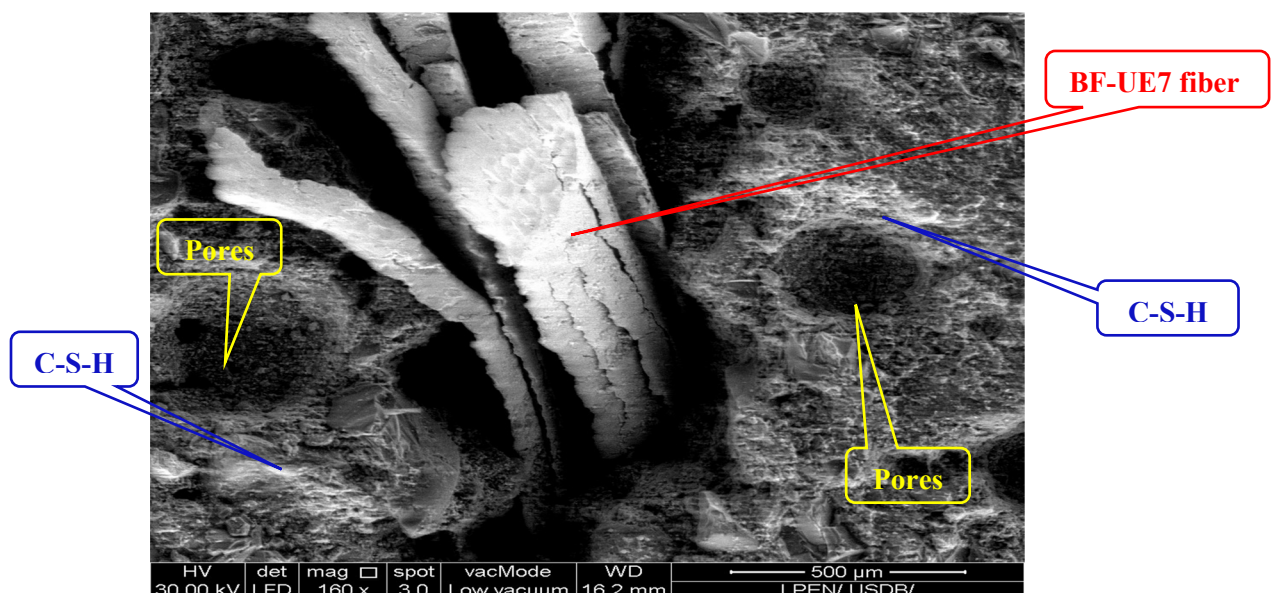


FIGURE I. 19. SEM – BF-UE7 FIBER REINFORCED SAND CONCRETE

I.3.5. High flow sand concrete

I.3.5.1. Definition

High Flow Sand Concrete (HFSC) is a type of sand concrete known for its effortless flow, under its weight while maintaining cohesion. It primarily consists of sand as the main aggregate, with little to no coarse aggregate. The flowability of this concrete is enhanced using additives such as superplasticizers, which allow the mix to fill complex molds without the need for mechanical vibration.

I. 3.5.2. Key properties

- *High flowability*: The concrete can flow and fill molds easily while maintaining a uniform mix.
- *Uniformity*: Provides an even distribution of fine aggregates without segregation.
- *Sand use*: Coarse aggregate is largely or entirely replaced by sand.
- *Ease of use*: Ideal for applications requiring pouring into narrow spaces or complex shapes.

I. 3.5.3. Applications of HFSC

High flow sand concrete is used in applications that require high workability and ease of pouring, such as:

I. 3.5.3.1. Complex architectural elements

High flow sand concrete is ideal for intricate architectural designs and structures that have complex shapes and details. Its high flowability allows it to fill molds with intricate patterns and textures, ensuring that all the fine details are captured accurately.

Examples: Decorative facades, sculptural elements, and detailed ornamental features in buildings. This concrete is also useful for creating complex geometries in precast concrete elements [Figure I.20](#)



FIGURE I. 20. COMPLEX ARCHITECTURAL ELEMENTS

I. 3.5.3.2. Structures with dense reinforcement

When concrete structures have a high density of reinforcement bars (rebar), such as in heavily reinforced columns or slabs, the mix must be able to flow around and fully encapsulate the

reinforcement without leaving voids. High flow sand concrete achieves this by easily flowing through tight spaces around the reinforcement.

Examples: High-rise building columns, thick slabs, and structural elements with closely spaced rebar
Figure I. 21 This ensures that the concrete effectively bonds with the reinforcement and maintains structural integrity.



FIGURE I. 21. STRUCTURAL ELEMENTS WITH CLOSELY SPACED REBAR

I. 3.5.3.3. Projects requiring precise surface finishing

For projects that demand a high-quality surface finish, such as smooth floors or fine-textured surfaces, high flow sand concrete is beneficial. Its consistent and smooth application helps achieve a fine surface finish with minimal surface defects. Examples: Smooth concrete floors **Figure I. 22**, polished surfaces, and architectural concrete elements where aesthetic quality and surface smoothness are crucial. This application is especially valuable in high-end residential or commercial projects where the visual appearance is a significant factor.



FIGURE I. 22. SMOOTH CONCRETE FLOORS

I. 3.5.3.4. Shotcrete applications

High flow sand concrete is well-suited for shotcrete applications **Figure I.23** due to its superior flowability and cohesive properties. This type of concrete enhances the spraying process by ensuring consistent coverage on complex and curved surfaces, reducing the risk of voids, and providing a strong bond between the cement paste and the substrate. Its ability to flow easily allows for efficient application and a high-quality finish.

Examples:

- Used for reinforcing and stabilizing walls, tunnels, and other structural elements.

- Effective in repairing and restoring damaged or aged concrete surfaces.



FIGURE I. 23. SHOTCRETE APPLICATIONS

I.3.5.4. Advantages and disadvantages of HFSC

I.3.5.4.1. Advantages

- **Cost-Effectiveness:** High flow sand concrete is more economical because it primarily uses sand as the aggregate, which is generally less expensive than coarse aggregates like gravel or crushed stone.
- **Improved Flowability:** Its excellent flow properties allow it to easily fill complex molds and cover intricate details without requiring extensive mechanical vibration.
- **Enhanced Surface Finish:** Provides a smooth and high-quality finish, making it suitable for applications where aesthetic appearance is important.

I.3.5.4.2. Disadvantages

- **Lower Strength:** The reduction or absence of coarse aggregates can result in lower compressive strength compared to conventional concrete mixes.
- **Potential for Shrinkage:** High flow sand concrete may be more prone to shrinkage and cracking due to the high water-cement ratio and the absence of coarse aggregate.

I.4. Conclusion

This chapter reviewed the literature on industrial waste, its recycling, and its use in civil engineering. Industrial waste includes various types, such as metallic waste (metallic shavings, metallic powder, and scraps) and synthetic fibers (polyester, polypropylene, carbon, and aramid fibers). Recycling industrial waste offers a sustainable solution that reduces environmental pollution.

Sand concrete was explored as a cost-effective material that uses sand as its primary component. Its properties can be improved by incorporating industrial waste. High-flow sand concrete, reinforced with mono fibers or hybrid (dual and triple) fibers, offers easy placement, superior quality, and enhanced structural performance by increasing compressive strength, reducing cracks, and providing economic benefits.

In summary, valorizing industrial waste presents effective solutions for improving the quality of construction materials while opening new avenues for future research focused on sustainability in civil engineering.

Chapter II

**Methodology and experimental
program for HFSC mix design**

Chapter II: Methodology and experimental program for HFSC mix design

II.1. Introduction

In this chapter, the materials used in reference sand concrete and mixed fiber-reinforced sand concrete (using three types of fibers) are explored, and their physical and chemical compositions, properties, and advantages are examined.

The methodology adopted to study the mix design of sand concrete is described, as well as the Norms and specimen followed to determine the physical, mechanical, chemical, physicochemical, and microscopic SEM properties of the mixtures.

A total of 23 different mixtures were investigated, utilizing three types of fibers. Each type of fiber was used to reinforce sand concrete separately, with five varying proportions (0.25%, 0.50%, 1.00%, 1.50%, 2.00%). After identifying the best mixture based on mechanical and physical properties, two types of fibers were then mixed together, followed by combining all three types of fibers.

II.2. Constituents of the mixes

In this study, the following materials were utilized for the production of sand concrete reinforced with mixed fiber:

I.2.1. Sand (S)

For the mix design of sand concrete, Class 0/2 dune sand sourced from a quarry located in Oued Z'hor, Skikda, Algeria [Figure II. 1](#) was used. Its physical properties are detailed in [TableII.4](#).



FIGURE II. 1. SAND CLASSE 0/2 – OUED Z'HOR

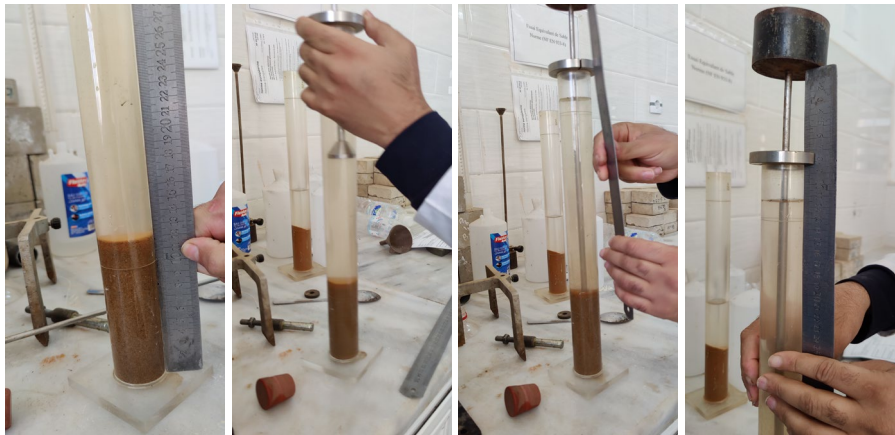
TABLE II. 1. PHYSICAL PROPERTIES OF SAND

Designation	Result
Sand Equivalent (Cleanliness) (%)	78.80
Methylene Blue Value	0.6
Fineness Modulus	2.39
Bulk Density (g/cm ³)	1.46
Absolute Density (g/cm ³)	2.47

The physical characteristics of sand concrete are given in the [Table II. 1](#) above. The values of these properties were determined using a number of laboratory tests to characterize the sand. The experiments comprised Sand Equivalent (Cleanliness), Methylene Blue Value, Particle Size (Granulometric) Analysis, Fineness Modulus, Bulk Density, and Absolute Density measurements. In the following sections of this study, we will delve into detailed explanations of each experiment conducted.

I.2.1.1. Sand equivalent (cleanliness)

The "Sand Equivalent Piston PS" [Figure II. 2](#) test (NF EN 933-8) is employed to determine the degree of cleanliness in sands. This test separates the sand from very fine particles that flocculate to the top of the test cylinder during washing. It is conducted exclusively on the 0/2 mm sand fraction, and the PS value must exceed 60 or 65, depending on the specific application.

**FIGURE II. 2.** SAND EQUIVALENT PISTON PS

$$PS = 100 \frac{h1}{h2}$$

h1: Clean sand + Fine elements,

h2: Clean sand

$$PS = 78.80\%$$

So; $70 \leq 78.80 \leq 80$; "Clean sand" with a low percentage of clay fines, perfectly suitable for high-quality concrete.

I.2.1.2. Methylene blue value

The "Methylene blue" [Figure II. 3](#) test (NF EN 933-9) is utilized to determine the cleanliness of sand. It is performed on the granular fraction 0/2mm of sands or, on fillers (0 / 0.125 mm) found within filler sand, gravel or all in aggregate. The objective is to identify the existence of clay fines and measure their concentration.

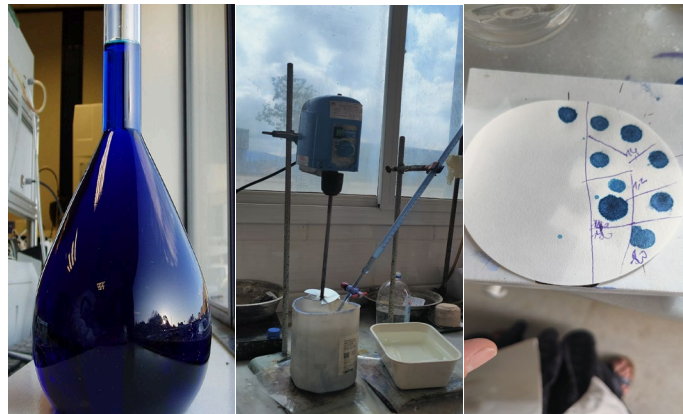


FIGURE II. 3. METHYLENE BLUE VALUE

After the test, it was found that:

$$V_{BS} = 0.6 ; 0.2 \leq V_{BS} \leq 1.5 \text{ Sandy clay loam, water-sensitive}$$

I.2.1.3. Particle size (granulometric) analysis

Particle size analysis (NF EN 933-1), determines the size and weight percentage of the different grain types, in a sample. This technique can be used for all aggregates sized 90 mm or smaller excluding fillers [Figure II. 4](#)



FIGURE II. 4. PARTICLE SIZE ANALYSIS

The results of the refusals are shown as a percentage of the initial dry mass and can be presented based on the findings in [Table II. 2](#)

TABLE II. 2. PARTICLE SIZE OF SAND 0/2 MM ACCORDING TO NF EN 933-1

Sieve (mm)	Partial retained mass (g)	Cumulative retained mass (g)	Cumulative retained (%)	Cumulative passings(%)
4.0	0.00	0.00	0.00%	100%
2.8	0.19	0.19	0.04%	99.96%
2.0	3.73	3.92	0.78%	99.22%
1.0	5.48	9.4	1.88%	98.12%
0.5	223.96	233.36	46.67%	53.33%
0.25	225.88	459.24	91.85%	8.15%
0.125	28.85	488.09	97.62%	2.38%
0.063	7.51	495.60	99.12%	0.88%
Pan	3.21	498.81	99.76%	0.24%

I.2.1.4. Fineness modulus

Fineness Modulus (FM) is an empirical calculation used to support the optimization of a sand concrete mix design. It is used to determine ‘degree of uniformity of the grading’. This can create a relationship between grading and consistence and/or the amount of cement or water to fill the voids. An example would be that sand with a high FM will have lower voids between the particles.

According to the (EN 12620) standard, the cumulative percentages of refusals for sieves with openings of 4, 2, 1, 0.5, 0.25, and 0.125 mm are summed. Based on these results, the fineness of our sand has been calculated as follows:

$$FM = \frac{0.78 + 1.88 + 46.67 + 91.85 + 97.62}{100} = 2.39$$

I.2.1.5. Bulk density

Bulk density [Figure II. 5](#) refers to the measure of mass within a specific volume of material. It can be calculated using the following formula:

$$\text{Bulk density} = \frac{\text{Mass}}{\text{Volume}}$$

According to the formula:

$$\text{Bulk density} = \frac{4724 - 3342}{945} = 1.46 \text{ g/cm}^3$$



FIGURE II. 5. BULK DENSITY OF SAND 0/2

I.2.1.5. Absolute density

The absolute density (EN 1097-6) of a material is determined by its mass, per unit volume which reflects the substances density, without accounting for any pores. To calculate this you can utilize a pycnometer [Figure II. 6](#) Follow these procedures:

- Measure the dry mass of the sample (M1): Completely dry the sample and weigh it.
- Fill the pycnometer with water and measure its mass filled with water only (M2).
- Add the dry sample to the pycnometer filled with water and measure the total mass (M3).
- Determine the density of water at the specific temperature (ρ_w).

The absolute density is then calculated using the following formula:

$$\text{Absolute density} = \rho_w \frac{M1}{M1 - (M3 - M2)}$$

According to the formula:

$$\text{Absolute density} = 0.998 \frac{500}{500 - (2110.46 - 1811.60)} = 2.47 \text{ g/cm}^3$$



FIGURE II. 6. ABSOLUTE DENSITY OF SAND 0/2

I.2.2. Cement (C)

Sulphate-resistant cement (SRC), also known as NA 442. CEM I 42.5 N SR3, from the Moukaoum Plus brand - LAFARGE ALGERIE, Algeria [Figure II. 7](#) (TDS. 1). This cement, with a density of 3.1g/cm³ and a Blaine fineness of 3450 cm²/g, underwent detailed chemical analysis as presented in [Figure II. 10](#) and [Table II. 3](#).



FIGURE II. 7. SRC CEMENT

I.2.3. Limestone filler (LF)

The term "Calcium Carbonate (CaCO₃)" is used to refer to the substance commonly known as limestone fillers. In this research, limestone fillers that're commercially available (ALCAL-F15) [Figure II. 8](#) (TDS. 2), with a density of 2.7 g/cm³, were sourced from the El-Kheroub unit of the National Aggregates Company (ENG) in Constantine, Algeria. The chemical properties of the limestone filler are described in [Figure II. 10](#) and [Table II. 3](#).



FIGURE II. 8. LIMESTONE FILLER

I.2.4. Silica fume (SF)

Silica fume, sold as SILTEK POWDER by TEKNACHEM company [Figure II. 9](#) (TDS. 3), in Sidi Bel Abbas, Algeria, was used in the research. This silica fume, with a density of 0.3 g/cm³ and chemical composition outlined in [Figure II. 10](#) and [Table II. 3](#), was incorporated into the study.



FIGURE II. 9. SILICA FUME

TABLE II. 3. CHEMICAL PROPERTIES OF CEMENT, LIMESTONE FILLERS AND SILICA FUME.

Designation	Cement	Limestone Fillers	Silica Fume
CaO	62.28	--	0.50
CaCO ₃	--	99.61	--
SiO ₂	23.20	0.04	95.01
Fe ₂ O ₃	5.40	0.02	1.00
Al ₂ O ₃	4.67	0.03	0.50
MgO	1.70	0.20	1.00
SO ₃	1.70	0.02	0.01
Na ₂ O	0.15	0.05	--

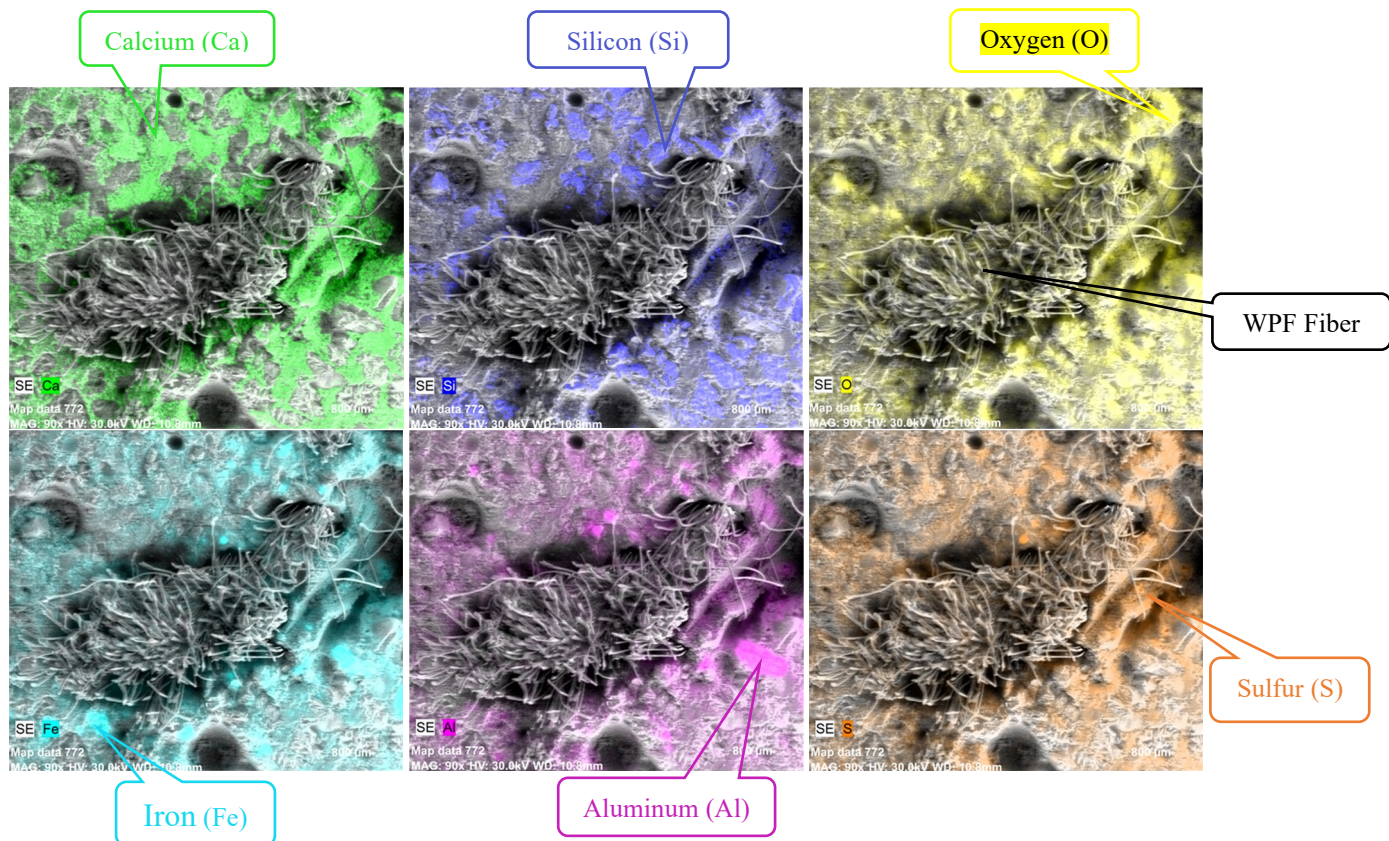
**FIGURE II. 10.** SEM-EDS CARTOGRAPHY OF CHEMICAL PROPERTIES OF CEMENT, LIMESTONE FILLERS AND SILICA FUME

Figure II. 10, illustrates the SEM-EDS cartography of the chemical properties of cement, limestone fillers, and silica fume. This figure shows the spatial distribution of different chemical elements within the studied samples using Scanning Electron Microscopy with Energy Dispersive X-ray Spectroscopy (SEM-EDS). The cartography provides a detailed

understanding of the chemical composition and the interactions of elements within these materials. By analyzing these distributions, the figure helps elucidate the contributions of each component to the enhancement of sand concrete properties. The most significant chemical compositions present will be outlined: **Ca** represents Calcium, **Si** represents Silicon, **O** represents Oxygen, **Fe** represents Iron, **Al** represents Aluminum and **S** represents Sulfur.

I.2.5. Fibers:

To enhance the characteristics of concrete, we have combined three types of fibers: macro metallic fibers, micro metallic fibers, and polystyrene fibers. These fibers were chosen based on their properties, which contribute to the quality of concrete as outlined:

I.2.5.1. Stainless steel fibers (SSF-316L)

The first type, Stainless Steel Shavings Fiber (SSF-316L), was procured from ALEMO, the Algerian National Company for Equipment and Machine Tools, located in El Kheroub, Constantine. These fibers, derived from spare part shavings, underwent sorting and cutting into lengths ranging from 25 to 40 mm and diameters of 0.75 to 2 mm, as illustrated in [Figure II.11](#). The physical and chemical properties of stainless steel 316L are detailed in [Table II. 4](#) and [Table II. 5](#), respectively (TDS. 4).

At ALEMO Company we offer a range of stainless steel options. For our study we decided to use 316L. This choice allows us to concentrate on one type avoiding any mix-ups and ensuring findings. This choice was made because of its acknowledged quality and the higher price of the raw materials. Yet SSF 316L was obtained for free as it was deemed merely metal shavings.



FIGURE II. 11. STAINLESS STEEL FIBERS (SSF-316L)

I.2.5.2. Bronze fibers (BF –UE7)

The second type consists of bronze shaving fibers (BF-UE7) procured from ALEMO, the Algerian National Company for Equipment and Machine Tools, located in El Khroub, Constantine. These fibers originate from the shavings of spare parts produced by cutting bronze rods. They are classified as microfibers due to their dimensions, which range from 6 to 8 mm in length and 0.1 to 0.3 mm in diameter, as shown in [Figure II. 12](#). [Table II. 4](#) and [Table II. 5](#) provide detailed information on the physical and chemical properties of the bronze shaving fibers (BF-UE7), respectively (TDS. 5).

Previously noted ALEMO Company provides many types of bronze shavings. But, to conduct a dependable study we opted for the UE7 variant. This selection was made based on its quality and the expensive cost of the raw materials used. However, BF-UE7 was acquired for free since it was regarded as simply metal shavings.



FIGURE II. 12. BRONZE FIBERS (BF-UE7)

I.2.5.3. Waste polyester fibers (WPF)

The third type differs out from the ones due, to its origin as polyester. These fibers (WPF), sourced from thread remnants utilized in shoe repair work are acquired from cobblers in Skikda, Algeria (TDS. 6).

These fibers are actually over 100 microfibers [Figure II. 10](#) that intertwine and stick together with the wax. They can either be used as macrofibers or be subjected to temperatures exceeding 50°C, leading the wax to melt and disperse them into microfibers, thus altering their diameter from 1 mm to 0.01 mm.

In this research the fibers were maintained in a bonded (interwoven) state in the form of macro fibers with a diameter of 1 mm. The length remained consistent, ranging from 10 to 12 mm as

illustrated in Figure II. 13. The physical and chemical properties of the polyester fibers (Cordonfil No. 6) are detailed in Table II. 4 and Table II. 5 respectively.



FIGURE II. 13. WASTE POLYSTYRENE FIBERS (WPF)

Table II. 4 and Table II. 5 detail the physical and chemical properties of the aforementioned fibers:

TABLE II. 4. THE PHYSICAL PROPERTIES OF FIBERS

Designation	SSF-316L	BF-UE7	WPF
Material	Metals	Metals	Synthetic
Density (g/cm ³)	7.81	8.80	1.38
Length (mm)	25 -- 40	6 – 8	10 -- 15
Diameter/ thickness (mm)	0.75 – 2.0	0.1 -- 0.3	1.0

TABLE II. 5. THE CHEMICAL PROPERTIES OF FIBERS

Designation	SSF-316L	BF-UE7	WPF
Fe	59.50	0.20	--
Cu	0.50	85.00	--
Cr	19.0	--	--
Ni	15.0	2.00	--
C	0.10	--	64.00
Mn	2.00	--	--
Zn	--	5.00	--
S	0.01	0.10	--
Si	0.75	0.01	--
Al	--	0.01	--
H	--	--	6.00
O	--	--	30.00

I.2.6. Water reducer (SP)

The superplasticizer used is of the type "Viscocrete 665", compliant with the EN 934-2 standard (Dupain & Saint-Arroman, 2009). It is a high water-reducing plasticizer for concrete, presented as a light brown liquid. The product "Viscocrete 665" is supplied by Sika-El Djazair. Its detailed characteristics are provided in Table II. 6 (TDS. 7):

TABLE II. 6. THE PROPERTIES OF WATER REDUCER VISCOCRETE665

Properties	Color	Density	pH	Dry extract	Content (Cl-)	Content (Na ₂ O)
Value	Brown liquid	1.085	5±1	32%	≤0.1%	≤0.1%

I.2.7. Water (W)

The water used for mixing is potable water provided from the civil engineering laboratory tap. Table II. 7 details the properties of the water:

TABLE II. 7. THE PROPERTIES OF WATER

Cl (mg/l)	pH	T°	Salinity	TDS (mg/l)	Conductivity (µs/cm)
0.1	7.3	28	0.2	297	541

I.3. Mix design

I.3.1. Experimental program

In the experimental program, high-flow sand concrete was selected as the reference concrete. A comprehensive study was conducted on three different types of fibers, each characterized by unique properties, with fiber content ranging from 0.25% to 2% for each type. No modifications were made to the initial composition of the reference concrete; instead, it was reinforced by adding fibers by mass. After each type was studied individually, the optimal composition for each fiber type was identified. Subsequently, two types were combined, followed by a combination of all three types. The formulations used are outlined in the following Table II. 8

TABLE II. 8. IDENTIFICATION OF THE MIXTURES

Mixtures	Fiber Identification	Fiber percentage
M0	Reference Concrete	0%
Stainless steel fibers type 316L		
M1	HFSC reinforced with 0.25% stainless steel shavings fibers type 316L (SSF-316L) by mass	0.25% SSF-316L
M2	HFSC reinforced with 0.50% stainless steel shavings fibers type 316L (SSF-316L) by mass	0.50% SSF-316L
M3	HFSC reinforced with 0.75% stainless steel shavings fibers type 316L (SSF-316L) by mass	0.75% SSF-316L
M4	HFSC reinforced with 1.00% stainless steel shavings fibers type 316L (SSF-316L) by mass	1.00% SSF-316L
M5	HFSC reinforced with 1.50% stainless steel shavings fibers type 316L (SSF-316L) by mass	1.50% SSF-316L
M6	HFSC reinforced with 2.00% stainless steel shavings fibers type 316L (SSF-316L) by mass	2.00% SSF-316L
Bronze fibers shavings type UE7		
M7	HFSC reinforced with 0.25% Bronze fibers shavings type UE7 (BF-UE7) by mass	0.25% BF-UE7
M8	HFSC reinforced with 0.50% Bronze fibers shavings type UE7 (BF-UE7) by mass	0.50% BF-UE7
M9	HFSC reinforced with 1.00% Bronze fibers shavings type UE7 (BF-UE7) by mass	1.00% BF-UE7
M10	HFSC reinforced with 1.50% Bronze shavings fibers type UE7 (BF-UE7) by mass	1.50% BF-UE7
M11	HFSC reinforced with 2.00% Bronze shavings fibers type UE7 (BF-UE7) by mass	2.00% BF-UE7
Waste Polyester fiber		
M12	HFSC reinforced with 0.25% Waste Polyester Fiber (WPF) by mass	0.25% WPF
M13	HFSC reinforced with 0.50% Waste Polyester Fiber (WPF) by mass	0.50% WPF
M14	HFSC reinforced with 1.00% Waste Polyester Fiber (WPF) by mass	1.00% WPF
M15	HFSC reinforced with 1.50% Waste Polyester Fiber (WPF) by mass	1.50% WPF
M16	HFSC reinforced with 2.00% Waste Polyester Fiber (WPF) by mass	2.00% WPF

Note :

As part of this study, 16 mixtures of high-flow sand concrete (HFSC) were prepared, including the reference mix (M0), stainless steel fiber reinforced HFSC (SSF-316L) with different proportions (M1–M6), bronze fiber reinforced HFSC (BF-UE7) with varying percentages (M7–M11), and waste polyester fiber reinforced HFSC (WPF) with different dosages (M12–M16). Laboratory experiments were conducted to assess the impact of each fiber type on the physical, mechanical, chemical, and physio-chemical properties of concrete to determine the optimal mix.

Based on the results obtained in Chapter III, hybrid (Dual and triple systems) mixtures are being studied, where the best-performing mixes from this initial study are combined to enhance performance and durability, relying on an in-depth analysis of previous findings.

I.3.2. Formwork

The mixture formulation was designed to achieve a compressive strength of 30 MPa with a water-to-cement ratio (W/C) of 0.60, a key factor in producing high-fluidity sand concrete. Utilizing the Sablocrete method ([Sablocrete, 1994](#)), the mix design for sand concrete was developed. Following extensive laboratory testing, minor adjustments were made to the theoretical results, leading to the final values reported for M0.

The reference concrete (M0) consists of high-flow sand concrete without fibers, while 16 additional samples were prepared by incorporating stainless steel shavings fibers (SSF-316L) at proportions of 0.25%, 0.5%, 0.75%, 1.0%, 1.5%, and 2.0%; bronze shavings fibers (BF-UE7) at 0.25%, 0.5%, 1.0%, 1.5%, and 2.0%; and waste polyester fibers (WPF) at 0.25%, 0.5%, 1.0%, 1.5%, and 2.0%. The detailed mix design proportions are presented in [Table II. 9](#)

TABLE II. 9. THE MIXTURES FORMULATION

Mix (kg/m ³)	S	C	FL	SF	W	SP	SSF- 316L	BF- UE7	WPF
Reference concrete									
M0	1267	450	100	50	270	3.6	--	--	--
HFSC reinforced with stainless steel fibers type 316L									
M1	1267	450	100	50	270	3.6	5.34	--	--
M2	1267	450	100	50	270	3.6	10.69	--	--
M3	1267	450	100	50	270	3.6	16.03	--	--
M4	1267	450	100	50	270	3.6	21.37	--	--
M5	1267	450	100	50	270	3.6	32.06	--	--
M6	1267	450	100	50	270	3.6	42.74	--	--
HFSC reinforced with bronze fibers shavings type UE7									
M7	1267	450	100	50	270	3.6	--	5.34	--
M8	1267	450	100	50	270	3.6	--	10.69	--
M9	1267	450	100	50	270	3.6	--	21.37	--
M10	1267	450	100	50	270	3.6	--	32.06	--
M11	1267	450	100	50	270	3.6	--	42.74	--
HFSC reinforced with waste polyester fiber									
M12	1267	450	100	50	270	3.6	--	--	5.34
M13	1267	450	100	50	270	3.6	--	--	10.69
M14	1267	450	100	50	270	3.6	--	--	21.37
M15	1267	450	100	50	270	3.6	--	--	32.06
M16	1267	450	100	50	270	3.6	--	--	42.74

I.3.3. Mix procedure

Sand, cement, fine limestone, and silica fume were first introduced into a mixer and blended for 1 minute until a homogeneous dry mixture was achieved. Following this, water and a superplasticizer were gradually added, with the mixing continuing for an additional 2 minutes, in accordance with the **NF EN 12350-1** standard (Dupain & Saint-Arroman, 2009). When high-flow sand concrete was prepared with single, dual, or triple fibers, the fibers were added after the water and superplasticizer had been incorporated into the mixture [Figure II. 14](#) .



FIGURE II. 14. MIX PROCEDURE

Upon completing the mixing process, the slump values, density, and air content of the fresh concrete were measured following the guidelines outlined in [Table II.13](#), ensuring its physical properties were accurately assessed. The freshly mixed concrete was then placed into lubricated molds under controlled laboratory conditions (20°C and 50% ± 5% relative humidity). After 24 hours, the solidified concrete specimens were demolded and stored in water at 20°C until testing.

For each mix, three specimens were tested to evaluate mechanical, chemical, and physicochemical properties, with average values reported. [Table II. 10](#) provides an overview of the tests conducted, along with the applicable standards, specimen dimensions, and required equipment for evaluating high-flow sand concrete reinforced with fibers in both its fresh and hardened states (Dupain & Saint-Arroman, 2009).

TABLE II. 10. NORMS, SPECIMEN DIMENSIONS OF CONCRETE

Concrete properties	Norms	Specimens dimensions
<i>Physical</i>		
Slump	NF EN 12350-2	Abrams cone, 30 cm tall
Density	NF EN 12350-6	(15x15x15)cm ³
Air content	NF EN 12350-7	1L Air Entrainment Meter
<i>Mechanical</i>		
Compressive strength	NF EN 12390-3	(10x10x10)cm ³
Flexural tensile strength	NF EN 12390-5	(7x7x28)cm ³
Split tensile strength	NF EN 12390-6	(15x15x15)cm ³
<i>Chemical</i>		
Sulfuric acid	NF EN 206-1	(7x7x7)cm ³ , 5% H ₂ SO ₄
Hydrochloric acid	NF EN 206-1	(7x7x7)cm ³ , 5% HCL
<i>Physio-chemical</i>		
Absorption by immersion	NBN EN 1015-18	(7x7x28)cm ³
Absorption by capillarity	NF EN 480-5	(7x7x14)cm ³
Sorptivity	NF EN 480-5	(7x7x14)cm ³
Shrinkage	NF P15-433	(4x4x16)cm ³
Swelling	NF P15-433	(4x4x16)cm ³
<i>Microstructure SEM</i>	---	1cm ²

I.4. Norms & specimen dimensions

I.4.1. Physical properties

I.4.1.1. Slump

The slump test, conducted using the Abrams cone according to the **NF EN 12350-2** standard [Figure II. 15](#), is the most widely used method due to its simplicity and ease of implementation. The objective is to observe the slump of a concrete cone, which is described as fluid if it exhibits significant subsidence.

The **NF EN 12350-2** standard classifies slump into five categories, corresponding to the following ranges:

S1 = Firm: (1 cm ≤ h ≤ 4 cm)

S2 = Plastic: (5 cm ≤ h ≤ 9 cm)

S3 = Very plastic: ($10 \text{ cm} \leq h \leq 15 \text{ cm}$)

S4 = Fluid: ($16 \text{ cm} \leq h \leq 21 \text{ cm}$)

The S5 class ($h \geq 22 \text{ cm}$) refers to self-compacting concretes.

For the reference concrete M0, the measured slump was 21 cm, qualifying it as a high-flow sand concrete due to its fluid behavior.



FIGURE II. 15. THE SLUMP TEST

I.4.1.2. Density

The density of fresh concrete is calculated by weighing an empty mold of known volume after applying a lubricant layer, and then reweighing it once filled with the concrete mixture, as per the **NF EN 12350-6** standard [Figure II. 16](#). The calculation formula is as follows:

$$\rho = \frac{(m - m_0)}{V}$$

ρ : Mass density of the concrete (g/cm^3)

m : Mass of the empty mold (g)

m_0 : Mass of the filled mold (g)

V : Volume of the mold (cm^3)



FIGURE II. 16. DENSITY TEST

I.4.1.3. Air content

The measurement of the entrapped air content is carried out using a 1-liter concrete air meter (Air Entrainment Meter) [Figure II. 17](#), in accordance with the **NF EN 12350-7** standard. The measuring device consists of two parts, an upper and a lower section, where the concrete is placed inside the lower section in the same manner as it is placed in molds. After filling with concrete, the upper part is carefully positioned and secured. Then, pressure is applied using the integrated manual pump until the device's needle indicates 0%. At this point, the valve separating the two parts of the device is opened, allowing the concrete to be compressed. The air content of the concrete is then directly displayed by the gauge on the air meter.



FIGURE II. 17. AIR CONTENT TEST

I.4.2. Mechanical properties

I.4.2.1. Compressive strength

The compression test is conducted according to the **NF EN 12390-3** standard using a hydraulic press with a capacity of 3000 KN **Figure II. 18**. The specimen, with dimensions of (10x10x10) cm³, is placed centrally between the two plates of the machine. A slow and constant compressive load is then applied until the specimen fractures. The resulting value represents the maximum compressive strength, which can be expressed by the following equation:

$$\sigma_{rup} = \frac{F_{max}}{S}$$

σ_{rup} : Compressive strength (MPa)

F_{max} : Fracture load (N)

S: Specimen surface area (mm²)

This test was conducted on three samples, and either the average or the best of the three measured values is selected to ensure greater accuracy in the results.



FIGURE II. 18. COMPRESSIVE TEST

I.4.2.2. Flexural tensile strength

The flexural tensile strength is measured using prismatic specimens of dimensions (7×7×28)cm³ **Figure II. 19**. The test is conducted with a three-point bending machine capable of applying a 100 kN load. The load is applied continuously and smoothly, without impact, until the specimen fails. In accordance with the **NF 12390-5** standard, the formula used to calculate the flexural tensile strength at failure is as follows:

$$R_t = \frac{3 Fl}{2 d^3}$$

R_t : Flexural tensile strength (MPa)

F : Applied load (N)

l : Distance between supports (mm)

d : Specimen side length (mm)

This test was conducted on three samples, and either the average or the best of the three measured values is selected to ensure greater accuracy in the results.



FIGURE II. 19. FLEXURAL TENSILE TEST

I.4.2.3. Split tensile strength

In this test, a compressive force is applied to the specimen along two opposing generating lines. This compressive force induces tensile stresses in the plane intersecting these two lines. Rupture, caused by these tensile stresses, occurs within this plane [Figure II. 20](#). The calculation allows for determining the split tensile strength corresponding to this rupture.

Typically, this test is conducted on a cylindrical specimen, or as in our case, on a cubic specimen with dimensions of 15×15×15 cm, in accordance with the EN12390-6 standard. The split tensile strength at rupture is given by:

$$R_s = 0,637 \frac{P}{d^2}$$

R_s : Split tensile strength (MPa)

P: Applied load (N)

d : Specimen side length (mm)

This test was conducted on three samples, and either the average or the best of the three measured values is selected to ensure greater accuracy in the results.



FIGURE II. 20. SPLIT TENSILE TEST

I.4.3. Chemical properties

To study the effect of fibers (SSF-316L, BF-UE7, and WPF) on the durability of high-flow sand concrete, whether mono, dual, or triple fiber reinforcement, various compositions were evaluated under aggressive environments (acids). After completing the flexural tensile test at 28 days with dimensions $(7 \times 7 \times 28) \text{ cm}^3$, which were stored in water at 20°C with 95% humidity, the specimens were cut into uniform cubes $(7 \times 7 \times 7) \text{ cm}^3$ (Figure III-14). Before placing the $(7 \times 7 \times 7) \text{ cm}^3$ test pieces in the chemical solution, the initial mass (M_i) was recorded

The resistance of the immersed samples to chemical attack is evaluated through mass loss according to **NF EN 206-1**. The test pieces are cleaned with water and allowed to dry at room temperature for 30 minutes before weighing, and the final mass M_{f3} , M_{f28} , and M_{f90} , is recorded. Measurements are taken after 1, 28, and 90 days of immersion.

$$\text{Weight loss (\%)} = \frac{(M_i - M_{f_d})}{M_i} 100$$

M_i : Initial mass of the test piece before immersion (g)

M_f : Final mass of the test piece after immersion for (d) days (g)

I.4.3.1. Weight loss in hydrochloric acid (HCL)

The chemical engineer from the research lab prepared the **5% hydrochloric acid (HCl)** solution, a strong acid, necessitating the use of gloves and all necessary safety precautions during the experiment. The specimens were immersed in the hydrochloric acid solution, which was replaced every 28 days due to the limited quantity of the chemical solution [Figure II. 21](#).



FIGURE II. 21. WEIGHT LOSS --- HYDROCHLORIC ACID (HCL)

I.4.3.2. Weight loss in sulfuric acid (H_2SO_4)

The chemical engineer from the research lab prepared a **5% sulfuric acid (H_2SO_4)** solution, a strong acid, requiring the use of gloves and full safety precautions during the experiment. The specimens were immersed in the sulfuric acid solution, which was replaced every 28 days due to the limited quantity of the chemical solution [Figure II. 22](#).



FIGURE II. 22. WEIGHT LOSS --- SULFURIC ACID (H_2SO_4)

I.4.4. Physio-chemical properties

I.4.4.1. Absorption by immersion

The process for evaluating water absorption by immersion involves placing prismatic concrete samples with dimensions $(7 \times 7 \times 28)$ cm³ in an oven at 105°C for 48 hours until they reach a constant mass [Figure II. 23](#). Subsequently, these samples are fully immersed in water at 20°C for 24 hours to ensure complete saturation of the material. After immersion, the samples are removed from the water, dried, and weighed to determine the absorption coefficient by immersion using the following formula. This procedure is conducted in accordance with the

NBN EN 1015-18 standard, which outlines the methodology for measuring water absorption in concrete.

$$Ab_{imr} = \frac{M_w - M_d}{M_d} 100$$

Ab_{imr} : Absorption coefficient by immersion (%)

M_w : Mass of the wet sample after immersion (g)

M_d : Mass of the dry sample after drying in the oven (g)

The absorption coefficient by immersion (Ab_{imr}) is calculated as the average of two samples or the best result among them.



FIGURE II. 23. ABSORPTION BY IMMERSION TEST

I.4.4.2. Capillary absorption

Testing the absorption of water by capillary in solid concrete involves using prismatic samples with dimensions 7 x 7 x 14 cm. The specimens are dried in an oven for 48 hours until they reach a constant weight, with their lateral surfaces shielded by aluminum foil. Subsequently, the samples are submerged in a water bath with a height of 5 mm for a duration of 72 hour [FigureII.24](#). Mass fluctuations and water penetration levels are recorded at the following intervals: 15, 30, 60, 120, 240, 360, 480, 720, 1080, 1440, 2880, and 4320 minutes, to evaluate the absorption properties. This procedure is conducted in accordance with the **NF EN 480-5** standard, which specifies the methodology for measuring water absorption by capillarity in concrete. The absorption coefficient by capillarity is calculated using the following formula:

$$Ab_{cap} = \frac{M_0 - M_t}{A}$$

Ab_{cap} : the coefficient of capillary absorption (g/mm^2)

M_0 : the initial mass of the sample before immersion (g)

M_t : the mass of the sample after immersion at time (t) (g)

A : the surface area of the sample in contact with water (mm²)

The coefficient of capillary absorption (Ab_{cap}) is calculated as the average of two samples or the best result among them.



FIGURE II. 24. CAPILLARY ABSORPTION TEST

I.4.4.3. Sorptivity

Sorptivity refers to the rate at which water is absorbed by concrete through capillary action over time and during saturation phases, rather than focusing solely on surface tension as in capillary absorption analysis. This property is crucial for understanding material behavior and predicting long-term damage.

The Sorptivity coefficient is calculated using the following formula:

$$Ab_{Srp} = \frac{M_0 - M_t}{A \cdot \sqrt{t}}$$

Ab_{Srp} : the Sorptivity coefficient (g/mm²·√min)

M_0 : the initial mass of the sample before immersion (g)

M_t : the mass of the sample after immersion at time (t) (g)

A : the surface area of the sample in contact with water (mm²)

t : time of immersion (min)

I.4.4.4. Shrinkage and swelling

The primary goal of incorporating fibers into high-flow sand concrete is to minimize shrinkage and swelling, as highlighted in Sablocrete (Sablocrete, 1994). This study explores how various

fiber systems, single (SSF-316L, BF-UE7, WPF), dual, or triple affect the shrinkage and swelling behavior of high-flow sand concrete.

The test involves comparing the length variation of a 4 x 4 x 16 cm specimen at different times (t) to its initial length at time (t_0), which is taken as the reference.

The test is conducted at a temperature of $20^{\circ}\text{C} \pm 2^{\circ}\text{C}$ and a relative humidity of at least $50\% \pm 5\%$. At the time of measurement, the dial gauge is zeroed against the Invar standard rod of length $L=160$. Let (t) represent the reading on the dial gauge at time t ; the specimen's length (l) at the given time is:

$$l = L + dl(t)$$

l : The length of the specimen at time t (mm)

L : The fixed length of the Invar (Invar) standard rod, which is 160 mm.

$dl(t)$: The value measured by the gauge at time t (μm).

The relative change in length, commonly denoted by (ε), is expressed as follows:

$$\varepsilon(t) = \frac{\Delta l(t)}{L} = \frac{dl(t) - dl(t_0)}{L}$$

ε : The relative change in length

Δl : The difference between the current length $l(t)$ and the length at the original time $l(t_0)$ (mm)

L : The fixed length of the Invar (Invar) standard rod, which is 160 mm.

$dl(t)$: The value measured by the gauge at time t (μm).

$dl(t_0)$: The value measured by the gauge at time t_0 (μm).

1.4.4.4.1. Shrinkage

When specimens are stored in air, $\Delta l(t)$ is typically negative (-), indicating a reduction in the specimen's length, commonly referred to as shrinkage. $\Delta l(t)$ is obtained by averaging the measurements from the two specimens taken from the same mold [Figure II. 25](#).

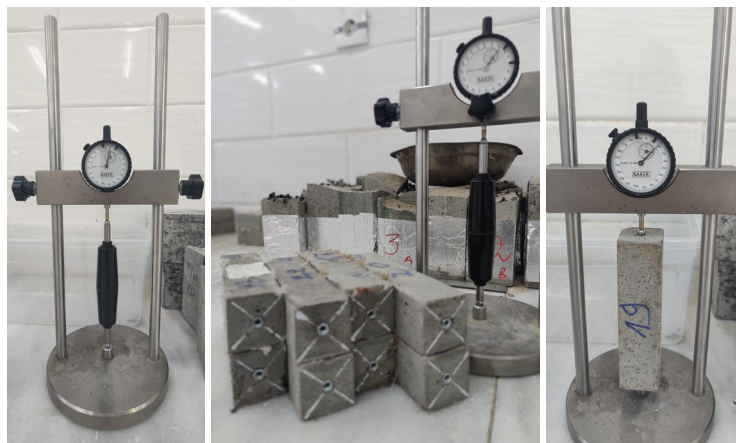


FIGURE II. 25. SHRINKAGE TEST

I.4.4.4.2. Swelling

When the specimen is stored in water, $\Delta l(t)$ can be positive (+), indicating swelling [Figure II.26](#). $\Delta l(t)$ is obtained by averaging the measurements from the two specimens taken from the same mold [Figure II. 26](#).



FIGURE II. 26. SWELLING TEST

I.4.5. SEM and EDS-cartography

I.1.5.1. Scanning electron microscope (SEM)

The SEM tests [Figure II. 27](#) were conducted at the Laboratory of Energy Processes and Nanotechnology, University of Saad Dahlab-Blida1, on two samples. After the mechanical tests, the specimens were cut into 10 mm diameter and 2 mm thick discs, cleansed with water, and oven-dried. A FEI Quanta 650 FEG Scanning Electron Microscope (SEM) [Figure II. 28](#) was employed to examine the microstructure of the samples. This analysis provided detailed insights into the physical properties of the material at a micro-scale, from 50 μm to 1 mm.

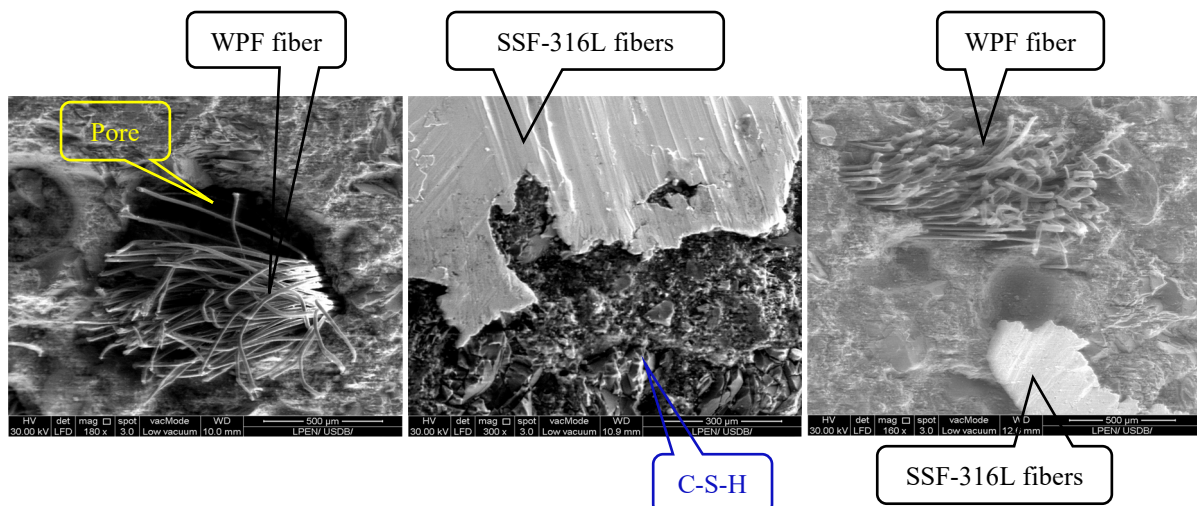


FIGURE II. 27. SCANNING ELECTRON MICROSCOPE

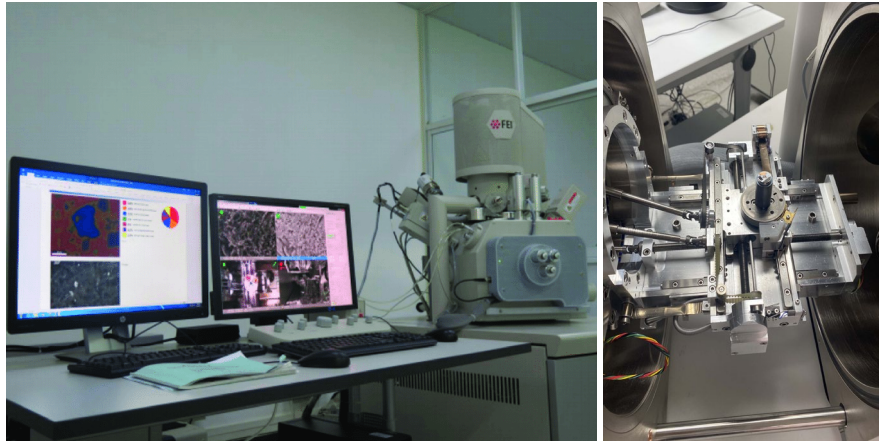


FIGURE II. 28. FEI QUANTA 650 FEG – SEM

I.1.5.2. SEM-EDS cartography

SEM imaging, Energy Dispersive X-ray Spectroscopy (SEM-EDS) was used for elemental analysis through a process known as EDS Cartography [Figure II. 30](#). This technique allows for the identification and mapping of the chemical elements present within the sample. EDS provides both qualitative and quantitative data on the distribution of elements.

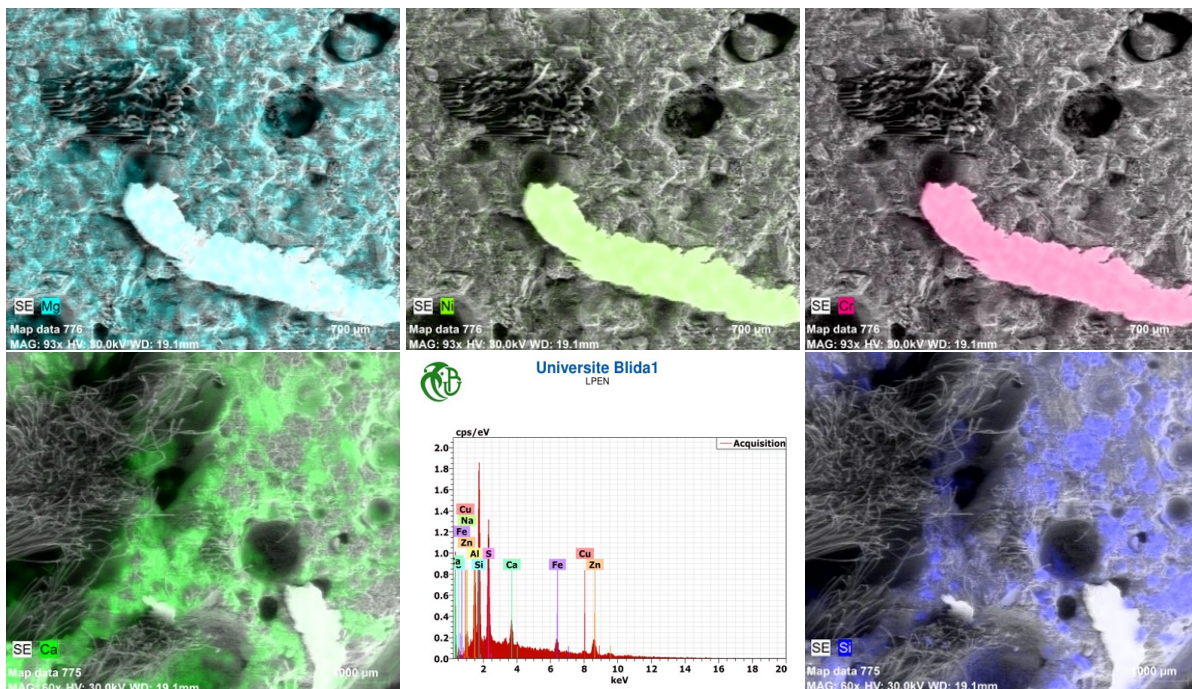


FIGURE II. 29. SEM-EDS CARTOGRAPHY

I.6. Conclusion

This chapter presents an investigation into high-flow sand concrete (HFSC) reinforced with mono fibers as well as hybrid systems (dual and triple combinations). The constituent materials of HFSC, including sand, cement, limestone fillers, silica fume, stainless steel fibers, bronze fibers, recycled polyester fibers, admixtures, and water, were meticulously selected and characterized in accordance with standardized methodologies.

A total of 24 HFSC mix designs were developed, incorporating three types of fibers, 316L stainless steel shavings, UE7 bronze shavings, and recycled polyester fibers, at varying ratios of 0.25%, 0.50%, 1%, 1.5%, and 2%.

This research presents a comprehensive study and practical applications conducted in accordance with established standards to enhance the physical, mechanical, chemical, and physio-chemical properties of high-flow sand concrete. It also includes microscopic analysis using SEM-EDS to examine the microstructural interactions in HFSC reinforced with mono, dual, and triple fiber systems.

Chapter III

Results and analysis

Chapter III : Results and analysis

III.1 Introduction

This chapter presents a comprehensive analysis of the experimental results obtained from the study of High-Flow Sand Concrete (HFSC) reinforced with three types of mono fibers: stainless steel fibers (SSF-316L), bronze fibers (BF-UE7), and waste polyester fibers (WPF). The objective is to evaluate the influence of each fiber type on the physical properties (slump, density, and air content), mechanical properties (compressive strength, split tensile strength, and flexural strength), chemical properties (in sulfuric and hydrochloric acid), and physico-chemical properties (shrinkage, swelling, absorption by immersion and capillarity, and sorptivity). Furthermore, a microstructural analysis is conducted using Scanning Electron Microscopy (SEM) to investigate the mechanisms by which these fibers affect the internal structure of the concrete.

In addition to assessing the effect of mono fiber types, the performance of hybrid fiber systems, including dual and triple combinations, is also examined. These systems aim to integrate the advantages of metallic (micro and macro) and synthetic fibers to enhance the concrete matrix, mitigate crack propagation, and improve durability in aggressive environments. The impact of these hybrid configurations on the physical, mechanical, physico-chemical, and chemical properties is analyzed, with a comparative assessment against mono-fiber systems to determine the most effective reinforcement strategy.

III.2. High flow sand concrete reinforced with SSF-316L

In this section, a comprehensive study will be conducted on the results obtained from various tests carried out on high-flow sand concrete reinforced with stainless steel shavings (SSF-316L). Its behavior in both the fresh and hardened states will be analyzed. The physical, mechanical, chemical, and physicochemical properties, as well as the microstructural analysis using SEM, will be examined for all the mixtures, providing a thorough interpretation of the results in comparison with previous studies.

III.2.1. Physical properties

Table III. 1 presents the results of the physical properties of the HFSC in the fresh state. The slump value, density, and air content of the mixtures were measured according to the standards outlined in the previous Chapter II.

TABLE III. 1. PHYSICAL PROPERTIES OF THE HFCS REINFORCED WITH SSF-316L

Mixtures	Slump (mm)	Density (g/dm ³)	Air Content (%)
M0 (0.00%)	215	2091	6.2
M1 (0.25%)	245	2108	5.6
M2 (0.50%)	215	2091	6.8
M3 (0.75%)	210	2092	7.0
M4 (1.00%)	245	2093	7.2
M5 (1.50%)	220	2106	6.2
M6 (2.00%)	195	2120	5.8

III.2.1.1 Slump

Table III. 1 shows the impact of SSF-316L on the workability of fresh high-flow sand concrete. The slump value for the M0 mix was 215 mm. It increased by 13.95% for the M1 (0.25%) and M4 (1.00%) mixes. The reason for the result is that evenly dispersed 316L stainless steel fibers improve the mixture's homogeneity and consistency and strengthen the concrete's cohesiveness by strengthening the bond between the fibers, sand, and cement matrix. This configuration makes the concrete easier to deal with by making the pumping and placing operation easier. It is evident that the inclusion of SSF-316L in mixes M2, M3, and M5 resulted in decreased workability. Furthermore, an increase in the SSF-316L content led to additional reduction in workability in mix M6, indicating a potential alteration in the properties of fresh concrete that could affect its strength and performance post-hardening (Zhang, et al., 2021) (Liu, et al., 2023)

III.2.1.2. Relationship between density & air content

Figure III. 1 illustrates the relationship between density and air content in different high-flow sand concrete (HFSC) mixes reinforced with SSF-316L:

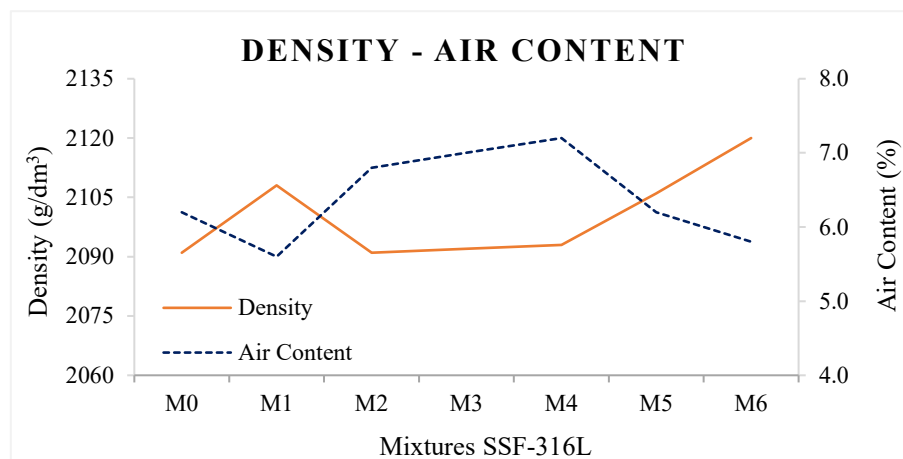
**FIGURE III. 1.** RELATIONSHIP BETWEEN DENSITY & AIR CONTENT OF MIXES WITH SSF-316

Table III. 1 shows the influence of adding SSF-316L shavings fibers to HFSC on its slump, density, and air content. The introduction of SSF-316L at 0.25% in mix M1 seems to improve workability, leading to an increase in density and a reduction in air content, as shown in Figure III. 1. The enhancement of the physical properties of HFSC results in improvements in its mechanical properties, particularly compressive strength, as shown in Figure III. 2.

The results reveal an inverse relationship between density and air content in HFSC reinforced with SSF-316L fibers. The optimal fiber contents for both density and air content were found at 0.25% and 2%, respectively (Iqbal , et al., 2015). These findings suggest that selecting the appropriate fiber ratio improves the concrete's properties by reducing air voids and enhancing the cohesion of the matrix. From an economic standpoint, the 0.25% fiber content is the most advantageous.

III.2.2. Mechanical properties

The mechanical properties of HFSC in its hardened state have been evaluated. The experiments conducted to assess these properties include compressive strength, flexural tensile strength, and splitting tensile strength. These tests were performed in accordance with the norms outlined in the previous Chapter II.

III.2.2.1. Compressive strength

Figure III. 2 illustrates the compressive strength results at 3, 7, 28, and 90 days for high-flow sand concrete reinforced with 316L Stainless Steel Shavings Fibers (SSF-316L):

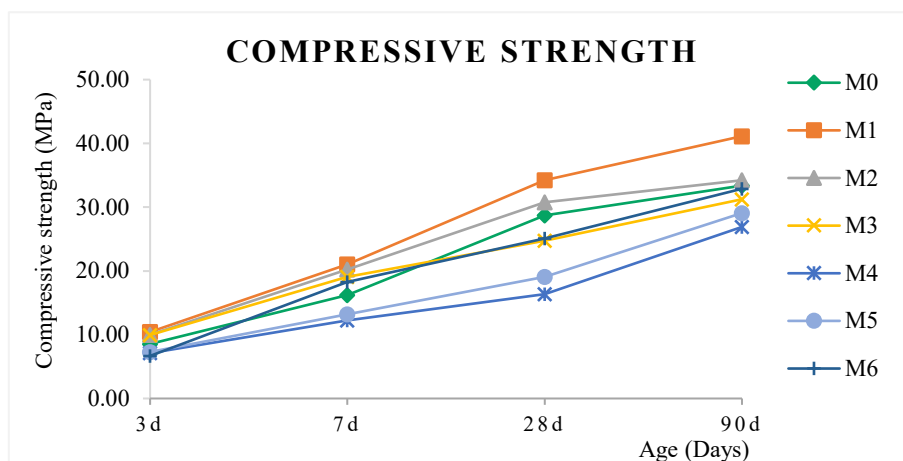


FIGURE III. 2. COMPRESSIVE STRENGTH OF MIXES WITH SSF-316L

The addition of Stainless Steel Shavings Fiber (SSF-316L) to high-flow sand concrete led to a notable enhancement in compressive strength. As shown in [Figure III. 2](#), the effect of SSF-316L on compressive strength initially increased, followed by a decrease at higher fiber contents. The optimal fiber content was determined to be 0.25%, with mix M1 exhibiting a 23.21% higher compressive strength compared to the reference mix M0.

This improvement can be attributed to several factors, including an increase in concrete density and a reduction in air content, as indicated in [Table III. 1](#), which helps mitigate the formation of micro-cracks. Additionally, SSF-316L fibers function as small reinforcement bars within the concrete matrix, effectively distributing stresses and preventing crack propagation ([Ding & Bai, 2018](#)).

III.2.2.2. Flexural tensile strength

The test aims to investigate the impact of incorporating SSF-316L as reinforcement on the flexural tensile strength of high-flow sand concrete at 3, 7, 28, and 90 days, as shown in the histogram in [Figure III. 3](#).

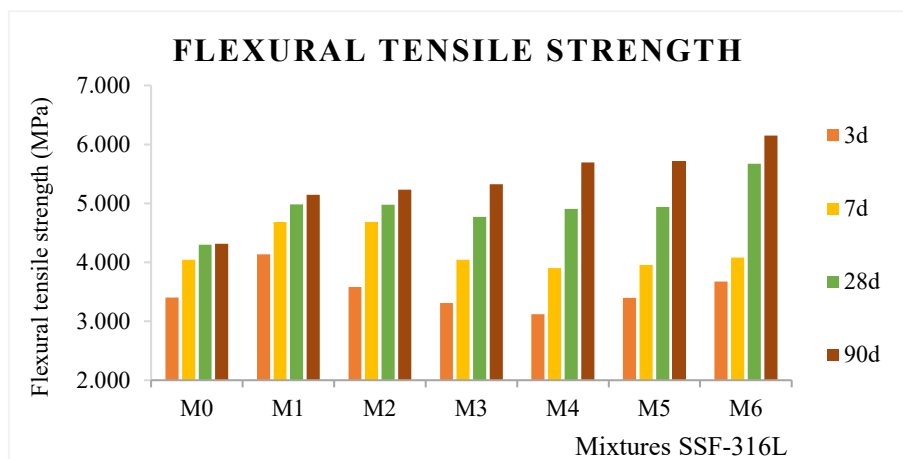


FIGURE III. 3. FLEXURAL TENSILE STRENGTH OF MIXES WITH SSF-316L

As illustrated in [Figure III. 3](#), increasing the content of SSF-316L fibers led to a substantial improvement in flexural tensile strength. The optimal mix was identified as M6, containing 2.0% fiber. The flexural strength of this mix showed an increase of 52.18% compared to the reference mix M0. This enhancement can be attributed to the fibers' role in improving the concrete's density and reducing its porosity ([Jinlin, et al., 2021](#)), which in turn enhances its resistance to bending. Moreover, SSF-316L fibers contribute significantly to the prevention of micro-crack formation by effectively distributing stresses across the concrete matrix, thus

improving overall durability and reducing the potential for crack propagation under applied loads (Kalpana & Tayu, 2020).

III.2.2.3. Split tensile strength

The test evaluates the effect of SSF-316L reinforcement on the split tensile strength of high-flow sand concrete at 3, 7, 28, and 90 days, as depicted in Figure III. 4.

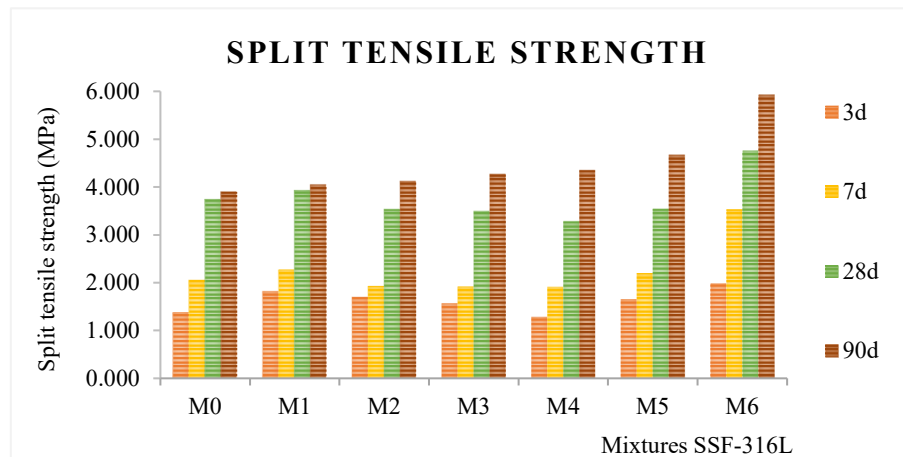


FIGURE III. 4. SPLIT TENSILE STRENGTH OF MIXES WITH SSF-316L

In terms of split tensile strength, an increase of 42.36% was observed at a 2% fiber ratio in mix M6 compared to the reference mix M0. This improvement can be attributed to the fibers acting as bridging elements between the cracked regions of the concrete, facilitating efficient stress transfer across the cracks. As a result, the concrete's resistance to large-scale cracking is enhanced. Additionally, the superior mechanical properties of SSF-316L fibers, particularly their corrugated shape, play a crucial role in preventing the further propagation of cracks, as confirmed by the findings of Fox et al. (Zhang, et al., 2020) (Ran, et al., 2021).

III.2.3. Physio-chemical properties

III.2.3.1. Absorption by immersion

In this study, HFSC was reinforced with SSF-316L to investigate its effect on water absorption after immersing the samples in water for 24 hours:

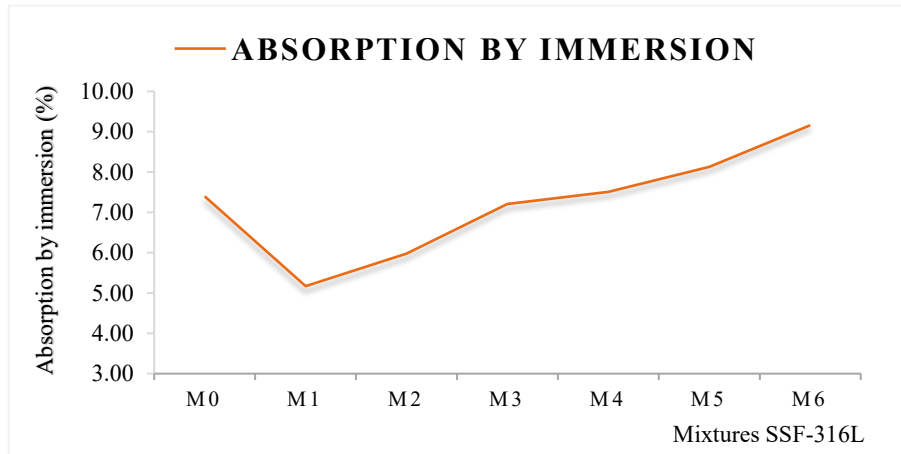


FIGURE III. 5. ABSORPTION BY IMMERSION OF MIXES WITH SSF-316L

As shown in [Figure III. 5](#), the mixture with 0.25% SSF-316L (M1) achieved the lowest water absorption rate of 5.17% compared to 7.40% for the reference concrete (M0). This indicates a significant improvement in resistance to water penetration due to enhanced density, reduced air content, and minimized porosity ([Faris, et al. \(2021\)](#)).

III.2.3.2. Capillary absorption

[Figure III. 6](#) shows the effect of different ratios of SSF-316L (0%, 0.25%, 0.5%, 0.75%, 1%, 1.5%, and 2%) on the capillary absorption of HFSC at 4320 minutes:

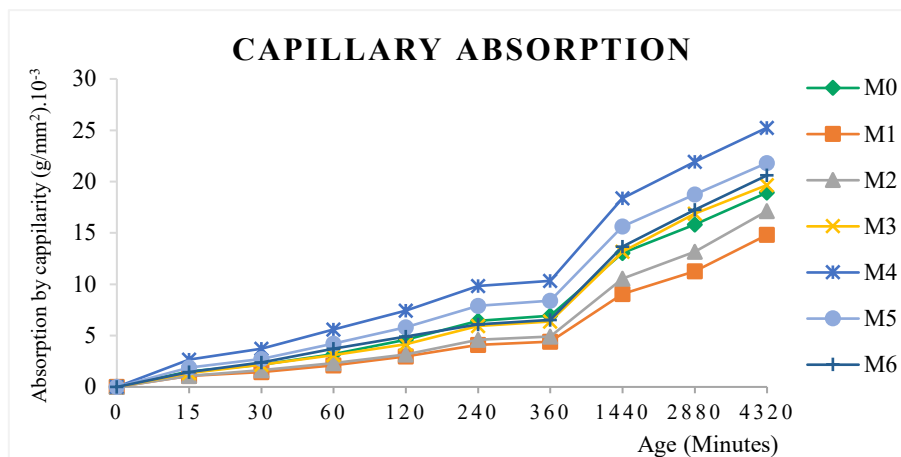


FIGURE III. 6. CAPILLARY ABSORPTION OF MIXES WITH SSF-316L

In the initial minutes, capillary absorption is primarily influenced by the surface porosity (outer surface) of the HFSC, with minimal differences observed between the various ratios of SSF-316L fibers. Over time, absorption becomes related to the internal matrix structure of the HFSC.

HFSC reinforced with 0.25% SSF-316L fiber, it show a reduction in capillary absorption (M1) compared to the reference mixture (M0), as the SSF-316L fiber enhance internal cohesion, reduce micro voids, and lower porosity. However, as the SSF-316L fiber content increases, the formation of new micro voids within the HFSC occurs, resulting in an increase in capillary absorption.

III.2.3.3. Sorptivity

The results of sorptivity are shown in [Figure III. 7](#), it measures the capillary absorption as a function of time. It determines the amount of water absorbed per unit of time for HFSC reinforced with SSF-316L fibers:

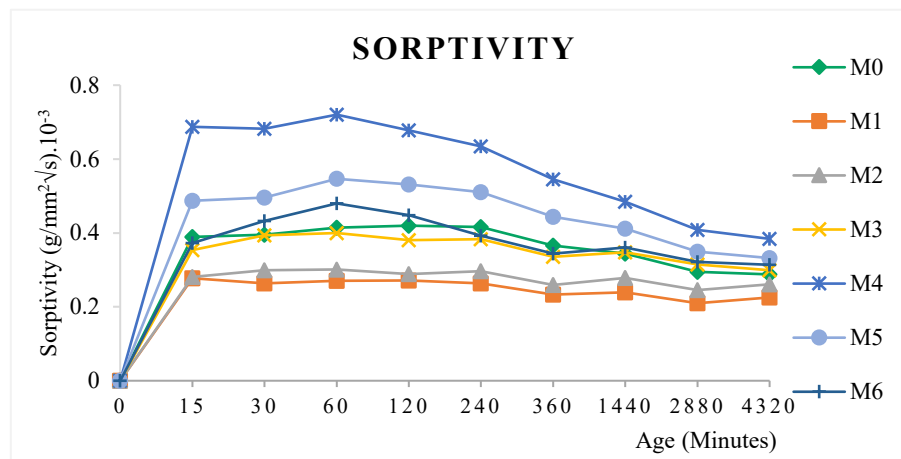


FIGURE III. 7. SORPTIVITY OF MIXES WITH SSF-316L

In HFSC reinforced with SSF-316L, capillary absorption starts with high values and decreases after 60 minutes. The mix M1 (0.25% SSF-316L) reduces sorptivity compared to M0, as the fibers enhance density, reduce air content, and decrease porosity. The sorptivity results show a similar trend to capillary absorption, considering that sorptivity incorporates the time factor in the measurement.

III.2.3.4. Shrinkage

The shrinkage strain results for HFSC reinforced with SSF-316L fibers are presented in [Figure III. 8](#):

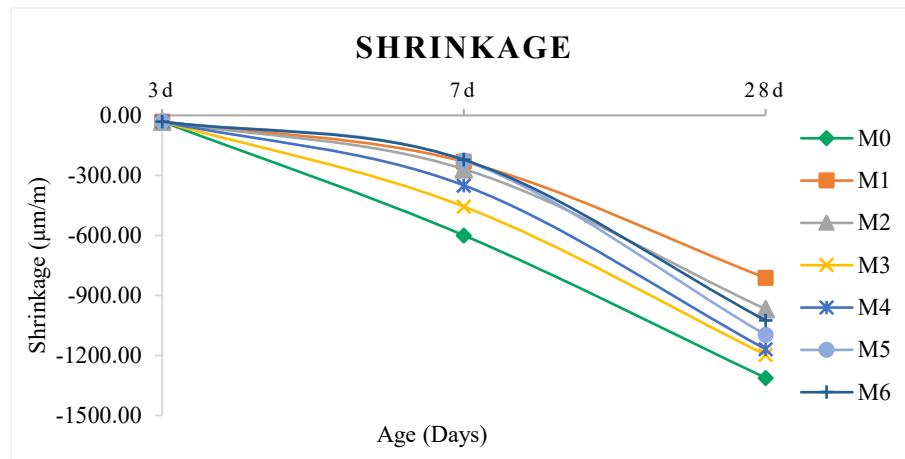


FIGURE III. 8. SHRINKAGE STRAIN OF MIXES WITH SSF-316L

In 7 days, mix M6 (2% SSF-316L) reduced shrinkage, indicating that a higher SSF-316L content reduces shrinkage in the early term.

In 28 days, mix M1 (0.25% SSF-316L) reduced shrinkage, suggesting that a lower SSF-316L content reduces shrinkage in the long term.

In all mixtures, HFSC reinforced with SSF-316L reduced shrinkage compared to the reference mix (M0). This reflects the effectiveness of SSF-316L in enhancing the cohesion of the concrete matrix. (Sayahi, et al., 2020)

III.2.3.5. Swelling

The swelling results for HFSC reinforced with SSF-316L fibers are presented in Figure III. 9

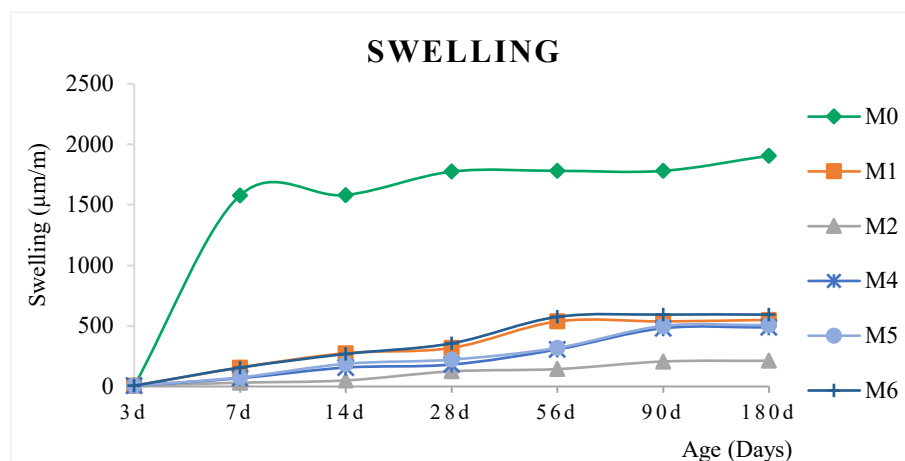


FIGURE III. 9. SWELLING OF MIXES WITH SSF-316L

All mixtures (M1 to M6) exhibited a reduction in swelling compared to the reference mixture (M0), confirming the role of SSF-316L in enhancing the physio-chemical properties of HFSC.

The best performance was observed in M1 and M2, with 0.25% and 0.50% SSF-316L achieving swelling reductions of 71% and 89%, respectively, at 180 days compared to the reference mixture (M0). However, increasing the SSF-316L ratio to 2.00% (M6) resulted in a lower reduction in swelling compared to M1 and M2, due to poor fiber distribution and the formation of pores within the HFSC.

Additionally, the results indicated that swelling increased gradually during the early term (7, 14, and 28 days) but became nearly constant in the long term.

III.2.4. Chemical properties

III.2.4.1. Weight loss in sulfuric acid (H_2SO_4)

Research was conducted to evaluate the durability of HFSC reinforced with SSF-316L fibers at ratios of 0.25%, 0.5%, 0.75%, 1%, 1.5%, and 2%. The samples were exposed to 5% H_2SO_4 for 90 days, with weight loss measured to assess resistance to chemical attack, as illustrated in Figure III. 10

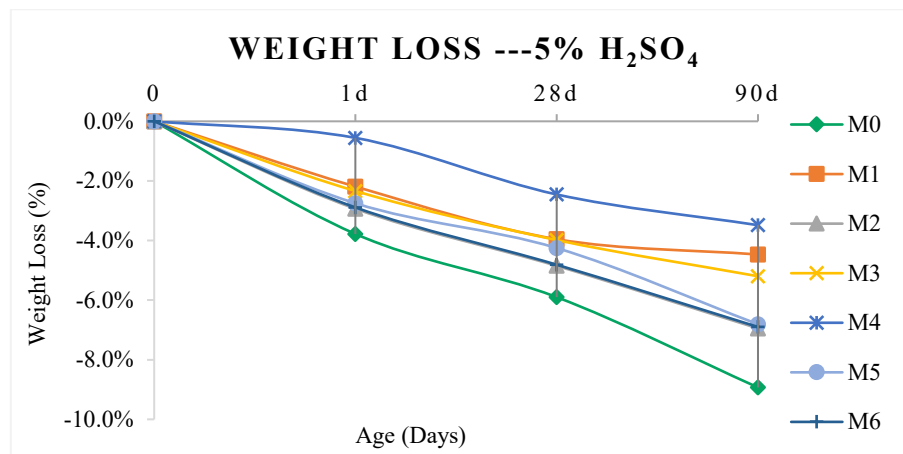


FIGURE III. 10. WEIGHT LOSS OF MIXES WITH SSF-316L EXPOSED IN SULFURIC ACID

Based on Figure III. 10, it's clear that the best combinations for HFSC with SSF-316L exposed to 5% H_2SO_4 are M1 and M4, with 0.25% and 1% fiber content, showing weight losses (Wf) of 4.5% and 3.50%, respectively. On the other hand, M2, M3, M5, and M6 also performed better than the reference concrete M0. This is because SSF-316L fibers reinforce the HFSC structure and prevent cracking caused by sulfate attack.

III.1.4.2. Weight loss in hydrochloric acid (HCl)

Figure III. 11 illustrates a study conducted to assess the durability of HFSC reinforced with SSF-316L fibers at ratios of 0.25%, 0.5%, 0.75%, 1%, 1.5%, and 2%, exposed to 5% HCl for 90 days by evaluating the weight loss due to chemical attack.

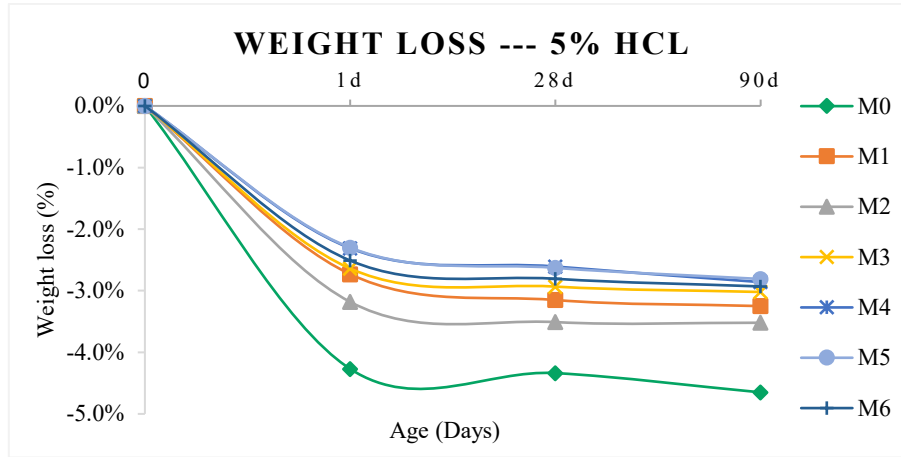


FIGURE III. 11. WEIGHT LOSS OF MIXES WITH SSF-316L EXPOSED HYDROCHLORIC ACID

Figure III. 11, it's evident that HFSC reinforced with SSF-316L exhibits resistance to 5% HCl acid attack compared to mix M0, resulting in less weight loss. Among the different mixes, mix M5 reinforced with 1.5% of SSF-316L by mass demonstrated superior performance and reduced weight loss caused by acid attack. These results agree with those found by (Dsouza, et al., 2018)

III.2.5. SEM

A scanning electron microscope (SEM) be used to examine specimens analyzing their structure and physical proprieties within a scale of 50 μ m to 1 mm.

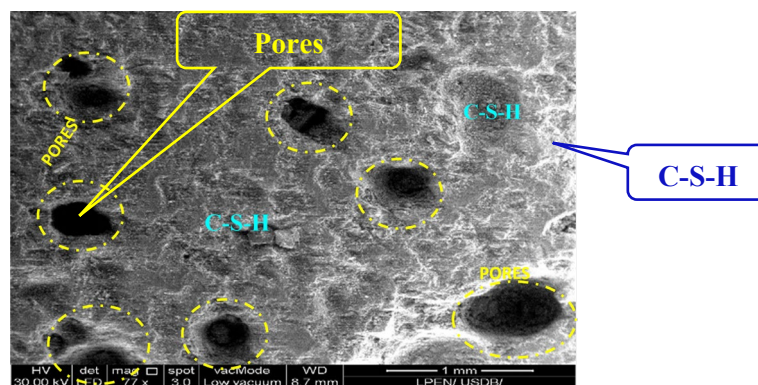


FIGURE III. 12. SEM OF M0 --- WITHOUT FIBERS

The incorporation of SSF 316L into mix M1 led to a reduction in pore diameter and quantity.

This led to a 9.67% reduction in air content and a 17 kg/m^3 increase in the density of the mixture compared reference concrete M0 [Figure III. 12](#). As a result there was an improvement in the mechanical properties of the HFSC.

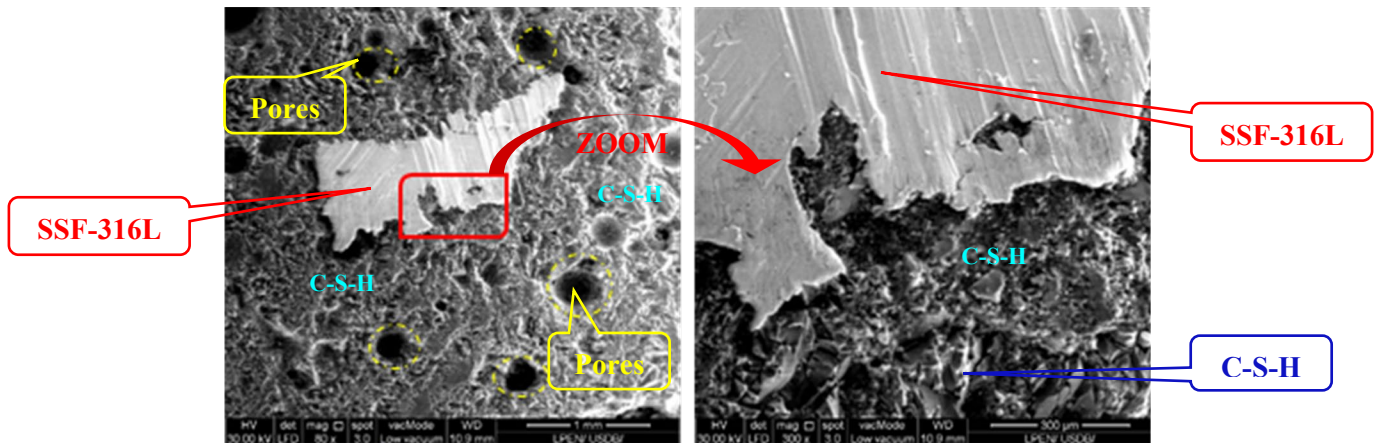


FIGURE III. 13. SEM OF MIX M1

[Figure III. 13](#) shows a cross section of a specimens from mix M1. The SSF-316L fibers have irregular edges blending well with C-S-H (calcium silicate hydrate). This enhanced bonding and cohesion between the sand concrete matrix and the fibers explain the progressively increasing flexural and split tensile strength results ([Sun, et al., 2024](#)).

III.2.6. Evaluation and justification for the optimal performance of SSF-316L in HFSC

The impact of stainless steel fibers (SSF-316L) on the physical, mechanical, chemical, and physico-chemical properties of high-flow sand concrete (HFSC) was evaluated:

Physical properties

The M1 mixture exhibited the best balance between workability and density, with the lowest air content. This improved the concrete's cohesion and reduced internal voids.

Mechanical properties

The M1 mixture achieved the highest compressive strength, while M6 demonstrated superior flexural and split tensile strength.

Physico-chemical properties

The M1 mixture showed superior performance in terms of reduced absorption by immersion, capillary absorption, and sorptivity, leading to lower porosity and shrinkage.

Chemical properties

The M1 mixture displayed exceptional resistance to acid attacks, particularly against sulfuric acid (H_2SO_4).

Additionally, SEM analysis confirmed the excellent bond between SSF-316L fibers and concrete's matrix, explaining the superior performance of the M1 mixture.

Based on these findings, the M1 mixture (0.25%) is considered the optimal mix.

III.3. High flow sand concrete reinforced with bronze fiber

In this section, a comprehensive analysis is conducted on the results obtained from High-Flow Sand Concrete samples reinforced with UE7 Bronze shavings fibers (BF-UE7). The physical properties (slump, density, and air content), mechanical properties (compressive strength, flexural tensile strength, and split tensile strength), chemical properties (effects of sulfuric and hydrochloric acid attacks), and physio-chemical properties (shrinkage, swelling, absorption by immersion and capillarity, and sorptivity) are examined. Additionally, microstructural analysis through Scanning Electron Microscopy (SEM) is included.

III.3.1. Physical properties

The results of the physical properties of the HFSC reinforced with UE7 Bronze shavings fibers (BF-UE7) in the fresh state. The slump value, density, and air content of the mixtures were measured according to the standards outlined in the previous Chapter II.

III.3.1.1. Slump

The effect of UE7 Bronze shavings fibers (BF-UE7) on the workability and consistency of High Flow Sand Concrete (HFSC) was evaluated by analyzing the slump test results, as shown in the curve in [Figure III. 14](#)

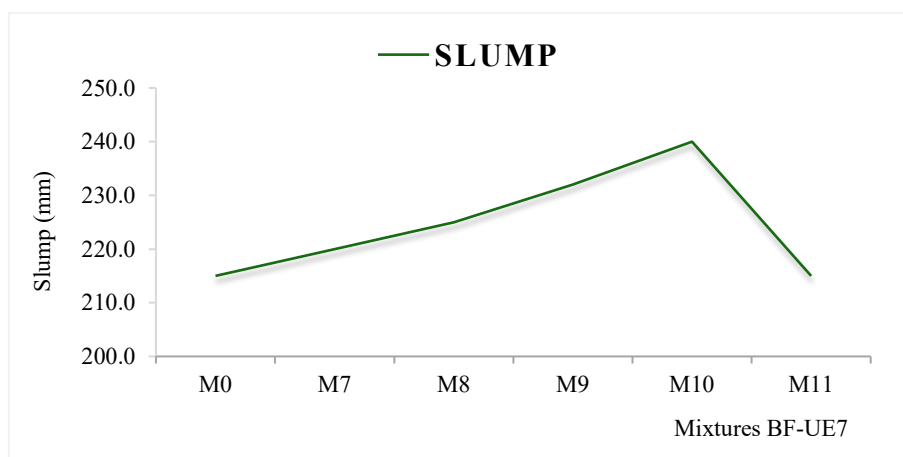


FIGURE III. 14. SLUMP OF MIXES WITH BF-UE7

The incorporation of bronze shavings fibers (BF-UE7) into High Flow Sand Concrete (HFSC) led to a slight enhancement in workability. As illustrated in [Figure III. 14](#), the mixes designated as M7, M8, and M9 demonstrated a notable increase in slump values compared to the reference concrete (M0), with percentage increases of 6.51%, 11.62%, and 58.14%, respectively. The maximum slump value was observed in mix M10, showing an increase of 51.16%.

This increase in slump can be attributed to the high-flow nature of the sand concrete, characterized by reduced coarse aggregate content, which minimizes interlocking or friction between the fibers and the aggregate. Furthermore, the straight and smooth geometry of the fibers reduces friction, thereby enhancing workability. These findings are consistent with the observations of ([Zhang, et al., 2024](#)), although their results contrasted with ours. This discrepancy can be explained by differences in the type of concrete and fibers employed in each study. However, in mix M11, the slump value decreased compared to M10. This reduction is attributed to the high fiber content, which led to fiber interlocking, consequently reducing the workability of the mix.

III.3.1.2. Density

The experiment is designed to examine how the density of High flow Sand Concrete (HFSC) changes when varying amounts of UE 7 Bronze Shavings Fiber (BF-UE7) are added gradually in increments of 0.25%, 0.5%, 1%, 1.5% and 2%. According to [Figure III. 15](#) displayed in the report, the findings will highlight how these fibers affect the density of the material:

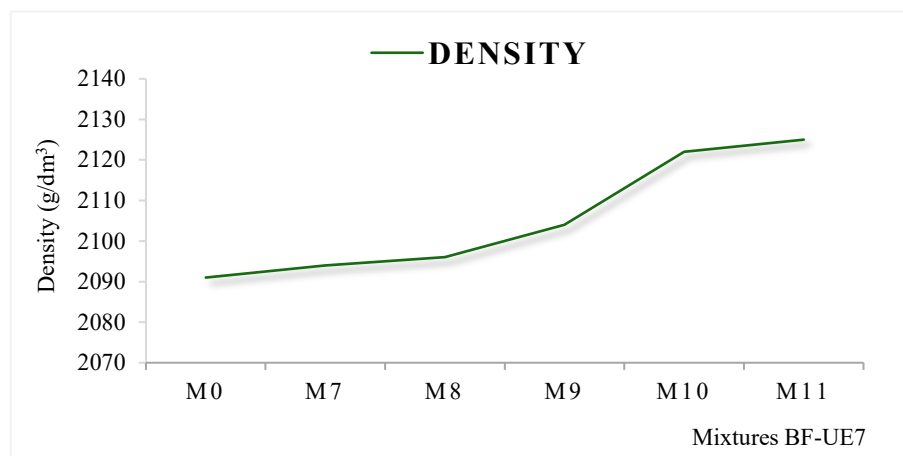


FIGURE III. 15. DENSITY OF MIXES WITH BF-UE7

([Faris, et al., 2021](#)) indicated in their study that the increase in the addition of steel fibers is directly proportional to the increase in concrete density. They attributed this to the difference in the bulk density of steel fibers, which is greater than that of concrete. This finding aligns

with the results obtained in this research, where it was observed that as the fiber content increased, the density of bronze fiber-reinforced High-Flow Sand Concrete (HFSC) also increased, reaching up to 2125 g/cm³ at 2% fiber content (M11). The reason for this increase is that the bulk density of bronze shavings fibers (BF-UE7) is approximately 8800 g/cm³, while the bulk density of the reference concrete (M0) is 2091 g/cm³.

III.3.1.3. Air content

The test aims to investigate how the air content of High-Flow Sand Concrete (HFSC) is affected by the addition of varying amounts of UE 7 Bronze Shavings Fiber (BF-UE7). The results illustrated in [Figure III. 16](#) of the study will demonstrate:

The air content test results reveal a substantial decrease in air content for most high-flow sand concrete (HFSC) mixtures. It was observed that with the incorporation of (BF-UE7) fibers at dosages ranging from 0.25% to 1.5%, the entrapped air content dropped from 4.8% to 4.4%, marking a 29.03% improvement in mix M10 compared to the reference concrete M0, which exhibited 6.2% entrapped air.

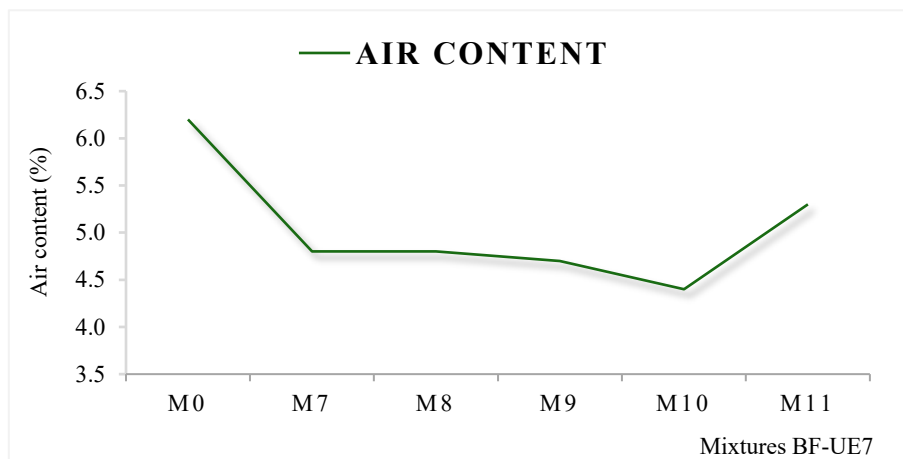


FIGURE III. 16. AIR CONTENT OF MIXES WITH BF-UE7

These findings are consistent with the observations made by [\(Wang & Gao, 2016\)](#) where air content decreases as the proportion of steel fibers increases. This reduction in entrapped air content can be attributed to the efficient dispersion of short fibers (microfibers), which optimize the concrete matrix by filling air voids and enhancing its compactness. The fibers exhibited an optimal and well-structured distribution, contributing to increased density and improved workability of the mixtures.

III.3.2. Mechanical properties

III.3.2.1. Compressive strength

The histogram in [Figure III. 17](#) illustrates the compressive strength results at 3, 7, 28, and 90 days for high-flow sand concrete reinforced with UE7 Bronze Shavings Fibers (BF-UE7):

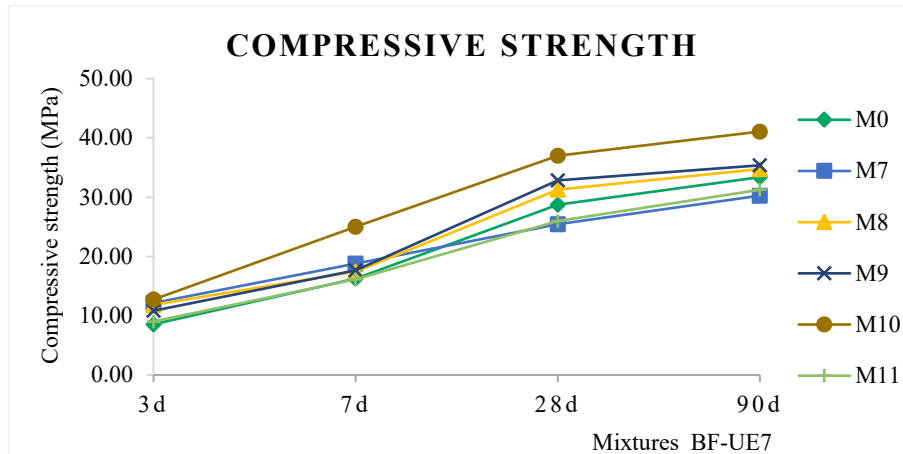


FIGURE III. 17. COMPRESSIVE STRENGTH OF MIXES WITH BF-UE7

After introducing UE7 Bronze Shavings Fibers (BF-UE7) into the high-flow sand concrete mixtures and a curing period of 90 days, an increase in compressive strength was observed with the mixes, with the M10 mix showing a peak improvement of 23.05% compared to the reference concrete (M0). These results are consistent with the findings of [\(Abubakar, et al., 2022\)](#), who noted that compressive strength rises with the increased content of copper wire fibers, with the highest strength observed at 1.5% fiber content after 28 days of curing. This behavior can be attributed to the ability of micro-fibers to enhance compressive strength by arresting the propagation of micro cracks, as corroborated by [\(Naser, et al., 2020\)](#).

[Figure III. 17](#) shows that after the 1.5% fiber content, there is a reduction in the compressive strength of the M11 mix. [\(Naser, et al., 2020\)](#) explained this reduction as being caused by an increase in air voids and this is also consistent with the air content results shown in [Figure III.16](#). Moreover, the decline in compressive strength observed in M11 can also be attributed to the non-uniform and inconsistent distribution of the fibers within the concrete matrix.

III.3.2.2. Flexural tensile strength

The test aims to investigate the impact of incorporating UE7 Bronze Shavings Fibers (BF-UE7) as reinforcement on the flexural tensile strength of high-flow sand concrete at 3, 7, 28, and 90 days, as demonstrated by the histogram in [Figure III. 18](#)

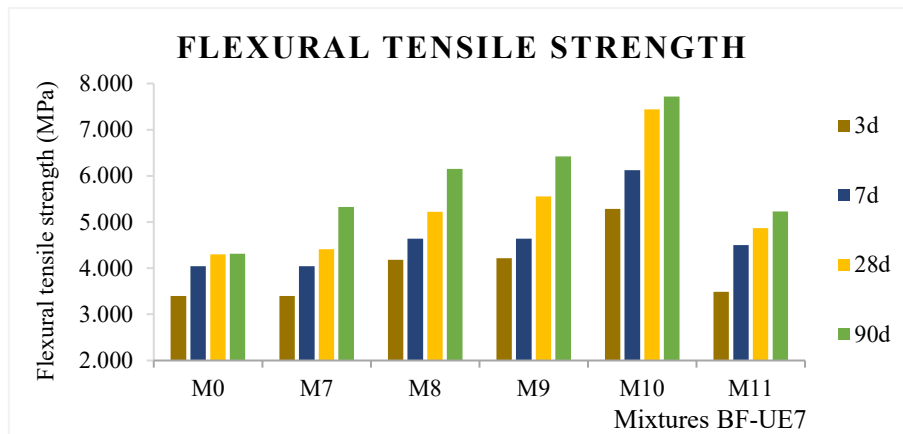


FIGURE III. 18. FLEXURAL TENSILE STRENGTH OF MIXES WITH BF-UE7

The high-flow sand concrete reinforced with UE7 bronze shavings fibers (BF-UE7) demonstrates a significantly higher flexural tensile strength compared to the reference concrete (M0). The strength increases steadily, reaching a peak improvement of 78.74% with the M10 mix, followed by a decline in the M11 mix. These results were recorded after 90 days of curing. For Bronze shavings fibers (UE7-BF), the increase in flexural tensile strength ranges from 21% to 78%, with the highest improvement (78%) observed at a 1.5% fiber ratio, which is considered the optimal addition level for this fiber type. UE7-BF, categorized as microfibers, are highly effective in arresting micro-cracks and preventing their evolution into macro-cracks. This behavior is consistent with the findings of (Naser, et al., 2020), who documented similar outcomes regarding the crack-bridging capabilities of microfibers in enhancing flexural performance.

III.3.2.3. Split tensile strength

Figure III. 19 illustrates the evaluation of split tensile strength in high-flow sand concrete reinforced with UE7 Bronze Shavings Fibers (BF-UE7), measured at 3, 7, 28, and 90 days.

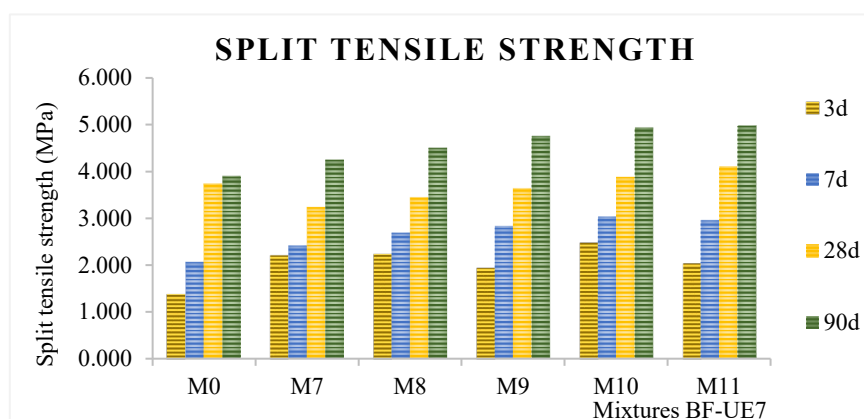


FIGURE III. 19. SPLIT TENSILE STRENGTH OF MIXES WITH BF-UE7

Incorporating UE7 Bronze Shavings Fibers (BF-UE7) into high-flow sand concrete resulted in a notable enhancement of split tensile strength over a 90-day curing period. The improvements ranged from 9% to 28%, with the maximum strength observed at a 2% fiber content. This optimal performance aligns with the findings of (Shobana & Brinila Bright, 2017). The fibers bridged the cracks in the central regions.

III.3.3. Physio-chemical properties

III.3.3.1. Absorption by immersion

In this study, HFSC was reinforced with BF-UE7 fibers to investigate their effect on water absorption by immersion over 24 hours. The results, as shown in Figure III. 20:

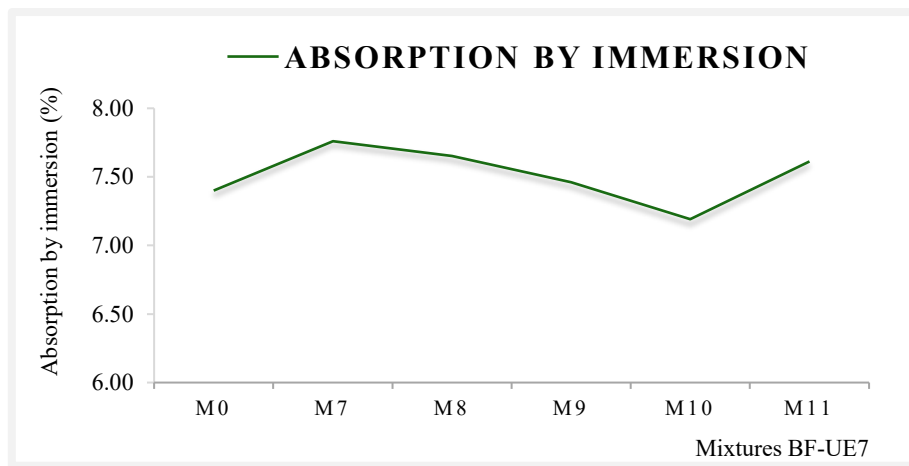


FIGURE III. 20. ABSORPTION BY IMMERSION OF MIXES WITH BF-UE7

The mix M10 (1.50% BF-UE7) achieved the best results in water absorption by immersion among the Bf-UE7 reinforced mixtures. However, when compared to SSF-316L, its performance was inferior. These results indicate that incorporating Bf-UE7 bronze fibers into HFSC didn't lead to a significant improvement in resistance to water absorption by immersion. (Huang, et al., 2024). The absorption coefficient decreased compared to the reference concrete, suggesting that there were partial improvements in absorption properties. However, the lack of connectivity between the internal pores and the incomplete connectivity of the voids in the matrix limited the enhancement in water resistance.

III.3.3.2. Capillary absorption

Figure III. 21 shows the effect of different ratios of BF-UE7 (0%, 0.25%, 0.5%, 1%, 1.5%, and 2%) on the capillary absorption of HFSC at 4320 minutes:

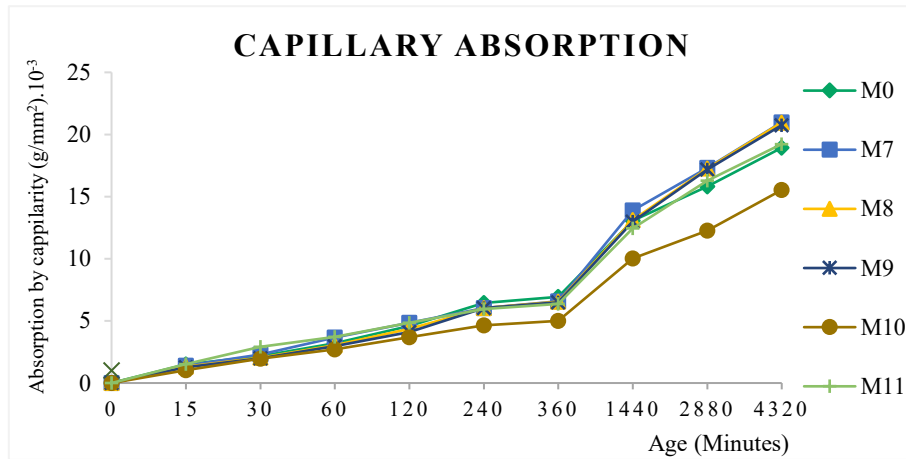


FIGURE III. 21. CAPILLARY ABSORPTION OF MIXES WITH BF-UE7

The optimal ratio for reducing capillary absorption in HFSC reinforced with Bf-UE7 is 1.50% (M10). This percentage effectively enhances density, reduces air content, and minimizes porosity. It isn't recommended to use percentages lower or higher than 1.50%, as they may lead to the formation of additional voids, negatively affecting the concrete matrix. (Oliveira, et al., 2006)

III.3.3.3. Sorptivity

The sorptivity results are presented in Figure III. 22 illustrating capillary absorption over time. This evaluates the rate at which water is absorbed per unit of time in HFSC reinforced with BF-UE7 fibers.

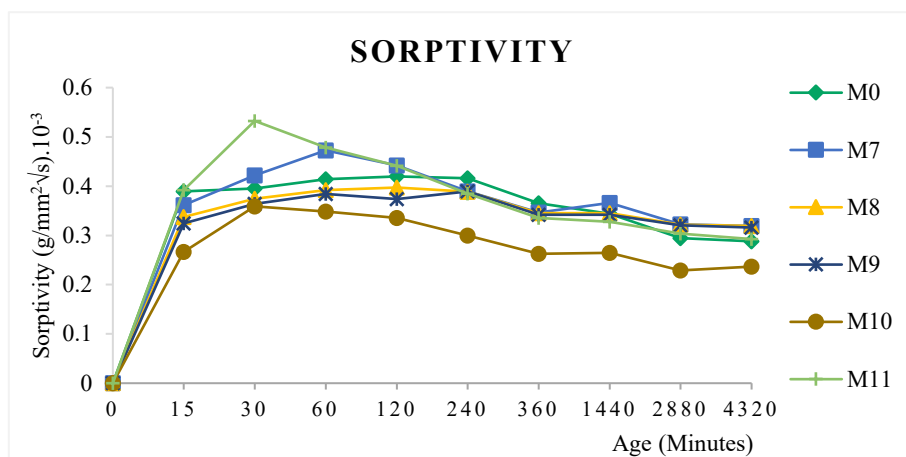


FIGURE III. 22. SORPTIVITY OF MIXES WITH BF-UE7

In HFSC reinforced with BF-UE7, capillary absorption starts with high values and decreases over time. The mix M10 (1.50% Bf-UE7) achieves the lowest sorptivity compared to the reference mix M0, as this optimal percentage enhances the concrete's density, reduces air content, and minimizes porosity. The sorptivity results are consistent with the capillary absorption trends. (Oliveira, et al., 2006)

III.3.3.4. Shrinkage

The shrinkage strain results for HFSC reinforced with BF-UE7 fibers are presented in [Figure III. 23](#)

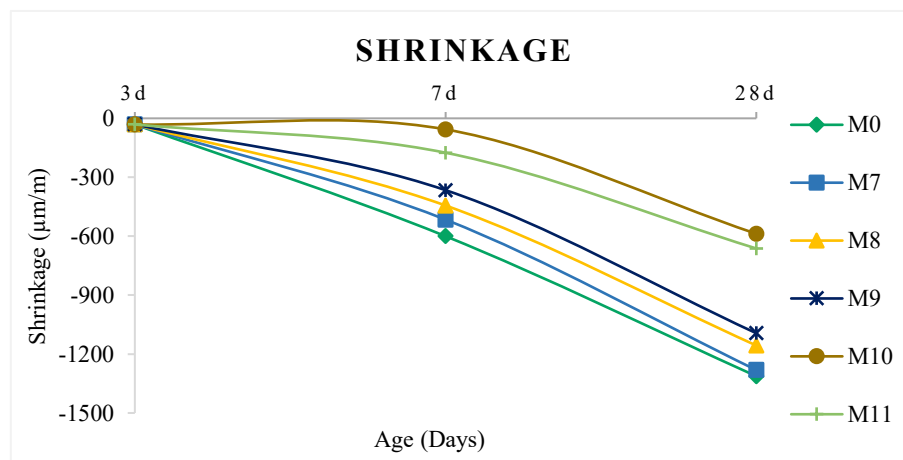


FIGURE III. 23. SHRINKAGE OF MIXES WITH BF-UE7

All the mixtures of HFSC reinforced with BF-UE7 fibers showed a reduction in shrinkage compared to the reference mix (M0), highlighting the positive effect of BF-UE7 fibers in reducing shrinkage in HFSC.

M10 (1.50% BF-UE7) exhibited the best overall performance, particularly in reducing shrinkage in both the early term and long term.

III.3.3.5. Swelling

The swelling results for HFSC reinforced with BF-UE7 fibers are presented in [Figure III. 24](#)

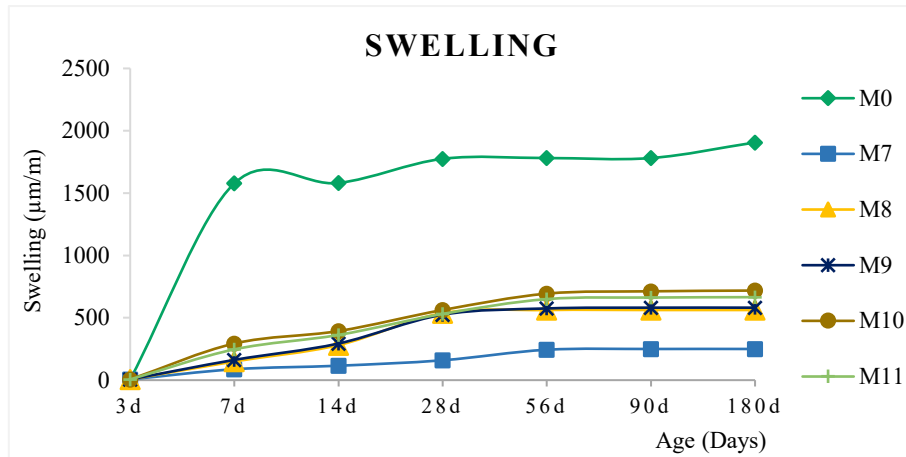


FIGURE III. 24. SWELLING OF MIXES WITH BF-UE7

The M7 mixture (0.25% BF-UE7) recorded the lowest swelling strain, stabilizing at 250.0 μm after 90 days and achieving an 87% reduction compared to M0 at 180 days.

All mixtures (M7 to M11) demonstrated reductions in swelling relative to the reference mixture (M0), highlighting the role of BF-UE7 fibers in enhancing the physio-chemical properties of HFSC. Swelling increased progressively during the early term (7, 14, and 28 days). However, after 90 days, the mixtures nearly constant swelling values.

III.3.4. Chemical properties

III.3.4.1. Weight loss in sulfuric acid (H_2SO_4)

The effect of bronze shavings (BF-UE7 microfibers) added at varying ratios (0.25%, 0.5%, 1%, 1.5%, and 2%) on the durability of high-flow sand concrete was investigated by exposing the mixtures to a 5% sulfuric acid (H_2SO_4) solution. The weight loss was measured at the initial state, as well as after 1 day, 28 days, and 90 days, as illustrated in [Figure III. 25](#)

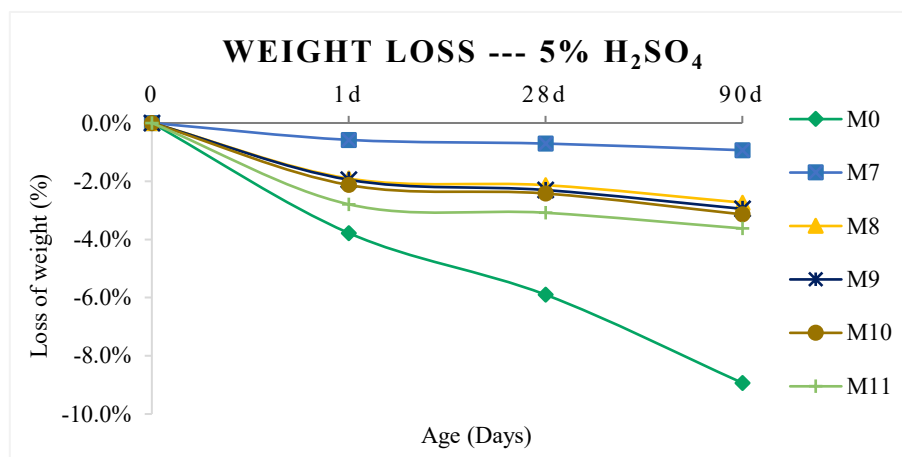


FIGURE III. 25. WEIGHT LOSS OF MIXES WITH BF-UE7 EXPOSED SULFURIC ACID

The reference concrete (M0), without fibers, showed a weight loss of 8.93% after 90 days of exposure to sulfuric acid (H_2SO_4). In comparison, the fiber-reinforced mixes (M7 to M11) recorded reduced weight loss ranging from 0.58% to 3.62%. The addition of BF-UE7 microfibers effectively reduced corrosion and enhanced the resistance of HFSC to sulfuric acid-induced degradation. (Dhanaraj & Sakthieswaran, 2016)

Bronze corrodes in high concentrations of sulfuric acid (H_2SO_4), especially in the presence of oxygen or additional sulfate ions, leading to the degradation of copper and the formation of copper sulfate ($CuSO_4$), which dissolves and weakens the fiber structure.

This explains the deterioration of mix M10, despite its excellent physical, mechanical, and physico-chemical properties.

III.3.4.2. Weight loss in hydrochloric acid (HCl)

Figure III. 26 illustrates the impact of incorporating bronze shavings (BF-UE7 microfibers) at varying ratios (0.25%, 0.5%, 1%, 1.5%, and 2%) on the durability of high-flow sand concrete (HFSC) when exposed to 5% hydrochloric acid (HCl). The weight loss was recorded at the initial state, as well as after 1 day, 28 days, and 90 days:

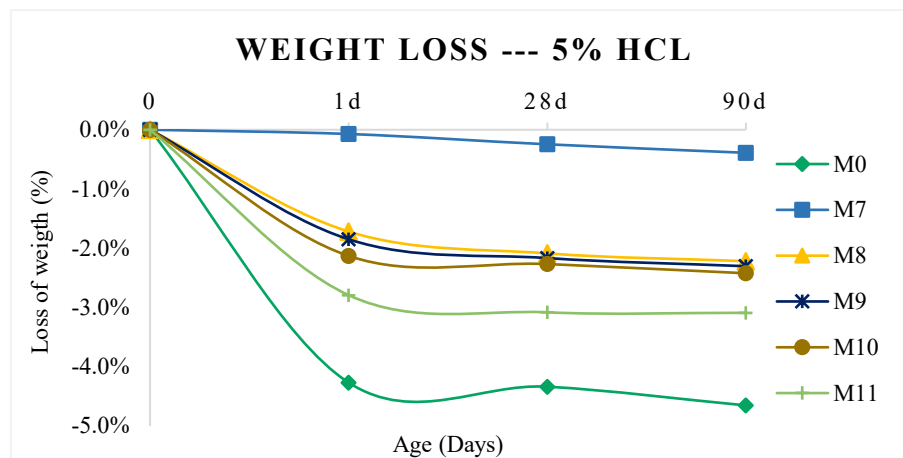


FIGURE III. 26. WEIGHT LOSS OF MIXES WITH BF-UE7 EXPOSED HYDROCHLORIC ACID

Micro fiber reinforced samples (M7 to M11) showed a notable reduction in weight loss compared to the reference concrete (M0). The mix with 0.25% BF-UE7 fibers (M7) exhibited the best performance, with a weight loss of only 0.39% after 90 days, effectively minimizing degradation caused by 5% HCl exposure. These results highlight the efficiency of microfibers (BF-UE7) in improving the Attack acid resistance of HFSC.

Copper in bronze can react with hydrochloric acid (HCl) to form copper chloride (CuCl_2), which is soluble in water, leading to the gradual corrosion of the fibers. This explains the deterioration of mix M10, despite its excellent physical, mechanical, and physico-chemical properties.

III.3.5. SEM

The improvement in the properties of HFSC reinforced with BF-UE7, as illustrated in [Figure III. 27](#), was examined using Scanning Electron Microscopy (SEM).

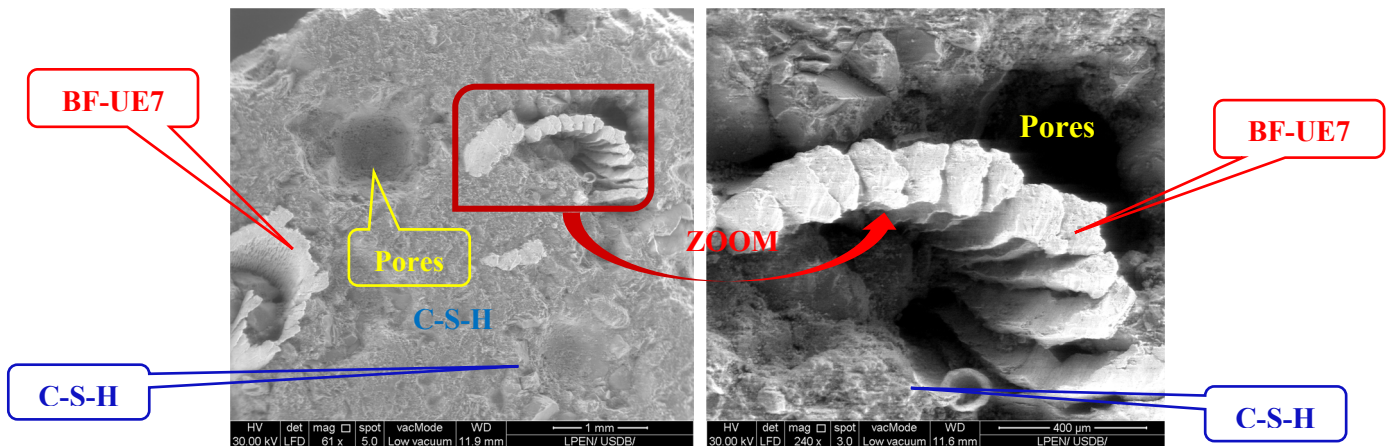


FIGURE III. 27. SEM OF M10 REINFORCED WITH BF-UE7

The [Figure III. 27](#) shows that the incorporation of BF-UE7 in the mix M10 led to a reduction in both the pore size and quantity, as the fibers filled the micro air pores. This resulted in a 29.03% reduction in air content and an increase in mix density by 31 kg/m^3 compared to the reference concrete (M0). As a result, these changes contributed to enhanced physical, mechanical, and physio-chemical properties of the HFSC. This improvement is also attributed to the bronze fibers having irregular edges, which allows for good cohesion and adhesion with C-S-H (calcium silicate hydrate).

III.3.6. Evaluation and justification for the optimal performance of BF-UE7 in HFSC

The Evaluation of bronze shavings fibers (BF-UE7) on HFSC Properties:

Physical properties

M10 demonstrated the best workability and density, with minimal air content, improving cohesion and reducing voids.

Mechanical properties

M10 achieved the highest compressive and flexural strength, while M11 showed superior split tensile strength.

Physico-chemical properties

M10 exhibited the lowest absorption by immersion, capillary absorption, and sorptivity, effectively reducing porosity and shrinkage. M7 was effective in minimizing swelling.

Chemical properties

M7 demonstrated resistance to acid attacks, particularly from H₂SO₄ and HCl.

The SEM analysis confirmed the efficient integration of BF-UE7 fibers within the cement matrix.

Based on these results, M10 is identified as the optimal mix.

III.4. High flow sand concrete reinforced with waste polyester fiber (WPF)

In this section, a comprehensive analysis is conducted on the results obtained from High-Flow Sand Concrete samples reinforced with waste polyester fibers (WPF). The physical properties (slump, density, and air content), mechanical properties (compressive strength, flexural tensile strength, and split tensile strength), chemical properties (effects of sulfuric and hydrochloric acid attacks), and physio-chemical properties (shrinkage, swelling, absorption by immersion and capillarity, and sorptivity) are examined. Additionally, microstructural analysis through Scanning Electron Microscopy (SEM) is included.

III.4.1. Physical properties

The results of the physical properties of the High-Flow Sand Concrete (HFSC) reinforced with Waste Polyester Fiber (WPF) in its fresh state are represented as follows: the slump values are shown in [Figure III. 28](#), the density measurements in [Figure III. 29](#), and the air content values [Figure III. 30](#). These properties were measured in accordance with the standards described in the previous Chapter II.

III.4.1.1. Slump

To assess the impact of Waste Polyester Fibers (WPF) on the workability and consistency of sand concrete, the results of the slump test were analyzed, as illustrated in the curve shown [Figure III. 28](#)

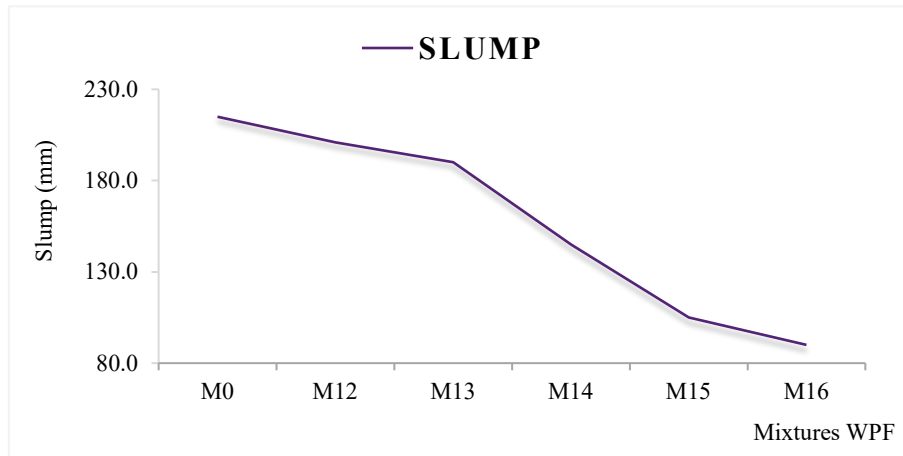


FIGURE III. 28. SLUMP OF MIXES WITH WPF

Upon incorporating Waste Polyester Fibers (WPF) into the sand concrete mixtures labeled M12, M13, M14, M15 and M16, a noticeable reduction in slump values was observed compared to the reference concrete (M0), with decreases of 6.51%, 11.62%, 32.55%, 51.16% and 58.14%, respectively. The addition of Waste Polyester Fibers (WPF) to the sand concrete led to a decrease in workability, as reflected by reduced bleeding and lower slump values. As shown in [Figure III. 28](#), all concrete mixes containing Waste Polyester Fibers (WPF) exhibited reduced workability compared to the base concrete (SC0). These results are consistent with the research findings of [\(Ali, et al., 2020\)](#).

III.4.1.2. Density

The test will examine the changes in the density of sand concrete when varying proportions of Waste Polyester Fibers (WPF) are gradually incorporated. The results, as illustrated in [Figure III. 29](#), will highlight the effect of these fibers on the concrete's density.

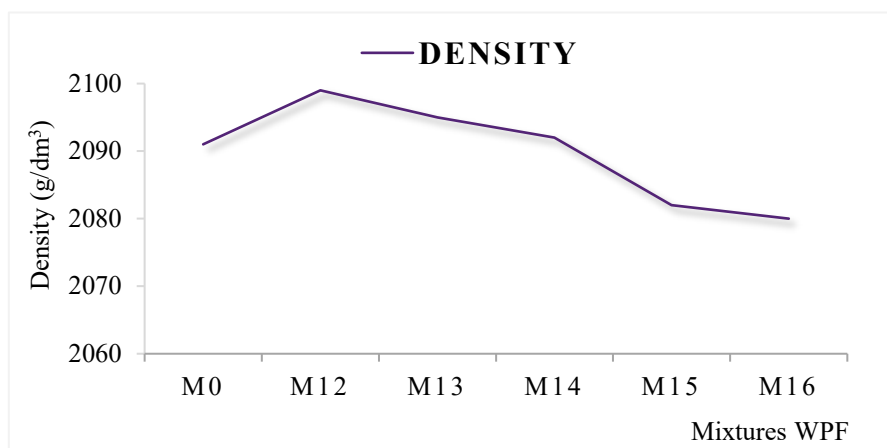


FIGURE III. 29. DENSITY OF MIXES WITH WPF

Figure III. 29 illustrates the increase in density of high-flow sand concrete (HFSC) reinforced with 0.25% to 0.5% Waste Polyester Fibers (WPF) in mixtures M12 and M13. The addition of 1%, 1.5%, and 2% WPF in mixtures M14, M15, and M16, however, results in a decrease in density compared to the reference concrete (M0).

The incorporation of 0.25% to 0.5% WPF reduces air voids in the HFSC, contributing to the observed increase in density. In contrast, adding 1%, 1.5%, and 2% WPF reduces the density due to the replacement of the sand-concrete matrix by the fibers.

These results align with the findings of Abdulridha Q.S. et al. (2022), who attributed the reduction in density to the higher air content trapped in concrete containing Waste Rope Fibers (WRF), as well as the lower density of these fibers (recycled polyester fibers = 1.38 g/cm³) compared to other concrete constituents.

III.4.1.3. Air content

This test to assess the changes in air content of high-flow sand concrete as varying proportions of Waste Polyester Fibers (WPF) are incrementally incorporated, as illustrated in Figure III. 30

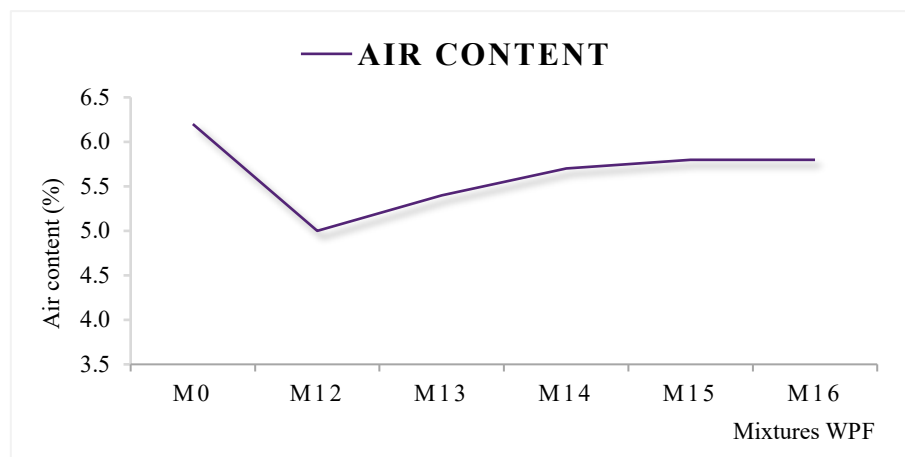


FIGURE III. 30. AIR CONTENT OF MIXES WITH WPF

The decrease in air content in high-flow sand concrete (HFSC) reinforced with 0.25% to 0.5% by mass of Waste Polyester Fibers (WPF) in mixes M12 and M13 is shown in Figure III. 30. Conversely, the incorporation of 1%, 1.5%, and 2% WPF in mixes M14, M15, and M16 causes an increase in air content compared to the reference concrete (M0).

This confirms the previous explanation regarding density provided by Abdulridha Q.S. et al. (2022), as the incorporation of 0.25% to 0.5% WPF replaces air voids in the HFSC. However, adding 1%, 1.5%, and 2% WPF disrupts the sand-concrete matrix, leading to an increase in air voids.

III.4.1.4. Relationship between density & air content

Figure III. 31 presents the relationship between density and air content in fresh High Flow Sand Concrete (HFSC) reinforced with Waste Polyester Fibers (WPF):

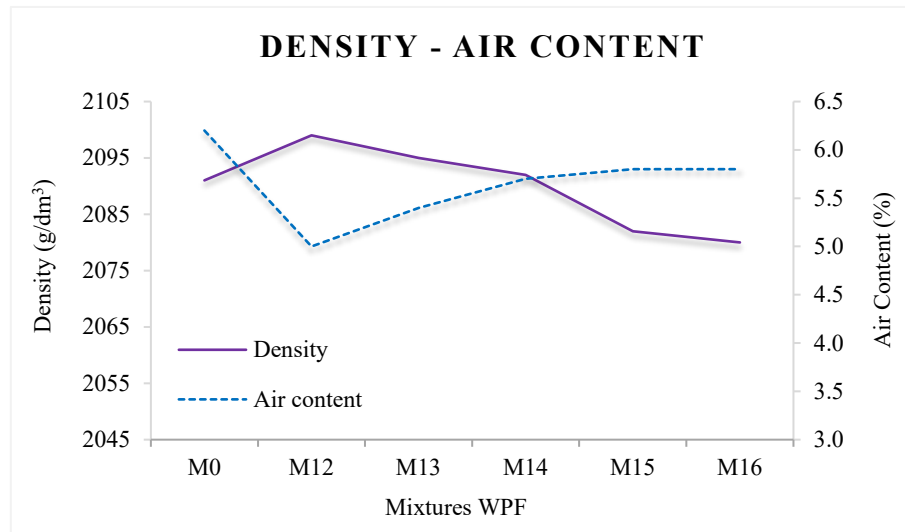


FIGURE III. 31. RELATIONSHIP BETWEEN DENSITY & AIR CONTENT OF MIXES WITH WPF

A clear inverse relationship was observed between density and air content in HFSC when WPF fibers were added. As the density increased, the air content decreased, suggesting that the fibers displaced the air present within the concrete. This indicates that the fibers occupied space within the HFSC matrix.

Furthermore, at a fiber content of 1%, a balance point was identified between density and air content. Beyond this threshold, as more fibers were added, the air content increased while the density decreased. This suggests that the fibers began to replace the concrete in the mix, as the density of the concrete is approximately 2091 g/dm³, while the density of the fibers is around 1380 g/dm³.

III.4.2. Mechanical properties

III.4.2.1. Compressive strength

The histogram in Figure III. 32 presents the compressive strength outcomes at 3, 7, 28 and 90 days for Waste Polyester Fibers (WPF)-reinforced sand concrete.

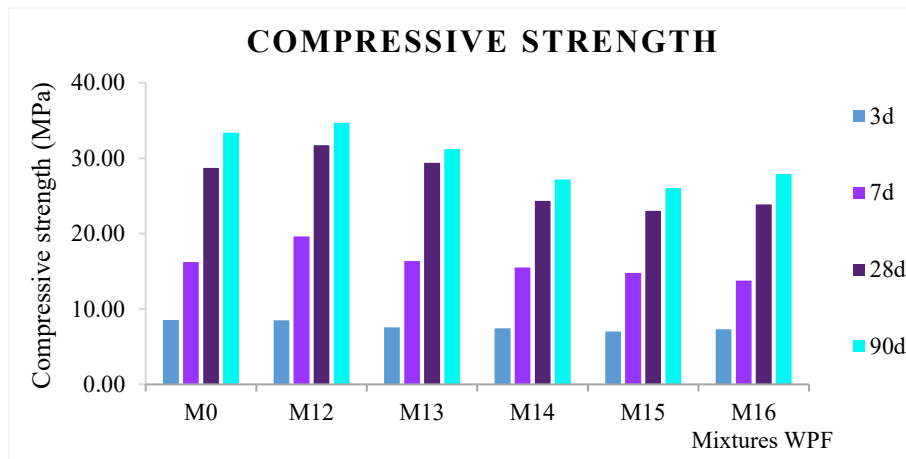


FIGURE III. 32. COMPRESSIVE STRENGTH OF MIXES WITH WPF

According to the results shown in [Figure III. 32](#), the addition of Waste Polyester Fibers (WPF) to the M12 mixture at a ratio of 0.25% led to an increase in compressive strength by 3.92% compared to the reference concrete (M0) after 90 days. However, in the M13, M14, M15, and M16 mixtures, as more Waste Polyester Fibers (WPF) were added, the compressive strength decreased, with the reduction reaching 21.95% in the M15 mixture compared to the reference concrete (M0) after 90 days.

These findings are consistent with the research by ([Christopher, et al., 2023](#)), which concluded that compressive strength decreases as the polyester fiber content increases from 0.5% to 1.0%. This reduction can be attributed to improper fiber distribution, as the fibers' highly porous microstructure leads to the formation of a weak interfacial zone between the fibers and the cement paste. The addition of excess fibers does not contribute to the development of strength, and the poor inter face between the fiber and cementitious matrix increases the air content and reduces the compressive strength.

III.4.2.2. Flexural tensile strength

The test aims to investigate the impact of incorporating waste polyester fiber (WPF) as reinforcement on the tensile strength of sand concrete at 3, 7, 28 and 90 days, as demonstrated by the curve in [Figure III. 33](#):

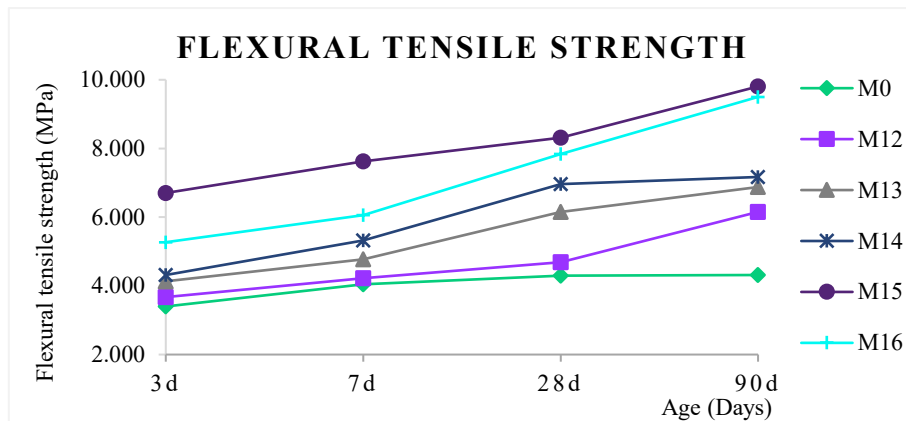


FIGURE III. 33. FLEXURAL TENSILE STRENGTH OF MIXES WITH WPF

According to the data illustrated in Figure III. 33, sand concrete incorporating Waste Polyester Fibers (WPF) exhibits significantly higher flexural tensile strength compared to the reference mix without fibers (M0). Specifically, M12, M13, M14, M15, and M16 show improvements of 42.56%, 59.35%, 66.12%, 127.20%, and 120.14%, respectively, after 90 days relative to the M0 mix. Based on this test and these parameters, the best mixture is M15, which incorporates 1.5% WPF.

The results indicate that incorporating waste polyester fibers improves the flexural tensile strength, consistent with the findings of (Fode, et al., 2024). In his study, it was noted that this improvement is due to the use of waste synthetic fibers, which enhance the ductility of the concrete matrix, thereby increasing the ultimate bending capacity of the cementitious material.

III.4.2.3. Split tensile strength

The objective of this test is to investigate the effect of including Waste Polyester Fibers (WPF) on the splitting tensile strength of sand concrete at 3, 7, 28 and 90 days. The results displayed in Figure III. 34 clearly highlight this impact

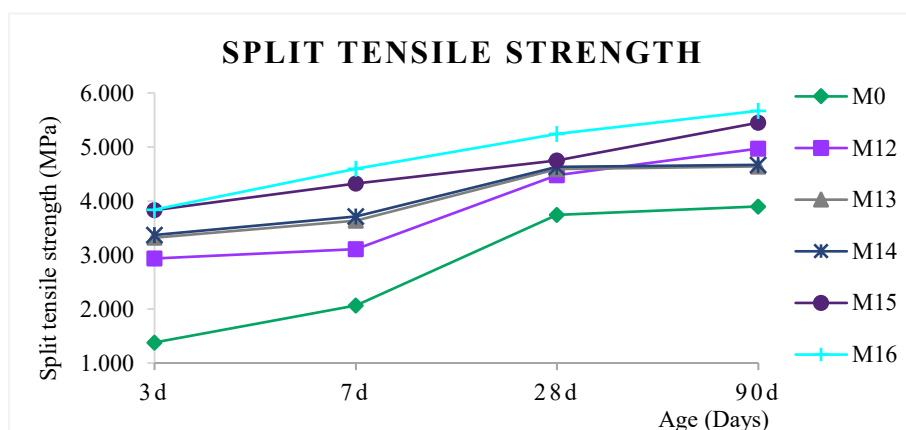


FIGURE III. 34. SPLIT TENSILE STRENGTH OF MIXES WITH WPF

Based on the findings presented in [Figure III. 34](#), it appears that sand concrete reinforced with Waste Polyester Fibers (WPF) demonstrates a higher splitting tensile strength compared to reference sand concrete without fibers (M0). The results show that M12, M13, M14, M15, and M16 exhibit increases in splitting tensile strength of 19.78%, 22.69%, 23.82%, 27.04% and 40.11%, respectively, at 28 days when compared to the mix M0.

These results indicate that the splitting strength is consistently enhanced by Waste Polyester Fibers (WPF), attributed to their high tensile properties. This is in accordance with the findings of [Wang .J et al. \(2023\)](#), who confirmed that it was shown that the strength of cement-stabilized concrete can be improved by the polyester fiber, particularly regarding the splitting tensile strength.

III.4.4. Physio-chemical properties

III.4.4.1. Absorption by immersion

In this study, HFSC was reinforced with Waste Polyester Fibers (WPF) to investigate their effect on water absorption by immersion over 24 hours. The results are presented in [Figure III. 35](#).

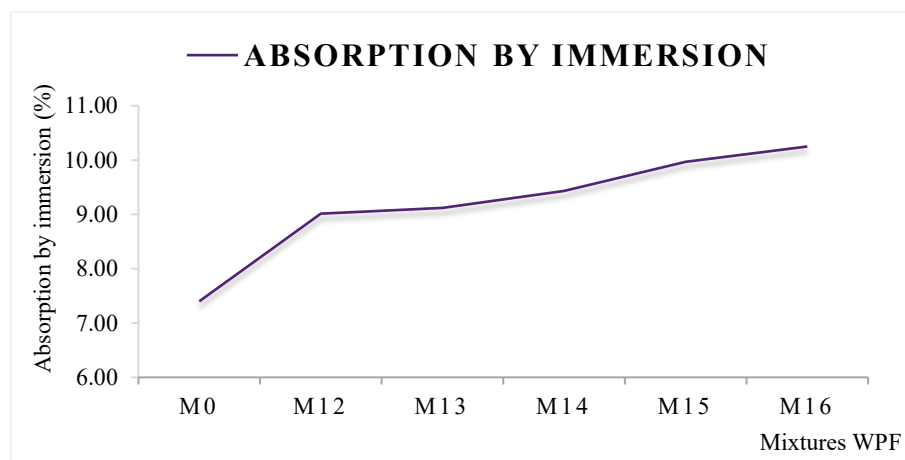


FIGURE III. 35. ABSORPTION BY IMMERSION OF MIXES WITH WPF

The results indicate that incorporating WPF into HFSC gradually increased water absorption by immersion compared to the reference mix (M0), suggesting that WPF may introduce new voids within the concrete matrix. Additionally, WPF is characterized by its ability to absorb water, contributing to the overall increase in water absorption by immersion.

III.4.4.2. Capillary absorption

The effect of different ratios of WPF (0%, 0.25%, 0.5%, 1%, 1.5%, and 2%) on the capillary absorption of HFSC at 4320 minutes, as shown in [Figure III. 36](#)

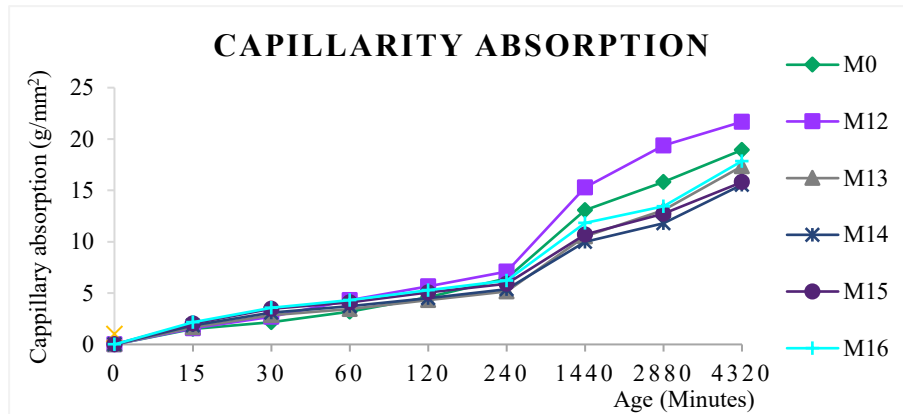


FIGURE III. 36. CAPILLARITY ABSORPTION OF MIXES WITH WPF

At early stages, the ratio of 0.50% (M13) shows the lowest capillary absorption in HFSC reinforced with waste polyester fibers (WPF). After 240 minutes, the M14 mix (1.00%) demonstrates better performance, while after 4320 minutes, the results for M14 and M15 (1.50%) converge. This underscores the importance of defining the specific application requirements of HFSC to determine the most suitable WPF fiber ratio for optimal performance.

III.4.4.3. Sorptivity

[Figure III. 37](#) presents the sorptivity results, reflecting the water absorption rate per unit of time for HFSC reinforced with WPF:

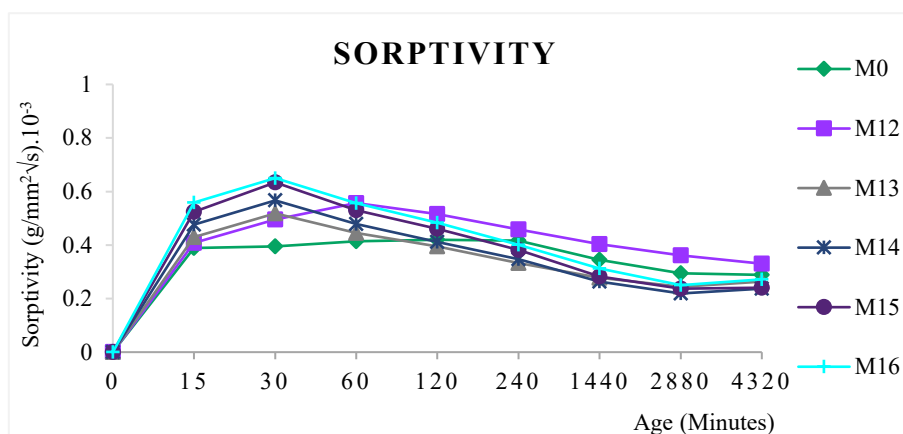


FIGURE III. 37. SORPTIVITY OF MIXES WITH WPF

At 30 minutes, the reference mix M0 (0% WPF) showed the lowest sorptivity values. As the WPF content increased, sorptivity gradually rose, peaking in M16 (2% WPF).

Over time, sorptivity decreased until reaching the lowest values in M14 (1% WPF) and M15 (1.5% WPF) at 4320 minutes. While WPF has an absorptive nature, it enhances concrete performance over time when used at specific ratios.

III.4.4.4. Shrinkage

The shrinkage strain results for HFSC reinforced with WPF fibers are presented in [Figure III.38](#)

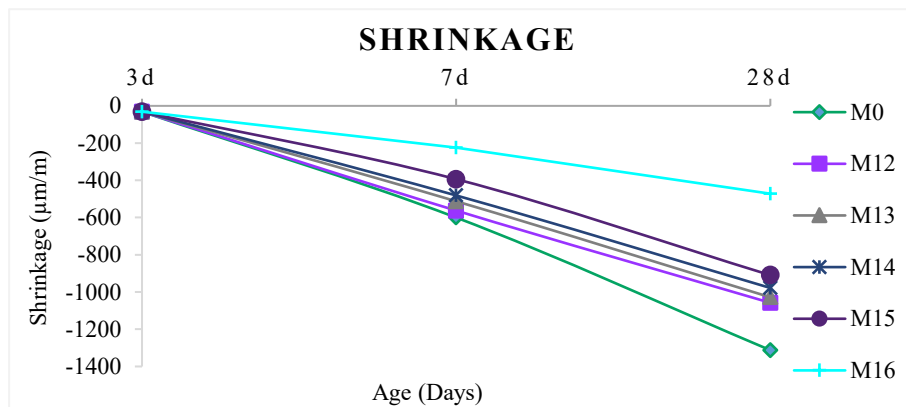


FIGURE III. 38. SHRINKAGE OF MIXES WITH WPF

All the mixtures of HFSC reinforced with WPF fibers showed a reduction in shrinkage compared to the reference mix (M0), highlighting the positive effect of WPF fibers in reducing shrinkage in HFSC.

M16 (2.0% WPF) exhibited the best overall performance, particularly in reducing shrinkage in both the early term and long term, reflecting the effectiveness of these fibers in enhancing the cohesion of the concrete matrix. (Wang, et al., 2023)

III.4.4.5. Swelling

The swelling results for HFSC reinforced with WPF fibers are presented in [Figure III. 39](#)

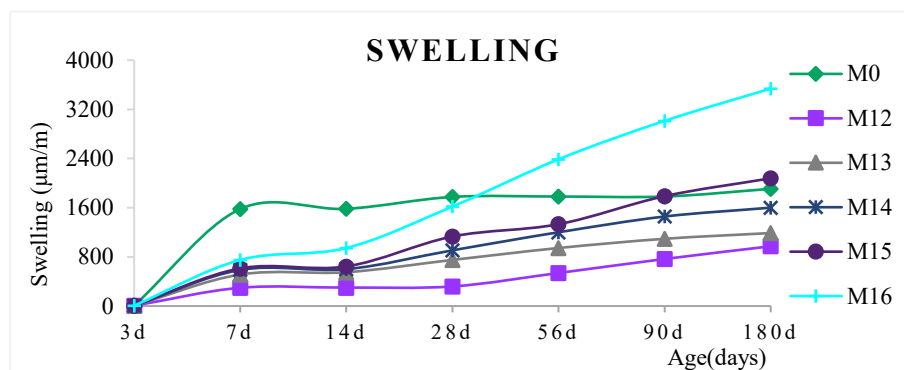


FIGURE III. 39. SWELLING OF MIXES WITH WPF

The M12 mixture (0.25% WPF) showed the best performance, with a 49.2% reduction in swelling at 180 days compared to the reference concrete (M0).

In the early term (3, 7, 14, and 28 days), all mixtures (M12 to M16) recorded lower swelling values than the reference concrete (M0). After 90 days, swelling in the M15 and M16 mixtures increased and surpassed the swelling of M0. This increase in swelling strain led to negative effects on the physio-chemical properties of HFSC.

III.4.4. Chemical properties

III.4.4.1. Weight loss in sulfuric acid (H_2SO_4)

The study evaluated HFSC with waste polyester fibers (WPF) at 0.25%, 0.5%, 1%, 1.5%, and 2% by mass. Durability was tested under 5% sulfuric acid (H_2SO_4) exposure, measuring weight loss at 0, 1, 28, and 90 days, as illustrated in [Figure III. 40](#)

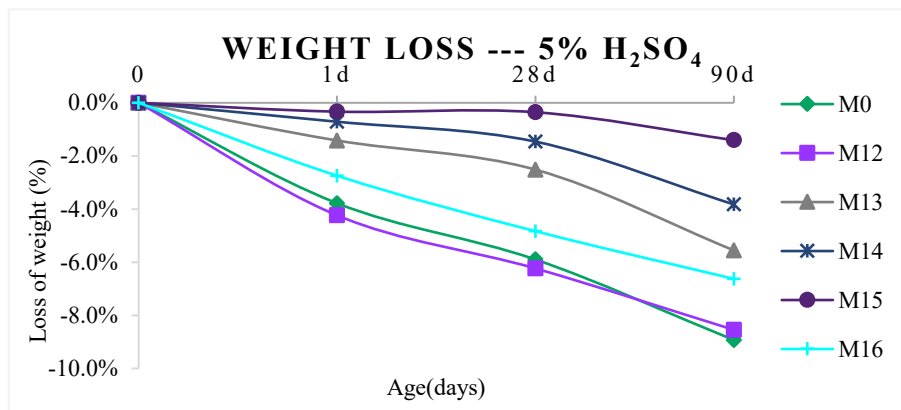


FIGURE III. 40. WEIGHT LOSS OF MIXES WITH WPF -- (H_2SO_4)

The results showed that the reference concrete (M0) lost 8.93% of its weight after 90 days of exposure to a 5% H_2SO_4 solution. The WPF-reinforced mixtures (M12 to M16) improved durability, with the M15 mix (1.5% WPF) achieving the lowest weight loss of 1.41% at 90 days.

III.4.4.2. Weight loss in hydrochloric acid (HCl)

Waste polyester fibers (WPF) were incorporated into HFSC at dosages of 0.25%, 0.5%, 1%, 1.5%, and 2% by mass. The samples were exposed to a 5% HCl solution, and weight loss was measured after 1, 28, and 90 days, as shown in [Figure III. 41](#)

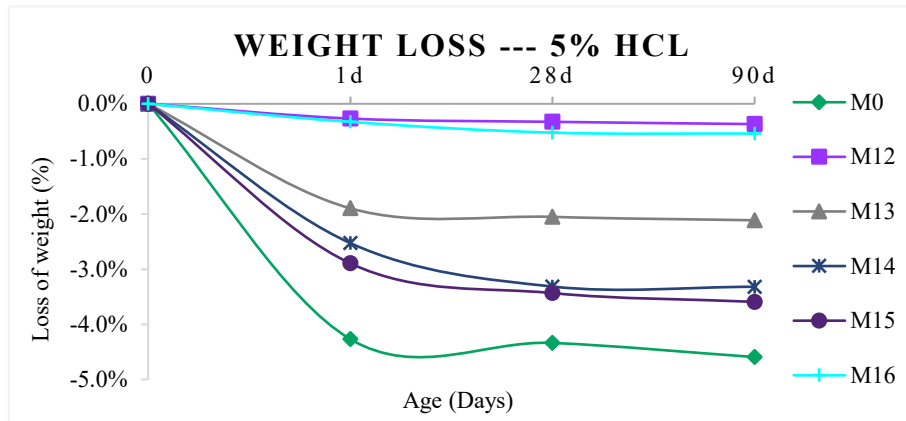


FIGURE III. 41. WEIGHT LOSS OF MIXES WITH WPF – (HCl)

The results indicate that incorporating WPF into HFSC enhances its durability against chemical attacks from 5% HCl, provided the WPF ratios are precisely selected. For example, a low dosage of 0.25% in mix M12 demonstrated improved durability, with a weight loss of 0.37% at 90 days. Conversely, when the WPF content exceeded 0.5% (M13), the loss of weight increased, peaking at 1.5% in mix M15. After this ratio, an improvement was observed.

III.4.5. SEM

The microstructure was examined using Scanning Electron Microscopy (SEM) to investigate the cause of the changes in the properties of HFSC reinforced with BF-UE7, as shown in Figure III. 42

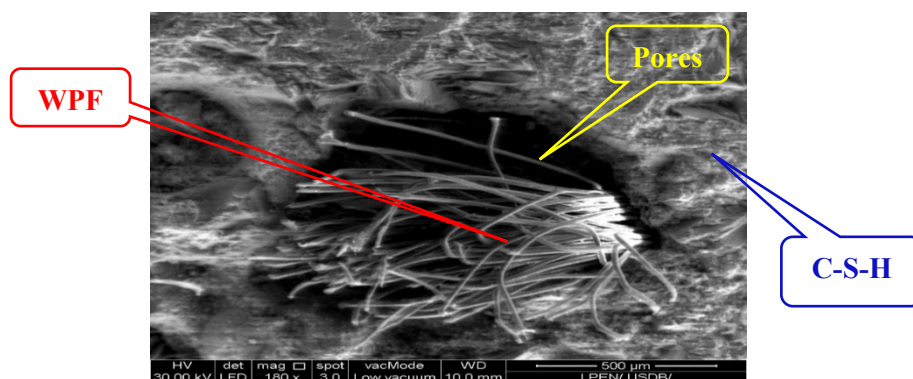


FIGURE III. 42. SEM OF MIXES WITH WPF

The incorporation of WPF in the mix M12 led to a reduction in pore size, with the fibers filling the air voids. This resulted in a 19% reduction in air content and an increase in the density by 8 kg/m^3 compared to the reference concrete (M0). Conversely, as the WPF dosage increased in mix M15 (1.5% WPF), the density decreased by 19 kg/m^3 . This is because the 0.25% WPF filled the air voids, while the higher dosage (1.5% WPF) replaced the cementitious matrix. This

explains the results of M15, where there was a 21.95% decrease in compressive strength, while the Flexural tensile strength increased by 127%.

III.4.6. Evaluation and justification for the optimal performance of WPF in HFSC

The Evaluation of waste polyester fibers (WPF) on HFSC properties:

Physical properties

M12 demonstrated optimal results for workability, density, and minimal air content, improving cohesion and reducing voids.

Mechanical properties

M12 achieved the highest compressive strength, while M15 exhibited superior flexural and split tensile strength.

Physico-chemical properties

Absorption by Immersion: M12 exhibited the lowest absorption.

Capillarity and Sorptivity: M12 excelled in the short term (0–30 minutes), whereas M15 showed better performance in the long term (after 30 minutes).

Shrinkage: M15 and M16 significantly reduced shrinkage.

Swelling: M12 effectively minimized swelling.

Chemical properties

M15 demonstrated better resistance to sulfuric acid (H_2SO_4), while M12 was more resistant to hydrochloric acid (HCl).

Based on these results, both M12 and M15 are selected due to their complementary strengths.

III.5. High flow sand concrete reinforced with hybrid fibers

In this section, a comprehensive analysis is carried out on the results obtained from High-Flow Sand Concrete samples reinforced with Hybrid fibers, including Dual fiber systems (micro and macro metallic fibers), Dual fibers (metallic and synthetic fibers), and Triple fiber systems (micro and macro metallic fibers combined with synthetic fibers). The physical properties (slump, density, and air content), mechanical properties (compressive strength, flexural tensile strength, and split tensile strength), chemical properties (effects of sulfuric and hydrochloric acid attacks), and physio-chemical properties (shrinkage, swelling, absorption by immersion and capillarity, and sorptivity) are assessed. Furthermore, microstructural analysis is conducted using Scanning Electron Microscopy (SEM).

III.5.1. Hybrid fiber integration in high-flow sand concrete

- After identifying the optimal mixtures from the previously studied fibers, a hybrid system is developed by combining three types of fibers as follows:
SSF-316L macro metallic fibers: Selected from M1 with a fiber content of 0.25%.
- **BF-UE7 micro metallic fibers:** Selected from M10 with a fiber content of 1.5%.
- **WPF macro synthetic fibers:** Selected from M12 with a fiber content of 0.25% and M15 with a fiber content of 1.5%.

These fibers were first integrated into dual systems, followed by a triple fiber system, as outlined in the mix design in [Table III. 2](#) , and the formwork in [Table III. 3](#) :

TABLE III. 2. MIX DESIGN FROM HYBRID (DUAL AND TRIPLE) FIBERS REINFORCED HFSC

Mixture	Fiber identification	Fiber %
M0	Reference concrete	0%
Best mixes in mono fiber reinforcement		
M1	Reference concrete reinforced with 0.25% stainless steel shavings fibers type 316L (SSF-316L) by mass	0.25% SSF-316L
M10	Reference concrete reinforced with 1.50% Bronze fibers shavings type UE7 (BF-UE7) by mass	1.50% BF-UE7
M12	Reference concrete reinforced with 0.25% Waste Polyester Fiber (WPF) by mass	0.25% WPF
M15	Reference concrete reinforced with 1.50% Waste Polyester Fiber (WPF) by mass	1.50% WPF
Dual fiber reinforcement		
M17	Reference concrete reinforced with 0.25% SSF-316L and 1.50% BF-UE7, by mass	M1+M10
M18	Reference concrete reinforced with 0.25% SSF-316L and 0.25% WPF, by mass	M1+M12
M19	Reference concrete reinforced with 1.50% BF-UE7 and 0.25% WPF, by mass	M10+M12
M20	Reference concrete reinforced with 0.25% SSF-316L and 1.50% WPF, by mass	M1+M15
M21	Reference concrete reinforced with 1.50% BF-UE7 and 1.50% WPF, by mass	M10+M15
Triple fiber reinforcement		
M22	Reference concrete reinforced with 0.25% SSF-316L + 1.50% BF-UE7+ 0.25% WPF, by mass	M1+M10+M12
M23	Reference concrete reinforced with 0.25% SSF-316L + 1.50% BF-UE7 + 1.50% WPF, by mass	M1+M10+M15

TABLE III. 3. FORMWORK FROM HYBRID (DUAL AND TRIPLE) FIBERS REINFORCED HFSC

Mix (kg/m ³)	S	C	FL	SF	W	SP	SSF-316L	BF-UE7	WPF
M0	1267	450	100	50	270	3.6	--	--	--
Best mixes in mono fiber reinforcement									
M1	1267	450	100	50	270	3.6	5.34	--	--
M10	1267	450	100	50	270	3.6	--	32.06	--
M12	1267	450	100	50	270	3.6	--	--	5.34
M15	1267	450	100	50	270	3.6	--	--	32.06
Dual fiber reinforcement									
M17	1267	450	100	50	270	3.6	5.34	32.06	--
M18	1267	450	100	50	270	3.6	5.34	--	5.34
M19	1267	450	100	50	270	3.6	--	32.06	5.34
M20	1267	450	100	50	270	3.6	5.34	--	32.06
M21	1267	450	100	50	270	3.6	--	32.06	32.06
Triple fiber reinforcement									
M22	1267	450	100	50	270	3.6	5.34	32.06	5.34
M23	1267	450	100	50	270	3.6	5.34	32.06	32.06

III.5.2. Physical properties

Table III. 4 presents the results of the physical properties of High-Flow Sand Concrete (HFSC) reinforced with Hybrid fibers (Dual and Triple systems) in its fresh state. The slump value, density, and air content of the mixtures were measured in accordance with the standards outlined in the previous Chapter II.

TABLE III. 4. PHYSICAL PROPERTIES OF MIXES WITH HYBRID FIBERS

Mixtures	Fiber identification	Slump (mm)	Density (g/dm ³)	Air content (%)
M0	Reference Concrete	215	2091	6.2
Best mixes mono fiber reinforcement				
M1	(0.25%) SSF-316L	245	2108	5.6
M10	(1.50%) BF-UE7	240	2122	4.4
M12	(0.25%) WPF	205	2099	5
M15	(1.5%) WPF	105	2072	5.8
Dual fiber reinforcement				
M17	M1+ M10	160	2145	5.2
M18	M1 +M12	130	2096	4.8
M19	M10+M12	120	2120	4.8
M20	M1+M15	70	2073.5	5.6
M21	M10+M15	70	2093	5.4
Triple fiber reinforcement				
M22	M1+M10+M12	90	2100	4.5
M23	M1+M10+M15	60	2093	4.8

III.5.2.1. Slump

The graph [Figure III. 43](#) shows the slump test results of a series of hybrid fiber reinforced concrete mixes. The best results for the fibers mixes M1, M10, M12 and M15 were selected and then combined to produce Hybrid fibers concrete. Among them, M17, M18, M19, M20, and M21 are dual fiber systems, and M22 and M23 are triple fiber systems.

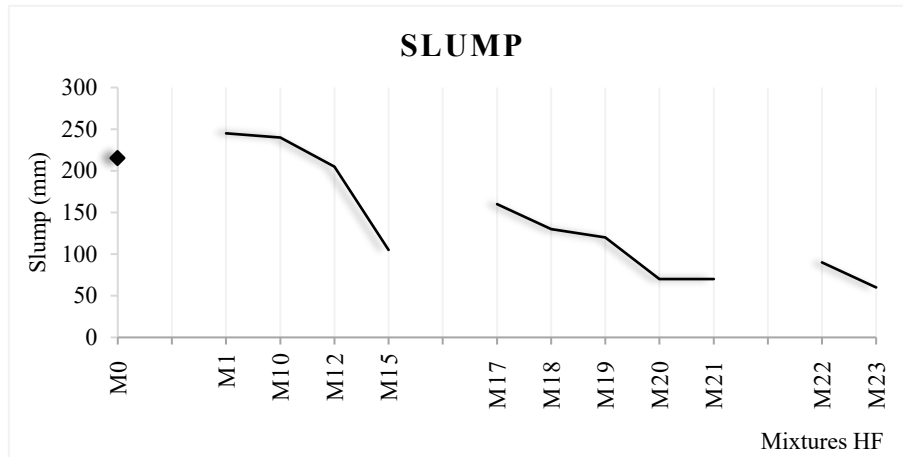


FIGURE III. 43. SLUMP OF MIXES WITH HYBRID FIBERS

The results show that the control mix (M0) achieved the slump value of 215 mm, indicating superior workability in the absence of fibers. However, a progressive decline in slump values was observed with the incremental addition of fibers, with the reduction occurring upon the inclusion of polyester fibers.

The incorporation of hybrid fibers reinforced with polyester fibers significantly reduces the workability of high-flow sand concrete (HFSC). When the M12 mix (0.25% PF) was combined with M1 and/or M10, the slump reduction was more pronounced compared to its combination with M15 (1.5% PF) along with M1 and/or M10

Triple fiber systems showed a greater slump reduction compared to dual systems, emphasizing the significant effect of higher fiber content on workability. (Aslani, et al., 2019)

III.5.2.2. Density

Density test results of various hybrid fiber (dual or triple systems) reinforced high-flow sand concrete (HFSC) mixes, including both dual and triple fiber systems, are presented in [Figure III. 44](#)

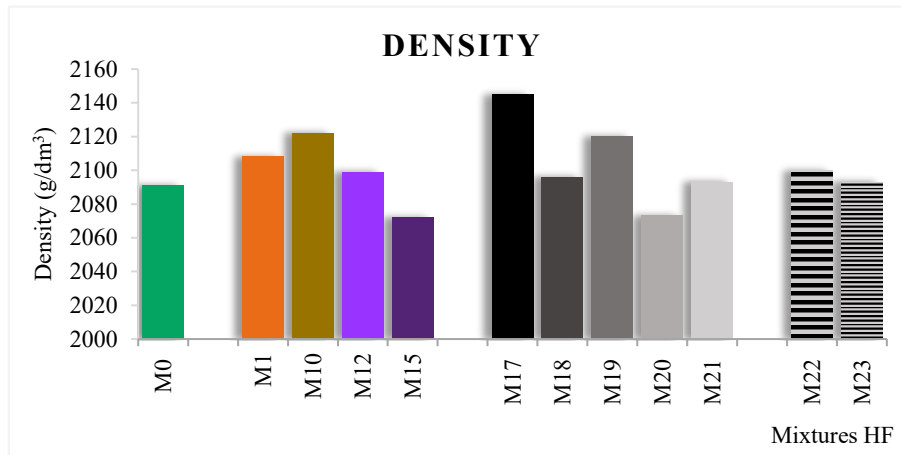


FIGURE III. 44. DENSITY OF MIXES WITH HYBRID FIBERS

Hybrid fiber mixtures exhibit a density range between 2072 g/dm³ and 2145 g/dm³. These mixtures include stainless steel shavings fibers (SSF-316L) as macro metallic fibers with corrugated surfaces, bronze fibers (BF-UE7) as micro metallic fibers with straight surfaces, and waste PET fibers (WPF) as synthetic fibers. A synergistic effect is observed from the use of dual or triple hybrid fiber systems, which provides a beneficial impact on concrete performance. Mixture M17 achieved the highest density (2145 g/dm³) compared to the reference concrete M0 (2091 g/dm³). This enhancement is attributed to stainless steel fibers (SSF-316L, 7810 g/dm³), which interconnect and reduce macro voids, and bronze fibers (BF-UE7, 8800 g/dm³), which fill micro voids. The synergistic effect of these fibers significantly improves the density and cohesion of the concrete matrix.

The densities of mixtures M18, M19, M20, M21, M22, and M23 are closely linked to the proportions of Waste Polyester Fibers (WPF) used. As the WPF content increases, the densities decrease, which can be attributed to the low density of polyester fibers (1380 g/dm³) compared to the concrete matrix. This effect is amplified by the relatively excessive volume of fibers introduced as reinforcement by mass, which occupies a significant portion of the concrete matrix, leading to a reduction in bulk density. (Aslani, et al., 2019)

III.5.2.3. Air content

Figure III. 45 presents air content results for various hybrid fiber (dual and triple systems) reinforced high-flow sand concrete (HFSC) mixes:

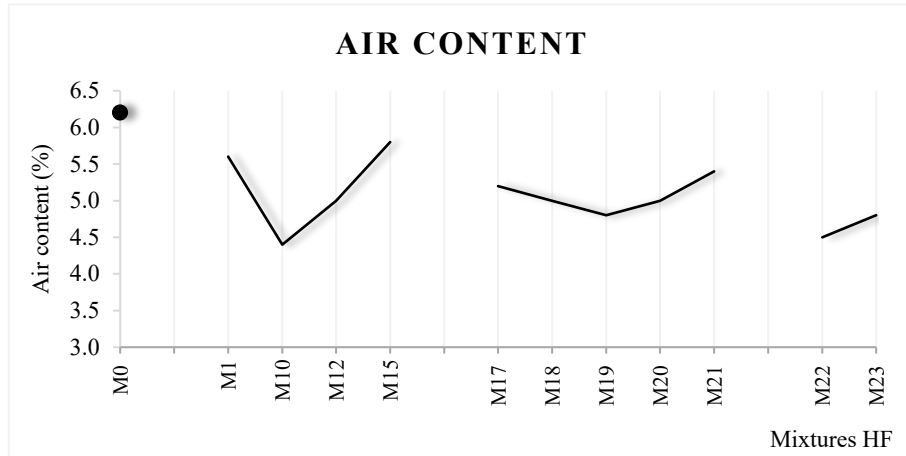


FIGURE III. 45. AIR CONTENT OF MIXES WITH HYBRID FIBERS

The air content in hybrid fiber mixtures ranges from 4.4% to 6.2%. The reference mixture M0 exhibits the highest air content (6.2%), while M10 shows the lowest (4.4%), indicating improved matrix compaction and reduced voids.

The addition of SSF-316L and BF-UE7 in M17 reduces air content moderately (5.2%). BF-UE7 fill micro voids, as seen in M10. While SSF-316L macro fibers may increase air content, the dual fiber system in M17, combining elements from M1 and M10, reduces air content compared to M1.

Mixtures M18 to M23 show a slight increase in air content with higher of WPF content, but their air content remains lower than M12 and M15, due to the void-filling effect of micro fibers of BF-UE7.

III.5.2.4. Relationship between density & air content

Figure III. 46 shows the relationship between density and air content in various high-flow sand concrete (HFSC) mixes reinforced with dual and triple hybrid fiber systems:

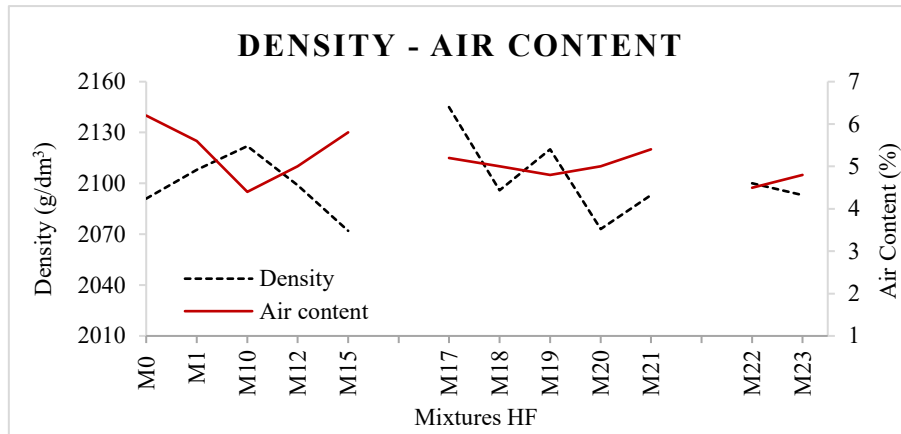


FIGURE III. 46. RELATIONSHIP BETWEEN DENSITY & AIR CONTENT OF MIXES WITH HYBRID FIBERS

The density in hybrid fiber mixtures shows a clear inverse relationship with air content. Bronze fibers (BF-UE7) fill micro voids and reduce air content due to their microfibers, which increase density with their high bulk density of 8900 g/dm^3 .

Conversely, Waste Polyester Fibers (WPF), with a low bulk density of 1380 g/dm^3 , decrease the overall density of the mixture. Their increased volume content occupies space within the concrete matrix.

Dual and triple hybrid fiber systems synergistically improve concrete performance, balancing both density and air content.

III.5.3. Mechanical properties

III.5.3.1. Compressive strength

The compressive strength results in [Figure III. 47](#) show that the performance of fiber-reinforced High-Flow Sand Concrete (HFSC) is affected by the type and proportion of fibers in single (mono) or hybrid (dual or triple) systems.

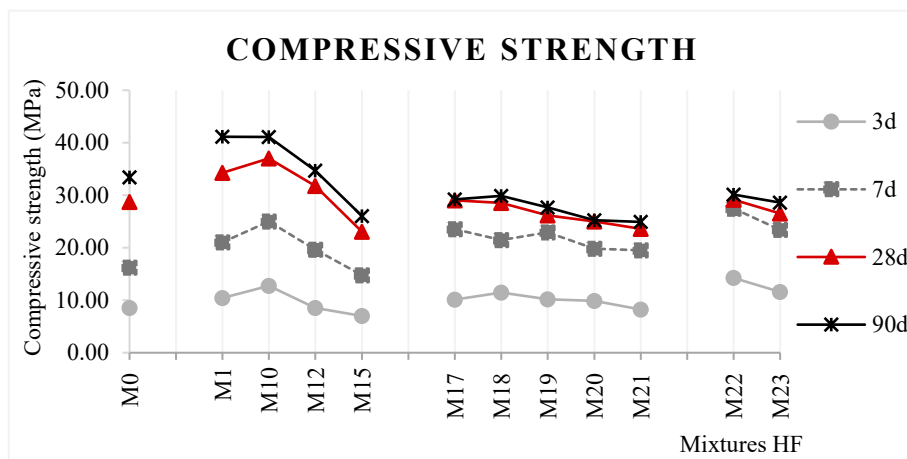


FIGURE III. 47. COMPRESSIVE STRENGTH OF MIXES WITH HYBRID FIBERS

Bronze fibers (BF-UE7) are micro-metallic fibers, effectively improved compressive strength. The M10 (1.5% BF-UE7) achieved the best mix strength of 41.08 MPa after 90 days.

Hybrid mixtures (dual or triple) showed better performance in the early term (3 and 7 days). The best mixture at 3 days, M22 (0.25% SSF-316L + 1.5% BF-UE7 + 0.25% WPF), reached a compressive strength of 14.24 MPa, representing a 66.5% improvement compared to M0. The high early strength is due to the quality and performance of the triple hybrid fibers (SSF-316L + BF-UE7 + WPF), rather than an overall enhancement of the HFSC mix.

In the long term (90 days), the mono fiber mix outperformed the hybrid mixtures, achieving the highest compressive strength (M1 and M10). Conversely, the incorporation of high proportions of WPF (1.5%) in M15, M20, M21, and M23 negatively impacted compressive strength, both in the early term (3 days) and the long term (90 days), with this decline attributed to the increased porosity of the concrete matrix. (Bao, et al., 2024)

III.5.3.2. Flexural tensile strength

Figure III. 48 shows the flexural tensile strength results of High-Flow Sand Concrete (HFSC) reinforced with mono, dual, and triple fibers.

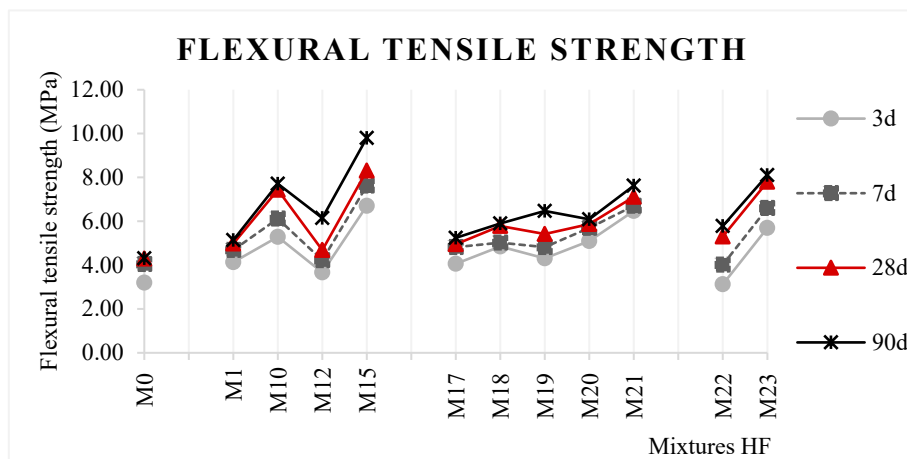


FIGURE III. 48. FLEXURAL TENSILE STRENGTH OF MIXES WITH HYBRID FIBERS

After 90 days, the flexural tensile strength of the M10 and M15 mixes was 78.74% and 87.84%, respectively, higher than that of the M0 mix. BF-UE7 effectively dispersed the stress and prevented the formation of microcracks, and WPF are characterized by ideal flexural tensile strength. (Kesavamoorthi & Ganesh, 2023).

Hybrid (dual and triple) fiber mixes such as M19, M20, M21, and M23 have shown superior performance compared to many mono fiber mixes (Abed, et al., 2023). The M23 mix had a

flexural tensile strength of 8.107 MPa after 90 days, which reduced the formation of microcracks due to BF-UE7 and the high proportion of WPF at 1.5%.

III.5.3.3. Split tensile strength

The split tensile strength results, presented in Figure III. 49, illustrate the performance of High-Flow Sand Concrete (HFSC) reinforced with mono, and hybrid fiber systems:

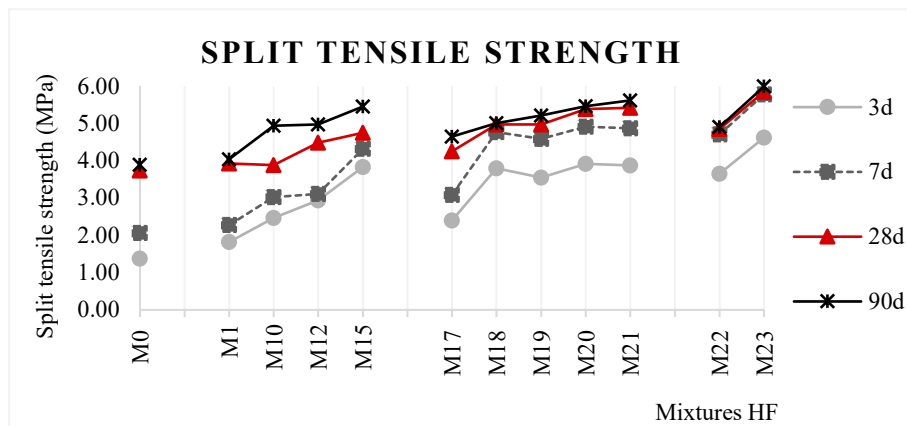


FIGURE III. 49. SPLIT TENSILE STRENGTH OF MIXES WITH HYBRID FIBERS

The best mixes in split tensile strength are M15 in mono fiber systems, M21 in dual fiber systems, and M23 in triple systems, with M23 achieving the highest split tensile strength increase of 54.02% at 90 days (Abed, et al., 2023). This performance is attributed to the hybrid combination of macro synthetic fibers (1.5% WPF) and both micro and macro metallic fibers (1.5% BF-UE7 and 0.25% SSF-316L).

The incorporation of hybrid fibers (dual, triple) demonstrated improvements in the split tensile strength of high-flow sand concrete (HFSC) both early and long term. (Khan, et al., 2022)

III.5.4. Physio-chemical properties

III.5.4.1. Absorption by immersion

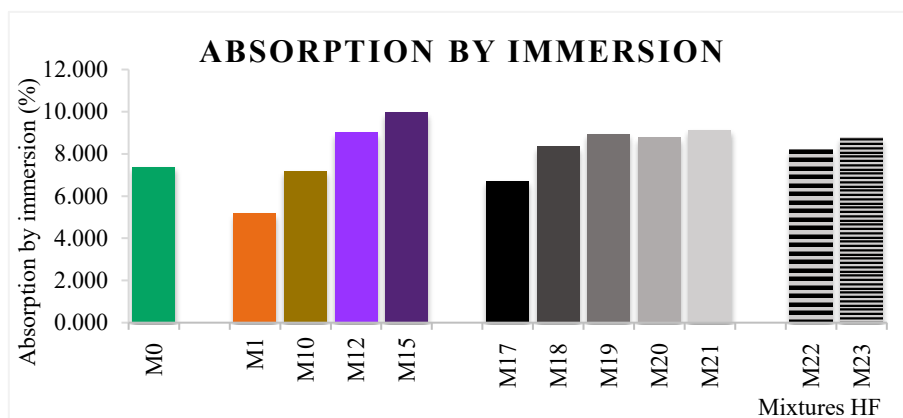


FIGURE III. 50. ABSORPTION BY IMMERSION OF MIXES WITH HYBRID FIBERS

The results in [Figure III. 50](#) showed that the performance of mono fibers was better than that of hybrid (dual, triple) fibers in reducing water absorption by immersion. SSF-316L fibers (M1) and BF-UE7 fibers (M10) achieved the lowest water absorption rates due to their role in improving density and reducing porosity. In contrast, WPF fibers increased water absorption due to their ability to absorb water and create additional voids within the HFSC. Moreover, the use of WPF, whether mono or in hybrid combinations (dual or triple), led to increased water absorption by immersion.

III.5.4.2. Capillary absorption

The effect of hybrid fibers (Dual and Triple systems) on the capillary absorption of HFSC, as shown in [Figure III. 51](#)

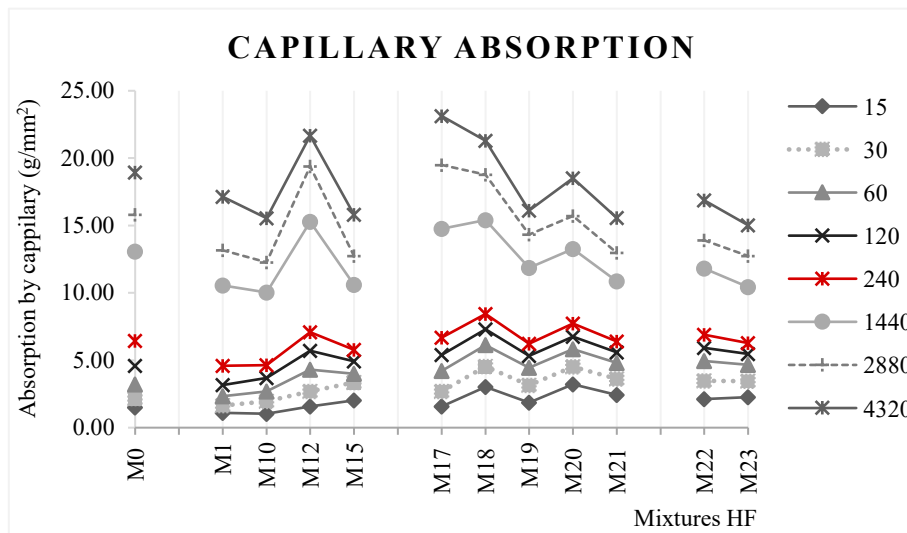


FIGURE III. 51. CAPILLARY ABSORPTION OF MIXES WITH HYBRID FIBERS

The optimal ratio for using mono fibers M1 (0.25% SSF-316L) and M10 (1.50% BF-UE7) effectively improved the concrete density, reduced air content and porosity, leading to a decrease in capillary absorption over the long term (4320 minutes).

The hybrid (dual fibers) mixture M17 (0.25% SSF-316L + 1.50% BF-UE7) showed the best performance in the early term (15 minutes), with the lowest capillary absorption. However, over time (after 240 minutes), this mixture became the highest in capillary absorption, as the hybrid fibers created fine bridges within the concrete matrix, which enhanced capillary absorption.

The mixtures containing WPF, whether in mono fibers or hybrid fibers, showed an increase in capillary water absorption due to the fibers' ability to absorb water and create additional voids within the HFSC.

III.5.4.3. Sorptivity

Figure III. 52 presents the sorptivity results, reflecting the water absorption rate per unit of time for HFSC reinforced with hybrid fibers

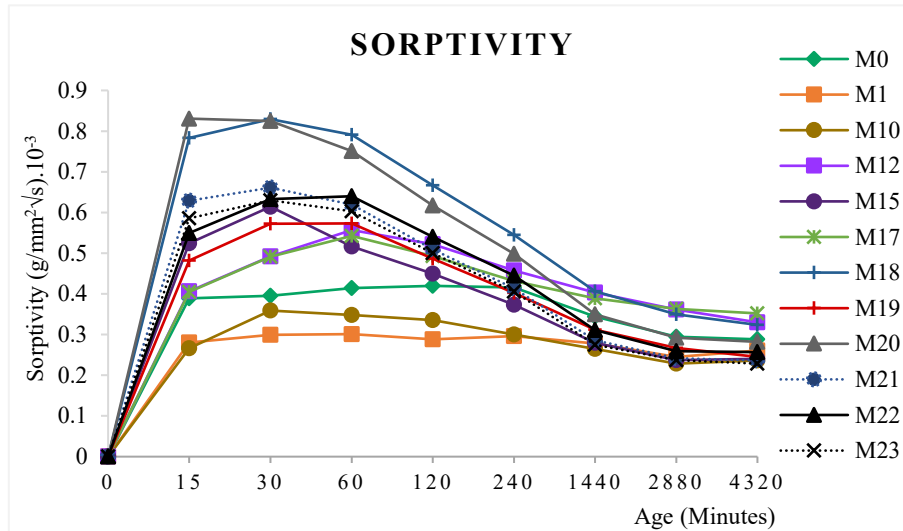


FIGURE III. 52. SORPTIVITY OF MIXES WITH HYBRID FIBERS

The best early-term (15–30 minutes) sorptivity performance was observed in M1 (0.25% SSF-316L) and M10 (1.50% BF-UE7), demonstrating enhanced density and reduced surface porosity.

For long-term performance (4320 minutes), M23 and M21 recorded the lowest sorptivity values, indicating improved internal structure density, which effectively resists capillary absorption.

The WPF, when used as a mono fiber or in hybrid (dual and triple) fiber reinforcements, exhibits higher sorptivity in the early term due to its absorptive nature. However, over time, sorptivity decreases, demonstrating improved performance in the long-term

III.5.4.4. Shrinkage

The shrinkage strain results for HFSC reinforced with hybrid fibers are presented in Figure III. 53

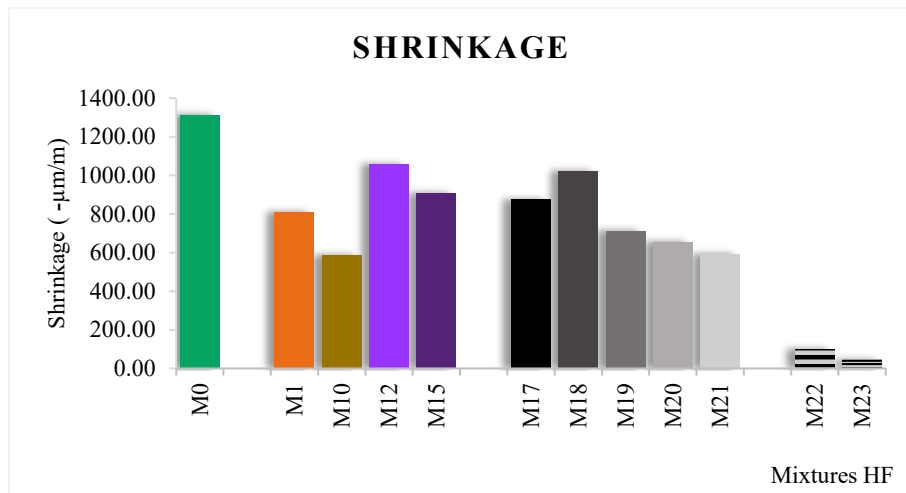


FIGURE III. 53. SHRINKAGE OF MIXES WITH HYBRID FIBERS

All fiber-reinforced high flow sand concrete mixtures demonstrated better performance than the reference mix M0 in reducing shrinkage.

Mixtures reinforced with hybrid fibers (dual and triple) more effective compared to those with mono fibers in reducing shrinkage. Specifically, the mix M23 (0.25% SSF-316 + 1.5% BF-UE7 + 1.5% WPF) exhibited the lowest shrinkage, with a reduction of 96.67% compared to the reference mix M0, This is consistent with the findings of (Abed, et al., 2023)

Note: The obtained results were negative (-), but for easier interpretation, they have been converted to positive (+) values.

III.5.4.5. Swelling

The swelling results for HFSC reinforced with WPF fibers are presented in Figure III. 54

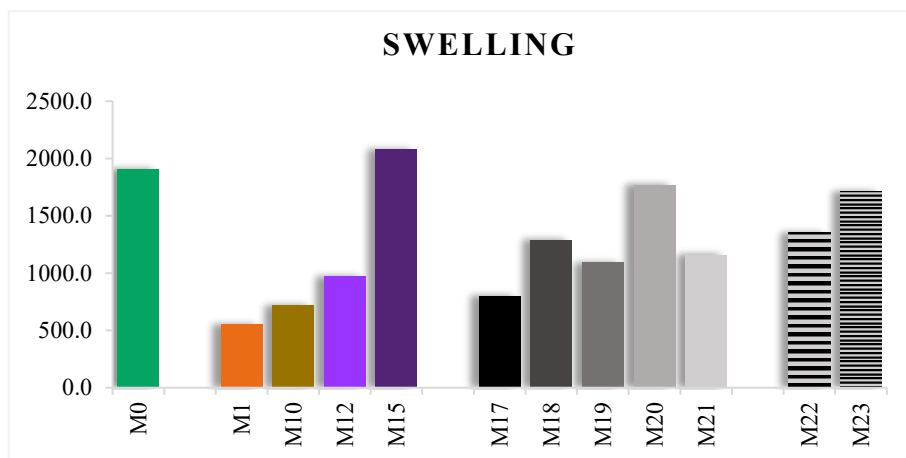


FIGURE III. 54. SWELLING OF MIXES WITH HYBRID FIBERS

The HFSC reinforced with hybrid (dual) fibers in mix M17 demonstrates a significant improvement in reducing swelling strain, enhancing the physio-chemical properties of the concrete matrix. This enhancement is attributed to the macro steel fibers (SSF-316L) and micro bronze fibers (BF-UE7), which exhibited high efficiency in mitigating swelling strain in mixes M1 and M10, with improvement rates of 71.2% and 62.1%, respectively, compared to the reference mixture (M0). This improvement stems from their ability to enhance matrix cohesion and prevent crack formation.

Conversely, waste polyester fibers (WPF) showed favorable performance at low dosages (0.25%). However, increasing the dosage led to elevated swelling due to void formation and poor fiber distribution, negatively affecting the performance of hybrid fibers reinforced with WPF.

III.5.5. Chemical properties

III.5.5.1. Weight loss in sulfuric acid (H_2SO_4)

The evaluated HFSC incorporated mono, dual, and triple fibers by mass. Durability was assessed under exposure to 5% H_2SO_4 , with weight loss measured at 90 days, as shown in [Figure III. 55](#).

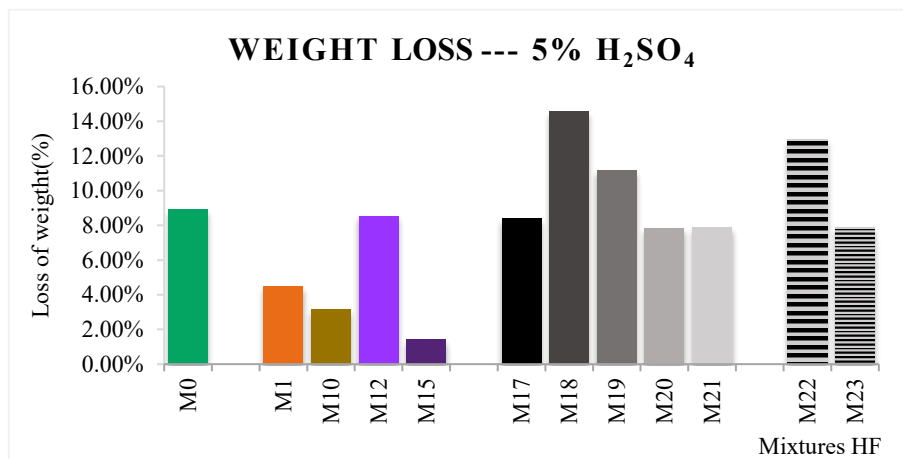


FIGURE III. 55. WEIGHT LOSS OF MIXES WITH HYBRID FIBERS EXPOSED SULFURIC ACID

The weight loss in hybrid mixtures (dual and triple) is higher compared to mono fiber mixtures, especially in the case of 0.25% polyester fiber (WPF) content, as observed in samples M18, M19, and M22. Conversely, the presence of 1.5% polyester fiber (WPF) significantly reduces weight loss due to (5 % H_2SO_4) sulfuric acid attack in M20, M21, and M23, as its higher content acts as an effective barrier. ([Khan, et al., 2022](#))

III.5.5.2. Weight loss in hydrochloric acid (HCl)

Figure III. 56 shows the weight loss of HFSC incorporated with mono and hybrid fibers by mass. Durability was evaluated under exposure to 5% HCl for 90 days.

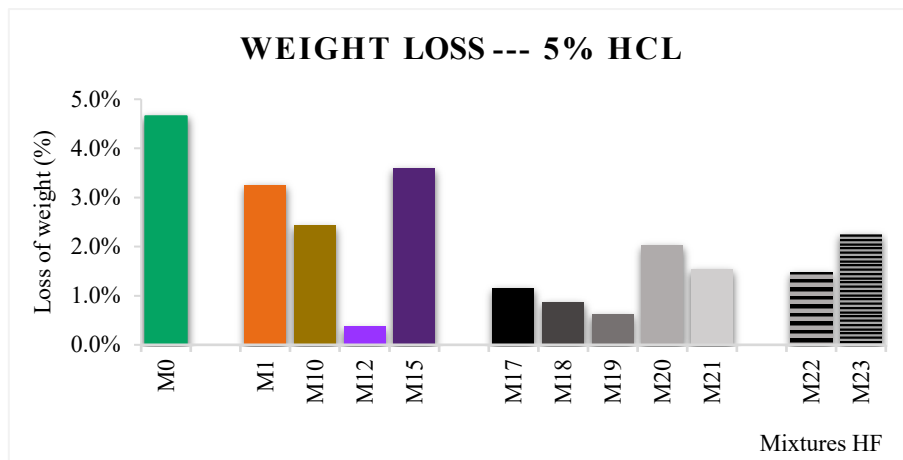


FIGURE III. 56. WEIGHT LOSS OF MIXES WITH HYBRID FIBERS EXPOSED HYDROCHLORIC ACID

The results showed that when HFSC was exposed to 5% hydrochloric acid (HCl), hybrid (dual and triple) mixes outperformed mono fiber mixes in terms of weight loss resistance. Moreover, mixes containing 0.25% WPF demonstrated better performance compared to those with 1.5% WPF. For example, samples M18, M19, and M22 exhibited low weight loss percentages (0.87%, 0.63%, and 1.48%, respectively), compared to higher WPF content samples such as M20, M21, and M23 (2.03%, 1.54%, and 2.25%). (Ammari, et al., 2020)

III.5.6. SEM

The enhancement in the properties of HFSC reinforced with hybrid fibers, as shown in Figure III. 57, was analyzed using Scanning Electron Microscopy (SEM).

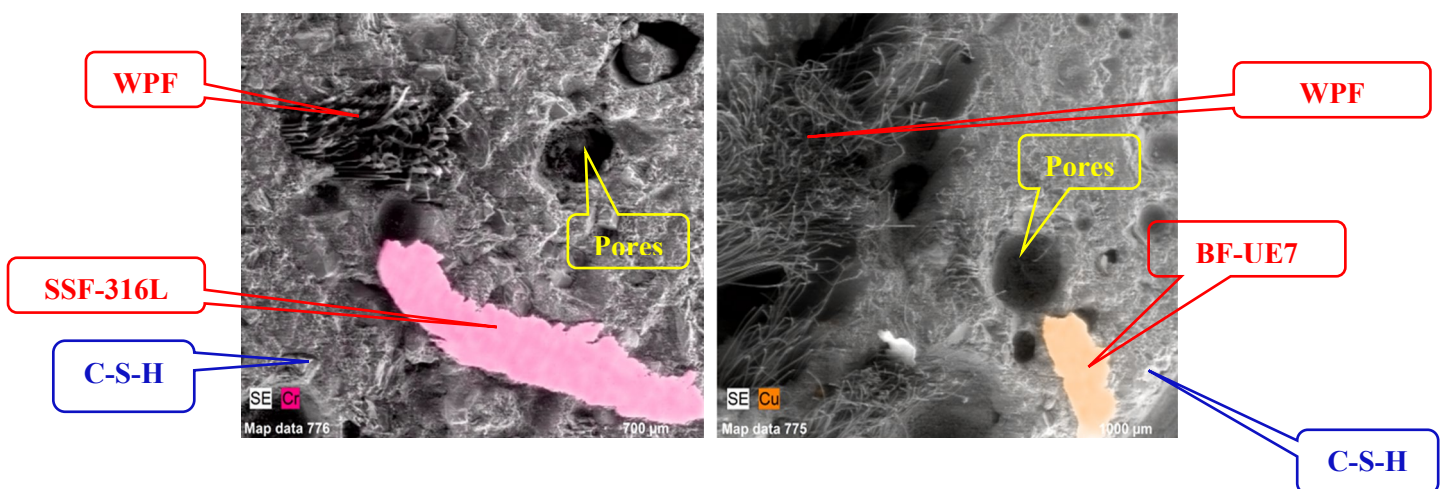


FIGURE III. 57. SEM OF MIXES WITH HYBRID FIBERS

The HFSC reinforced with hybrid (Dual and Triple) fibers has a positive effect on reducing porosity, resulting in a decrease in air content, as shown in Figure III. 45. Additionally, the mixture enhances flexural and split tensile strength, as evidenced by the results presented in Figure III. 48 and Figure III. 49. SSF-316L and BF-UE7 improves cohesion with C-S-H, while WPF contributes to better shrinkage resistance, as demonstrated in Figure III. 53. Figure III. 57 shows a reduction in both pore size and quantity compared to the reference concrete (M0) shown in Figure III. 12.

III.6. Conclusion

In conclusion, this study has demonstrated the effects of incorporating different types of industrial fibers on the physical, mechanical, chemical, and physio-chemical properties of High-Flow Sand Concrete (HFSC). The addition of stainless steel fibers (SSF-316L) significantly improved compressive strength at a 0.25% dosage (M1), while the mix with 2% SSF-316L (M6) exhibited a 42.36% increase in split tensile strength. This enhancement is attributed to the fiber's ability to bridge cracks, improving stress transfer and mitigating large-scale crack propagation. Additionally, SSF-316L reinforcement enhanced HFSC durability by reducing weight loss under exposure to sulfuric (H_2SO_4) and hydrochloric acid (HCl). Scanning Electron Microscopy (SEM) analysis confirmed these findings, revealing strong cohesion between SSF-316L and C-S-H phases, which contributed to the internal matrix integrity.

The incorporation of UE7 Bronze Shavings Fibers (BF-UE7) improved density while reducing porosity, leading to enhanced compressive, split tensile, and flexural strengths, with optimal performance observed at 1.50% fiber content (M10). Furthermore, BF-UE7 reinforcement significantly increased chemical resistance, minimizing weight loss when exposed to acidic environments. SEM imaging corroborated these results, showing reduced pore sizes and improved C-S-H phase distribution, which strengthened the concrete's microstructural cohesion.

Conversely, the integration of Waste Polyester Fibers (WPF) affected HFSC workability due to increased internal friction, leading to reduced density and increased air void content at higher dosages. Nevertheless, at an optimal 1.5% fiber content (M15), WPF reinforcement yielded a 40.11% increase in split tensile strength and a remarkable 127% enhancement in flexural strength, highlighting its effectiveness in crack mitigation and dynamic load resistance. Chemically, WPF-reinforced HFSC exhibited improved durability against acid exposure, with laboratory tests confirming its resistance to degradation in H_2SO_4 and HCl solutions. SEM

analysis further revealed refined fiber distribution, reduced porosity, and enhanced matrix stability, particularly at optimized dosages.

Regarding hybrid fiber systems, the study demonstrated that dual and ternary fiber combinations achieved a balance between improved mechanical performance and reduced structural deficiencies. Dual fiber blends (SSF-316L + BF-UE7) exhibited increased density and lower air void content, enhancing internal cohesion and mitigating early-age cracking. Mechanically, ternary fiber combinations (SSF-316L + BF-UE7 + WPF) outperformed mono-fiber mixtures in split tensile and flexural strength, recording increases of 18.7% and 21.3%, respectively. This superior performance is attributed to the synergistic effect between metallic and polymeric fibers, which collectively enhance resistance to dynamic loads. Chemically, hybrid fiber mixtures demonstrated superior resistance to acid-induced weight loss in 5% HCl exposure compared to mono-fiber samples. However, mono-fiber mixtures exhibited slightly better resistance to sulfuric acid (H_2SO_4), indicating the necessity of precise mix design adjustments for different aggressive environments.

SEM analysis confirmed that both mono and hybrid fiber reinforcements contributed to improved matrix cohesion, reduced air voids, and optimized C-S-H phase distribution, positively impacting concrete properties at the microstructural level. Based on these findings, the selection of an appropriate fiber type or combination should be dictated by specific performance requirements. Metallic fibers (SSF-316L and BF-UE7) are well-suited for enhancing mechanical strength, while polymeric fibers (WPF) effectively mitigate cracking. Hybrid fiber systems provide an optimal solution by balancing compressive and tensile strength with enhanced chemical durability, making them highly suitable for demanding structural applications exposed to harsh environmental conditions.

General conclusion

General conclusion

This thesis systematically examines the influence of industrial and recycled fibers—stainless steel shavings fibers (SSF-316L), bronze shavings fibers (BF-UE7), and waste polyester fibers (WPF)—on the performance of High-Flow Sand Concrete (HFSC). The study focuses on the impact of these fibers on physical, mechanical, physico-chemical, chemical, and microstructural properties, with the key findings summarized as follows:

Physical properties

- *SSF-316L* significantly improved workability and density in M1 (0.25%) while reducing air content, resulting in lower porosity. The increase in density is attributed to the high density of stainless steel fibers (7.9 g/cm^3).
- *BF-UE7* enhanced workability and density in M10 (1.5%) due to the high density of bronze fibers (8.1 g/cm^3).
- *WPF* reduced workability due to its porous nature and water absorption capacity. At low fiber content M12 (0.25%), density increased as the fibers occupied air voids. However, at higher content M15 (1.5%), density decreased because the polyester fibers displaced the HFSC matrix. Given that the density of polyester fibers is 1.38 g/cm^3 compared to 2.1 g/cm^3 for HFSC, this influenced the air void distribution.
- *Hybrid fiber systems* reduced workability due to the high fiber concentration, which complicated flowability. The addition of WPF further increased water absorption and fiber entanglement. Regarding density, it increased in M17 (M1 + M10) due to the combined high density of SSF-316L and BF-UE7 (7.9 and 8.1 g/cm^3 , respectively). However, as WPF was introduced, density decreased due to its lower density (1.38 g/cm^3) compared to HFSC, also affecting air content distribution.

Mechanical properties

- *SSF-316L* significantly enhanced compressive strength, particularly in the optimal mix M1 (0.25%). Flexural and split tensile strength peaked at M6 (2%), attributed to improved stress transfer and macro-crack bridging.
- *BF-UE7* at an optimal content of M10 (1.5%) improved compressive, flexural, and split tensile strength due to reduced porosity and enhanced micro-crack bridging.
- *WPF* exhibited optimal compressive strength in M12, while M15 was superior for flexural and split tensile strength.

- *Hybrid fiber systems* (dual and teriple) decreased compressive strength compared to mono-fiber mixes. In contrast, they improved flexural and split tensile strength.

Physico-chemical properties

- *SSF-316L* reduced absorption by immersion, capillary absorption, sorptivity, and shrinkage in M1. This improvement is attributed to the decrease in external surface porosity and the reduction in internal air content.
- *BF-UE7* enhanced resistance to absorption by immersion, capillary absorption, sorptivity, and shrinkage in M10. This confirms that the microfiber content contributed to reducing porosity within the concrete matrix.
- *WPF*, In terms of absorption by immersion, capillary absorption, and sorptivity, M12 demonstrated optimal performance in the early (short) term (0–30 minutes), while M15 showed superior efficiency in the long term (after 30 minutes). Shrinkage was reduced in M15 and M16, whereas M12 minimized swelling.
- *Hybrid fiber systems* led to an increase in absorption by immersion with higher WPF content. The best early-term (15–30 minutes) sorptivity performance was recorded in M1 and M10, while for long-term performance (4320 minutes), M23 and M21 exhibited the lowest sorptivity values. The hybrid fiber system reduced shrinkage and increased swelling.

Chemical properties

- *SSF-316L* demonstrated superior resistance to acid attacks and weight loss. The M1 mixture exhibited exceptional durability, particularly against sulfuric acid (H_2SO_4).
- *BF-UE7* effectively resisted acid attacks and weight loss, with the M7 mixture best performance.
- *WPF* enhanced resistance to acid attacks. M15 demonstrated high resistance to sulfuric acid (H_2SO_4), while M12 showed resistance to hydrochloric acid (HCl).
- *Hybrid systems* exhibited superior resistance to acid attacks and weight loss under hydrochloric acid (HCl) exposure compared to mono-fiber mixes. In contrast, mono-fiber mixes displayed better resistance to sulfuric acid (H_2SO_4).

Microstructural analysis (SEM)

SEM analysis confirmed that both mono and hybrid fiber reinforcements contributed to reducing air voids, leading to improved cohesion within the concrete matrix.

In conclusion, this study demonstrates that recycled fibers (SSF-316L, BF-UE7, and WPF) improve the properties of high-flow sand concrete. Environmentally, using these fibers offers a sustainable solution that reduces the environmental impact of industrial waste. Economically, these fibers are cost-free, which significantly lowers the cost of fiber-reinforced sand concrete, in addition to the sustainability benefits they provide.

Bibliography

Bibliography

Abed, S. et al., 2023. Influence of ternary hybrid fibers on the mechanical properties of ultrahigh-strength concrete. *Frontiers in materials*.

Abubakar, A., Mohammed, A., Duna, S. & Yusuf, U. S., 2022. Relationship between compressive, Flexural and split tensile strengths of waste copper wire fiber reinforced concrete. *Traektoria Nauki - Path of science*.

AFNOR, 1995. Bétons de sable . In: *Bétons* . s.l.:s.n.

Aghaee, K. & Khayat, K. H., 2024. Use of hybrid fibers and shrinkage mitigating materials in SGG for repair applications. *Construction and building materials - Elsevier*, Volume 413.

Al-Alusi, M. R. M., Kurdi, H. H., Al-Hadithi, A. I. & Hammad, A., 2024. An experimental investigation of the mechanical characteristics and drying shrinkage of single-size expanded polystyrene lightweight concrete reinforced with waste plastic fibers. *Construction and building materials*.

Aldaoood, A., Alkiki, I. M. & Abdulnafaa, M. D., 2022. Industrial waste and its impacts on the engineering properties of soil. *Al-Radidain Engineering Journal*, Volume 27, pp. 25-35.

Ali, M., Kumar, A., Rizvi, S. H. & Ahmed, I., 2020. Effect of polyester fiber on workability of high strength concrete. *Quest research journal*, 18(2), pp. 102-108.

Ali, M. et al., 2020. Effect of Polyester Fiber on Workability Property of High Strength Concrete. *QUEST RESEARCH JOURNAL*, 18(2), pp. 102-108.

Alla, S., Jayaram, M. & Asadi, S. S., 2021. An experimental investigation for replacement of river sand and cement with Robosand, fly-ash and silica fume in concrete to evaluate the influence in durability properties. *Materials Today: Proceedings*.

Ammari, M. S., Bedrina, M., Belhadj, B. & Merrah, A., 2020. Effect of steel fibers on the durability properties of sand concrete with barley straws. *Construction and building materials*.

Aslani, F. et al., 2019. Experimental analysis of fiber reinforced recycled aggregate self-compacting concrete using waste recycled concrete aggregates, polypropylene, and steel fibers. *fib Wiley*.

Atiyeh, M. & Aydin, E., 2020. Carbon fiber enriched cement-based composites for better sustainability. *Materials -MDPI*, Volume 13.

Bao, X. et al., 2024. Experimental investigation on axial compressive and splitting tensile behaviour of reinforced concrete with a low content of hybrid steel fibers. *Construction and building Materials -Elsevier*.

Bao, X. et al., 2024. Experimental investigation on axial compressive and splitting tensile behaviour of reinforced concrete with a low content of hybrid steel fibres. *Construction and building -Elsevier*.

Bao, X. et al., 2024. Investigation on the flexural behaviour and crack propagation of hybrid steel fibre reinforced concrete with a low fibre content for tunnel structures. *Construction and building materials*, Volume 417.

Bhandari, M. & Nam, I.-W., 2024. A critical review on the application of recycled carbon fiber to concrete and cement composites. *Recycling -MDPI*, Volume 9.

Bisley Company, 2021. *What are polypropylene fibres used for?*. [Online] Available at: <https://bisley.biz/news/what-are-polypropylene-fibres-used-for/> [Accessed 05 09 2024].

Bisley Company, 2021. *What is the use of carbon fiber reinforced concrete?*. [Online] Available at: <https://bisley.biz/news/what-is-the-use-of-carbon-fibre-reinforced-concrete/> [Accessed 20 08 2024].

Bisley company, 2021. *Why Polypropylene Fibre Is Used In Concrete*. [Online] Available at: <https://bisley.biz/news/why-polypropylene-fibre-is-used-in-concrete/> [Accessed 06 09 2024].

Chandratilaka, E., Baduge, K. S., Mendis, P. & Thilakarathna, P., 2021. Structural applications of synthetic fibre reinforced cementitious composites: A review on material properties, fire behaviour, durability and structural performance. *Structures*, Volume 34, pp. 550-574.

Cherian, C., Siddiqua, S. & Arnepalli, D. N., 2022. Utilization of recycled industrial solid wastes as building materials in sustainable construction. *Advances in Sustainable Materials and Resilient Infrastructure*,.

Christopher, c. G. et al., 2023. Experimental toughness and durability evaluation of FRC composite reinforced with steel-polyester fiber combination. *International journal of concrete structure and materials*.

Christopher, C. G. et al., 2023. Experimental Toughness and durability Evaluation of FRC Composite Reinforced with Steel Polyester Fiber Combination. *Internatinal Journal of Concrete Structures and Materials - Springer*.

Christopher, C. G. et al., 2023. Experimental toughness and durbility evaluation of FRC composite reinforced with steel-Polyester fiber combination. *International journal of concrete structures and materials -Springer*, Volume 17.

COHEN, 2024. COHEN USA. [Online] Available at: <https://www.cohenusa.com/blog/what-is-swarf-recycling-your-machining-scrap->

for-cash/

[Accessed 16 05 2024].

Dask, M. K. & Patro, S. K., 2018. Performance assessment of ferrochrome slag as partial replacement of fine aggregate in concrete. *European journal of environmental and civil engineering*.

Dhanaraj, R. & Sakthieswaran, N., 2016. Acid Attack on Reinforced Concrete Incorporated with Industrial Wastes. *Journal of advances in chemistry*, 12(22).

Ding, Y. & Bai, Y.-L., 2018. Fracture properties and softening curves of steel fiber-reinforced slag-Based Geopolymer mortar and concrete. *Materials-MDPI*.

Dogruyol, M., Ayhan, E. & Karasin, A., 2024. Effect of waste steel fiber use on concrete behavior at high temperature. *Case studies in construction materials*.

Dong, S., Ouyang, X., Yu, F. & Han, B., 2024. Self-heating curing and its influence on self-sensing properties of ultra-high performance concrete with hybrid stainless steel wires and steel fibers. *Sensors and actuators: A. Physical - Elsevier*, Volume 379.

Dsouza, N., Patil, N. & Swamy, R., 2018. Strength and durability aspects of steel fiber reinforced concrete. *International journal of civil engineering and technology*, Volume 9, pp. 948-957.

Dupain, R. & Saint-Arroman, J. C., 2009. *Granulats, sols, ciment et bétons*. Ecole française du beton: CASTEILLA.

Elite-indus, 2024. *Polyester fiber (Bitumen concrete reinforced fiber)*. [Online] Available at: <https://www.ahelite.com/Polyester-Fiber-Bitumen-Concrete-Reinforced-Fiber-pd948524.html>

[Accessed 03 09 2024].

Fang, C. et al., 2020. The influence of steel fibre properties on the shrinkage of ultra-high performance fibre reinforced concrete. *Construction and Building Materials*.

Faris, M. A. et al., 2021. Comparison of hook and straight fibers addition on Malaysian Fly ash-based geopolymer concrete on the slump, density, water absorption and mechanical properties. *materials -MDPI*.

Fode, T. A., Chande-Jande, A. Y. & Kivevele, T., 2024. Physical, mechanical, and durability properties of concrete containing different waste synthetic fibers for green environment - A critical review. *Heliyon -Elsevier*.

Gao, H. & Xia, Y., 2023. Research on the dispersion of carbon fiber and recycled carbon fiber in cement-based materials: a review. *Frontiers in materials*.

Guendouz, M., 2017. *Contribution à la formulation et à la caractérisation d'un éco-matériau de construction à la base de déchets plastique : application au béton de sable*. s.l.:s.n.

Guo, H. et al., 2021. Influence of a hybrid combination of steel and polypropylene fibers on concrete toughness. *Construction and building materials - Elsevier*, Volume 275.

Hadjoudja, M. et al., 2021. Effect of mineral additions and metal fibers on the resistance of cracking of the dune sand concretes. *Iranian journal of science and technology , Transactions of civil engineering*.

Haigh, R., 2024. The mechanical behaviour of waste plastic milk bottle fibres with surface modification using silica fume to supplement 10% cement in concrete materials. *Construction and building materials*.

Htet, P., Chen, W., Huang, Z. & Hao, H., 2024. Physical and mechanical properties of deflection-hardening hybrid fibre-reinforced recycled aggregate concrete. *Journal of building engineering*, Volume 90.

Huang, Y. et al., 2024. Effect of different shapes of steel fibers and polyglyoxal-nanofibers on performance of ultra - high performance concrete. *Nature portfolio*.

Iqbal , S., Ali, A., Holschemacher, K. & Bier, T., 2015. Mechanical properties of steel fiber reinforced high strength lightweight self-compacting concrete. *Construction and building materials*, pp. 325-333.

James , J. & Pandian, K., 2016. Industrial Waste as Auxiliary additives to cement Lime stabilization of soils. *Advances in civil engineering*, Volume 2016.

Jayalath, A. et al., 2024. Mechanical properties and life cycle greenhouse gas analysis of textile waste fiber-based concrete. *Construction and building materials*.

Jinlin, R. et al., 2021. Mechanical properties of concrete reinforced with corrugated steel fiber under uniaxial compression and tension. *Structures*, Volume 34, pp. 1890-1902.

Kalpana, M. & Tayu, A., 2020. Experimental investigation on lightweight concrete added with industrial waste (steel waste). *Materials today: Proceedings*, pp. 887-889.

Kassimi, F. & Khayat, K. H., 2020. Shrinkage of high-performance fiber-reinforced concrete with adapted rheology. *Construction and building materials*.

Kazemian, M. & Shafei, B., 2022. Mechanical properties of hybrid fiber-reinforced concretes made with low dosages of synthetic fibers. *Fib Wiley*.

KDO CHEMICAL, 2023. *Applications and Advantages of Polypropylene Fiber*. [Online] Available at: <https://www.kdochem.com/news/applications-and-advantages-of-polypropylene-fiber.html>

[Accessed 9 9 2024].

Kesavamoorthi , R. & Ganesh, M., 2023. Impact resistance of micro and macro crimped steel fibre reinforced self-compacting concrete with SCM. *Case studies in construction Materials*.

Khan, M., Cao, M., Chu, S. H. & Ali, M., 2022. Properties of hybrid steel basalt fiber reinforced concrete exposed to different surrounding conditions. *Construction and building materials*.

Ladjel, M., Chemrouk, M., Bouziadi, F. & Boulekbache, B., 2022. Experimental and numerical investigation of the shrinkage of dune sand concrete containing limestone fillers subjected to different curing temperatures. *Materials and structures*.

Liu, S., Zheng, W. & Wang, Y., 2023. Utilization of waste foundry sand and fly ash in the production of steel fiber reinforced concrete. *Journal of cleaner production*, Volume 433.

Liu, S., Zheng, W. & Wang, Y., 2023. Utilization of waste foundry sand and fly ash in the production of steel fibre reinforced concrete. *Journal of cleaner production*.

Li, Y.-F. et al., 2021. An experimental study on mechanical behaviors of carbon fiber and microwave-assisted porolysis recycled carbon fiber-reinforced concrete. *Sustainability - MDPI*, Volume 13.

Li, Y.-F. et al., 2021. Mechanical properties of aramid / Carbon hybrid fiber reinforced concrete. *Materials - MDPI*, Volume 14.

Malagavelli, V. & Rao Patura, N., 2011. Polyester Fibers in the Concrete an Experimental Investigation. *Advanced materials research*, pp. 125-129.

Malek, M., Jackowski, M., Lasica, W. & Kadela, M., 2020. Characteristics of recycled polypropylene fibers as an addition to concrete fabrication based on portland cement. *Materials*.

Martinez-Berrera, G., Gencel, O. & Martinez-Lopez, M., 2022. Performance improvement of polymer concrete produced with unsaturated resin, by a post-cure process, polyester fibers and gamma radiation. *Journal of building Engineering*.

Meddah, M. S. & Bencheikh, M., 2009. Properties of concrete reinforced with different kinds of industrial waste fibre materials. *Construction and building Materials*, pp. 3196 - 3205.

Murthi, P., Lavanya, V., Bahrami, A. & Poongodi, K., 2023. Performance evaluation of polypropylene fiber- reinforced pavement quality concrete made with waste granite powder. *Buildings*, Volume 13.

Naser, M. H., Naser, F. H. & Dhahir, M. K., 2020. Tensile behavior of fiber reinforced cement mortar using wastes of electrical connections wires and galvanized binding wires. *Construction and building materials*.

NBM&CW, 2022. *Polypropylene fiber reinforced concrete : An overview*. [Online] Available at: <https://www.nbmcw.com/product-technology/construction-chemicals->

[waterproofing/concrete-admixtures/pfrc.html](https://www.researchgate.net/publication/325111111/waterproofing/concrete-admixtures/pfrc.html)

[Accessed 02 09 2024].

Oliveira, L. A. P., Gomes, J. p. c. & Pereira , C. N. g., 2006. Study of sorptivity of self-compacting concrete with mineral additives. *Journal of civil engineering and management*, XII(3), pp. 215-220.

Patil, G. M. & Prakash, S. S., 2024. Effect of macro-synthetic and hybrid fibres on the behaviour of square concrete columns reinforced with GFRP rebars under eccentric compression. *Structures*, Volume 59.

Rahman, S. S., Siddiqua, S. & Cherian, C., 2022. Sustainable applications of textile waste fiber in the construction and geotechnical industries: A retrospect. *Cleaner engineering and technology*.

Ran, J. et al., 2021. Mechanical properties of concrete reinforced with corrugated steel fiber unde uniaxial copression and tension. *Structures - Elsevier*.

Rastogi, D. & Sharma, U., 2012. Utilization on industrial waste in the construction industry. *International journal of research in engineering and technology*, Volume 01, pp. 307-312.

Rihia, C., 2020. *Valorisation des dechets dans un beton de sable à base des fibres vegetales*. s.l.:s.n.

Ruziev, J. & Kim, W., 2023. A study on the flexural performance of para-aramid fiber reinforced concrete beams with recyvlcd coarse aggregates. *International journal of concrete structures and materials -Springer Open*, Volume 17.

Sablocrete, 1994. *Béton de Sable*. Paris: Presses de l'école nationale des Ponts et chaussées.

Sayahi, F., Hedlund, H., Emborg, M. & Cwirzen, A., 2020. Effect of steel fibres extracted from recycled tyres on plastic shrinkage cracking in self-compacting concrete. *Magazine of Concrete Research*.

Shobana, B. & Brinila Bright, B. N., 2017. Experimental investigation on high performance concrete by using electric copper wire. *International journal of innovative research in sciencen engineering and technology*, 6(5).

Sun, H., Luo, L., Li, X. & Yuan, H., 2024. The treated recycled aggregates effects on workability, mechanical properties and microstructure of ultra-high performance concrete Co-reinforced with nano-silica and steel fibers. *Journal of building Engineering*.

Surendra P, S., 1992. Do fibers Increase the tensile strength of cement based matrix ?. *Materials journal*.

Talikoti, R. S. & Kandekar, S. B., 2019. Stenrgth and durability study of concrete structures using aramid-fiber reinforced polymer. *fibers-MDPI*, Volume 7.

Wang , R. & Gao, X., 2016. Relationship between flowability, Entrapped air content and strength of UHPC mixtures containing different dosage of steel fiber. *Applied sciences - MDPI*.

Wang, j. et al., 2023. Investigation on Shrinkage Characteristics of Polyester-Fiber-Reinforced Cement-Stabilized Concrete Considering Fiber Length and Content. *Buildings*.

Yeheyis , M. et al., 2012. An overview of construction and demolition waste management in canada: a lifecycle analysis approach to sustainability. *Clean Technologies and environmental policy*, Volume 15, pp. 81-91.

Yeswanth, M. & Praveenkumar, S., 2022. A study on polyester fiber reinforced concrete with addition of silica fume. *International research journal of modernization in engineering technology and science*, 04(1).

Yousef, 2023. *The Engineers Post*. [Online] Available at: <https://www.theengineerspost.com/types-of-metals/> [Accessed 14 05 2024].

Zhang, L., Zhao, J., Fan, C. & Wang, Z., 2020. Effect of surface shape and content of steel fiber on mechanical properties of concrete. *Advances in civil engineering - Hindawi*.

Zhang, P. et al., 2021. Effect of steel fiber on impact resistance and durability of concrete containing nano -SiO₂. *DE GRUYTER - Nanotechnology*, Volume 10, pp. 504-517.

Zhang, X. et al., 2024. Research and devlopment of steel fiber reinforced concrete filling material and its application in gob-side entry retaining technology in deep mines. *Buildings - MDPI*.

Zhao, M., Li, J., Li, C. & Shen, J., 2024. Experimental study and prediction of the long-term strength development of high-flowability concrete made of mixed sand and high-content fly ash. *Construction and building materials*.

Zheng, Z. & Feldman, D., 1995. Synthetic fibre reinforced concrete. *Progress in Polymer Science*, Volume 20, pp. 185-210.

**Technical
data sheet
(TDS)**

TDS. 1

Cement (C)

Sulphate-Resistant Cement (SRC)

Moukaoum - LAFARGE ALGERIE, Algeria



Mokaouem Plus

مقاوم بلوس



Ciment Portland

NA 442 - CEM I 42,5 N-SR 3

Mokaouem est un ciment gris résistant aux sulfates, résultat de la mouture d'un clinker contenant un faible taux d'aluminates de calcium avec une proportion de gypse inférieure à celle d'un ciment portland composé.

Mokaouem

NA 442 - CEM I 42,5 N-SR3

Mokaouem NA 442 -CEM I 42,5 N-SR3 selon la NA 442 v 2013 et la EN 197-1II est conforme à la norme nationale NA 442 v 2013 et à la norme Européenne EN 197-1 avec un taux en C3A < 3%.

AVANTAGES PRODUIT



- Tout en étant un ciment de haute performance, **Mokaouem** protège la structure contre les agressions chimiques de l'environnement externe.
- Une meilleure durabilité pour les structures en béton.
- Une faible chaleur d'hydratation.











APPLICATIONS RECOMMANDÉES

- Les fondations et les structures à réaliser dans un milieu agressif
- Les travaux maritimes
- Les stations de dessalement et d'épuration
- Les travaux hydrauliques
- Les barrages et les digues de soutènement collinaire



FORMULATION CONSEILLÉE

	Ciment 	Sable (sec)  0/5	Gravillons (sec)  8/15mm 15/25mm	Eau (litres) 
Dosage pour béton C25/30	X 1 	+ X7 	+ X5  + X4 	+ 25 L

Remarque: un bidon = 10 Litres

Formulation de béton à suivre dans le cas de l'absence d'une étude délivrée par un laboratoire"

CARACTÉRISTIQUES TECHNIQUES

• Analyses chimiques

	Valeur
Perte au feu (%) (NA5042)	0,5 à 3 %
Teneur en sulfates (SO3) (%)	1,8 à 3
Teneur en oxyde de magnésium MgO (%)	1,2 à 3
Teneur en Chlorures(NA5042) (%)	0,01 à 0,05

• Temps de prise à 20° (NA 230)

	Valeur
Début de prise (min)	> 60
Fin de prise (min)	240 à 400

• Composition minéralogique

	Valeur
Taux d'aluminate C3A	<3.0%

• Résistance à la compression

	Valeur
2 jours (MPa)	≥10
28 jours (MPa)	≥42.5

• Propriétés physiques

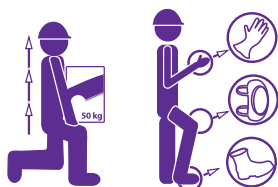
	Valeur
Consistance Normale (%)	25 à 28
Finesse suivant la méthode de Blaine (cm ² /g) (NA231)	3200 à 3800
Retrait à 28 jours (µm/m)	< 1000
Expansion (mm)	≤2,0
Chaleur d'hydratation	<270j/g

Ces valeurs sont données à titre indicatif et ne peuvent être considérées comme absolues

CONSIGNES DE SÉCURITÉ

1- PROTÉGEZ VOTRE PEAU : Portez les équipements adaptés dans vos chantiers: casques, lunettes, gants, genouillères, chaussures et vêtements de sécurité.

2- MANUTENTION : levez le sac en pliant les genoux et en gardant le dos droit.



Conditionnement:



LAFARGE ALGÉRIE

TDS. 2

Limestone Filler (LF)

Calcium Carbonate (CaCO₃)

(ALCAL-F15)

National Aggregates Company (ENG), Constantine, Algeria

المؤسسة الوطنية للحصى

ENTREPRISE NATIONALE DES GRANULATS

Société par actions (SPA) au capital de 3 000 000 000 DA - RC:99B007759

Cité Administrative Lot N°135 Ouled Fayet - Alger

Tél : 023 29 63 37/ 38/ 39 / 40 - Fax : 023 29 63 30 / 31

e-mail : dc@eng.dz - Site web : www.eng.dz

UNITE CARBONATE DE CALCIUM



LEADER ALGERIEN EN

GRANULATS

SABLE, GRAVILLON

BALLAST, ENROCHEMENT

CARBONATE DE CALCIUM

PIERRES ORNEMENTALES

POUZZOLANE

USINE EL KHROUB: BP N° 13,
EL Khroub Constantine.

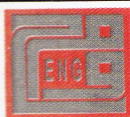
Tél/Fax.: 031 98 01 25 | 26

Mobile: 0660 40 32 14 | 0660 20 81

E-mail : elkhroubcaco3@eng.dz
engcaco3@eng.dz

DÉPÔT ROUIBA : 0660 37 68 16

DÉPÔT ORAN : 0660 37 68 14



ALCAL F15

Fiche technique

Le gisement El-khroub occupe la partie sud ouest du massif Oum Settas au sud-est de Constantine, il est constitué de calcaire d'origine néritique caractérisé par une grande pureté chimique et une blancheur élevée.

Caractéristiques chimiques

CaCO ₃	99,61%
CaO	55,94%
SiO ₂	0,04%
Na ₂ O	0,05%
AL ₂ O ₃	0,03%
MgO	0,20%
Fe ₂ O ₃	0,02%
K ₂ O	0,01%
P ₂ O ₅	0,01%
TiO ₂	0,01%
SO ₃	0,02%
Perte au feu	43,67%
Ph	9

Caractéristiques physiques

Dureté (MOHS) :	3
Poids spécifique :	2,7
Densité apparente non tassée :	0,94
Blancheur (ELREPHO 070) :	L* ≥ 94 ; a* ≤ 0,60 ; b* ≤ 5
Prise d'huile (NF.T 30.022) :	19g/100g de poudre
Humidité à l' ensachage :	0,01%
Indice de réfraction :	1,71

Les éléments toxiques:

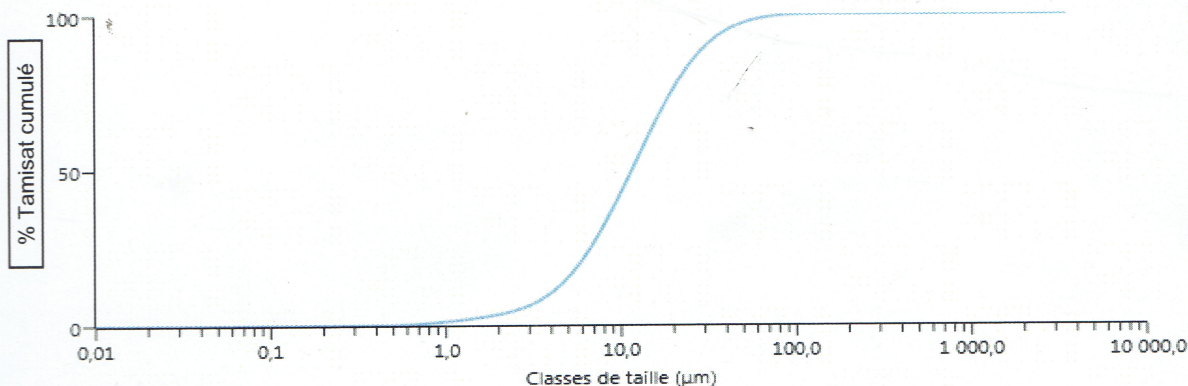
Cyanure	0,045 µg / gr
Mercure	0,35 µg / gr
Arsenic	0,08 µg / gr
Fluor	0,02mg / gr

Répartition granulométrique

Inférieur à 10µm : 43%

Diamètre médian : 11,6 µm

Inférieur à 100µm : 99%



diffraction laser (3000)

Les valeurs figurants dans cette fiche technique sont des valeurs caractéristiques moyennes de la production

Conditionnement

Big-bag (1tonne)
Palettes houssées (48 sacs de 25kg)

Principales utilisations

Peinture mate en phase aqueuse et phase solvant
Peinture hydrodispersible
Enduit en peinture
Enduit base ciment
Composites
Poudre et crème à récurer
Mastic
Améliorant de pain
boue de forage

TDS. 3

Silica fume (SF)

SILTEK POWDER

TEKNACHEM company, Sidi Bel Abbes, Algeria



SILTEK POWDER

FUMÉE DE SILICE ACTIVE SÉLECTIONNÉE À HAUTE PURITÉ

DESCRIPTION

C'est un produit en poudre, constitué par une excellente silice active micronisée, communément appelée « fumée de silice ».

SILTEK POWDER par sa haute composition en silice et micro silicates actives et par sa grande surface spécifique, est considéré, aujourd'hui, comme l'un des meilleurs produits à haute activité pouzzolane.

CARACTERISTIQUES

SILTEK POWDER est constitué de 93 à 98% de particules sphériques de SiO₂ amorphes avec des dimensions de quelques dixièmes de microns, c'est ainsi que sa surface spécifique s'élève à environ 220.000 cm²/g (Blaine). Cette caractéristique lui permet de capter et de fixer l'hydrate de calcium [Ca(OH)] et de le transformer, en un premier temps, en silicate hydraté et successivement en silicate de calcium stable et irréversible.

Cette particularité permet de modifier le comportement des bétons à l'état humide, comme à l'état durci.

ACTION DE SILTEK POWDER

Pour obtenir une bonne maniabilité des bétons, il faut utiliser une quantité d'eau toujours supérieure à celle nécessaire pour l'hydratation du ciment.

Ce qui amène, à la pâte durcie, la formation de capillaires et cavités. Ces dernières sont d'autant nombreuses que la quantité d'eau est élevée.

En outre, durant la dilatation, il se forme une certaine quantité de chaux libre qui se dépose dans les cavités disponibles. Ce comportement rend vulnérable, par effet d'agents externes, le conglomerat durci, en réduisant la durée de vie.

SILTEK POWDER, ajouté au mélange, en raison de 2 à 5% du poids du ciment, capte et réagit avec la chaux libre, et remplit ainsi les vides présents dans la pâte cimentaire, ce qui rend plus compact, plus imperméable et plus résistant le conglomerat et par conséquent plus durable et avec un meilleur aspect.

MODE D'UTILISATION

SILTEK POWDER est principalement utilisé dans tous les bétons et les mortiers de hautes performances.

SILTEK POWDER est utilisé dans la préparation de :

- Coulis de protection.
- Coulis pour injection de consolidation.
- Coulis expansifs.
- Bétons et mortiers à haute résistance mécanique.
- Bétons et mortiers à haute imperméabilité.
- Bétons pré comprimés résistants à l'action chimique.
- Bétons et mortiers pour utilisation sous-marine, spécialement en milieu agressif.
- Mortiers thixotrope pour réfection et réparation.

Et dans toutes les configurations où il est demandé aux mortiers ou aux bétons des caractéristiques supérieures, telles que :

- Résistances mécaniques.
- Résistances chimiques.
- Résistances à l'usure et à l'abrasion.
- Imperméabilité.
- Stabilité et cohésion.
- Durabilité.

Il est aussi utilisé pour réduire le ressuage des bétons.



Siège & Usine :

B.P. 203 Zone Industrielle de Sidi-Bel-Abbès
Tél.: + 213 (0) 48 70 34 63
Fax: + 213 (0) 48 70 34 62
E-mail: info@teknachem.com
WWW.TEKNAICHEM.COM

Antenne d'Alger :

Rue de la Soummam lot N° 06 Z.I. Oued Smar Alger
Tél./Fax: + 213 (0) 23 92 05 62

Antenne de Sétif :

Zone d'Activité Artisanale 6^{ème} Tranche - Sétif
Tél.: + 213 (0) 36 93 90 10 - Fax: + 213 (0) 36 93 90 60

Les informations contenues dans la présente fiche technique, bien que représentant le stade le plus avancé de la connaissance, ne dispensent pas l'utilisateur de procéder à des tests préliminaires dans ses propres conditions d'emploi ou à faire appel à l'assistance technique de la société. Par conséquent **TEKNA CHEM ALGERIE SARL** décline toutes responsabilités pour l'emploi inapproprié du produit.





SILTEK POWDER

FUMÉE DE SILICE ACTIVE SÉLECTIONNÉE À HAUTE PURETÉ

SILTEK POWDER est conseillé aussi, pour compléter et corriger la courbe granulométrique d'une composition de mélanges hydrauliques.

GRANULOMETRIE

Dans le **SILTEK POWDER** la dimension moyenne des particules est de 0.1 μm (micron). Les très petites dimensions des particules de cette poudre comportent une énorme surface spécifique, qui requiert une quantité d'eau supérieure. Alors pour optimiser l'efficacité du **SILTEK POWDER**, dans la production du béton, il est toujours conseillé l'emploi conjoint d'un super fluidifiant de la gamme **TEKNACHEM**.

DONNEES TECHNIQUES

Etat physique :Poudre
 Couleur :Argent
 Granulométrie :de 0,05 à 0,15 μm
 Densité (g/cm³ à 20°C) :environ 0,3
 Solubilité dans l'eau :Insoluble

COMPOSITION

SiO₂ :> 95 %
 CaO :< 0,5 %
 MgO :< 1 %
 Fe₂O₃ :< 1 %
 Al₂O₃ :< 0,5 %
 Autres composants :des traces

DOSAGE

La marge de dosage moyenne est de 3 à 5 % du poids du ciment en fonction du mélange et des caractéristiques voulues.

D'autres dosages peuvent être utilisés, après des essais préliminaires.

CURE

Les réactions, en milieu pouzzolane, sont assez longues et arrivent dans un environnement humide. C'est pour cela, qu'il est demandé, une cure du mortier ou du béton, de manière à éviter des séchages trop rapides. Pour cela, il est conseillé de protéger les surfaces, durant la première phase de durcissement, avec des toiles de polyéthylène et d'appliquer, successivement sur les surfaces exposées une pellicule de **TEKCURING** surtout par temps chaud ou en présence de courants d'air.

CONDITIONNEMENT

SILTEK POWDER est disponible en :

- Big-bags de 500 kilogrammes.
- Sacs de 6 kilogrammes.

STOCKAGE ET VALIDITE

Stocké dans un endroit sec et dans les sacs d'emballage d'origine, parfaitement fermés, le **SILTEK POWDER** a une validité de 12 mois.

L'humidité, éventuellement absorbée par le produit, ne porte pas préjudice à son efficacité, mais rend difficile et peu précis son dosage, en plus d'une distribution non homogène du mélange fini. Il est, par conséquent, conseillé de refermer soigneusement les sacs après chaque prélèvement.



Siège & Usine :

B.P. 203 Zone Industrielle de Sidi-Bel-Abbes
 Tél. : + 213 (0) 48 70 34 63
 Fax : + 213 (0) 48 70 34 62
 E-mail : info@teknachem.com
 WWW.TEKNACHEM.COM

Antenne d'Alger :

Rue de la Soummam lot N° 06 Z.I. Oued Smar Alger
 Tél./Fax : + 213 (0) 23 92 05 62

Antenne de Sétif :

Zone d'Activité Artisanale 6^{ème} Tranche - Sétif
 Tél. : + 213 (0) 36 93 90 10 - Fax : + 213 (0) 36 93 90 60

Les informations contenues dans la présente fiche technique, bien que représentant le stade le plus avancé de la connaissance, ne dispensent pas l'utilisateur de procéder à des tests préliminaires dans ses propres conditions d'emploi ou à faire appel à l'assistance technique de la société. Par conséquent la **TEKNACHEM ALGERIE SARL** décline toutes responsabilités pour l'emploi inapproprié du produit.



TDS. 4

Stainless steel Fibers (SSF-316L)

Stainless Steel Shavings- 316L

ALEMO, El Kheroub, Constantine



EOS Acier inoxydable 316L

L'acier inoxydable d'EOS 316L (EOS StainlessSteel 316L) est un alliage à base de fer résistant à la corrosion qui a été optimisé spécialement pour le traitement sur les systèmes EOSINT M280.

Ce document fournit des informations et des données sur les pièces fabriquées avec de la poudre EOS StainlessSteel 316L (numéro d'article EOS 9011-0032) sur les spécifications de système suivantes:

- Système EOSINT M280 400W avec PSW3.6 et jeu de paramètres 316L_Surface 1.0
- Système EOSINT M280 200W avec PSW3.6 et jeu de paramètres 316L_Surface 1.0

Description

Les pièces construites en EOS StainlessSteel 316L ont une composition chimique correspondant à ASTM F138 "Spécification standard pour les barres et fils en acier inoxydable forgé 18Cr-14Ni-2.5Mo pour implants chirurgicaux (UNS S31673)". Ce type d'acier inoxydable se caractérise par une bonne résistance à la corrosion et des preuves de l'absence de substances lixiviables à des concentrations cytotoxiques.

Ce matériau est idéal pour

- Produits de consommation - montres, autres bijoux, montures de lunettes, décorations, éléments fonctionnels dans un boîtier électronique et des accessoires
- Automobile / Industriel - Usines courantes de produits non corrosifs, alimentaires et chimiques
- Industrie aérospatiale / turbines - Matériaux d'entrée de gamme pour la technologie de frittage laser, pièces de montage, supports, échangeurs de chaleur

Les pièces construites en EOS StainlessSteel 316L peuvent être usinées, grenillées et polies. Le recuit en solution n'est pas nécessaire car les propriétés mécaniques « brut » de fabrication » indiquent les valeurs souhaitées (ASTM A403). Les pièces ne sont pas idéales dans la plage de température de 427 ° C à 816 ° C où il se produit une précipitation de carbures de chrome. En raison de la méthode de construction par couches, les pièces présentent une certaine anisotropie qui peut être constatées dans les propriétés mécaniques.

Données techniques

Données générales du processus

EOS StainlessSteel 316L	
Précision [1]	
- petites pièces	approx. $\pm 20\text{-}50\ \mu\text{m}$
- grandes pièces	approx. $\pm 0.2\ \%$
Epaisseur minimale de paroi [2]	approx. 0.3 - 0.4 mm
Epaisseur de couches	20 μm
Rugosité de surface [3]	
- brut de fabrication	$R_a\ 13 \pm 5\ \mu\text{m}; R_z\ 80 \pm 20\ \mu\text{m}$
- après grenailage	$R_a\ 5 \pm 2\ \mu\text{m}; R_z\ 30 \pm 10\ \mu\text{m}$
- après polissage	$R_z\ \text{up to } < 1\ \mu\text{m}$ (peut être très finement poli)
Taux de volume [4]	2 mm^3/s (7.2 cm^3/h)

[1] Basé sur l'expérience des utilisateurs en matière de précision dimensionnelle pour les géométries typiques, par ex. $\pm 40\ \mu\text{m}$ lorsque les paramètres peuvent être optimisés pour une certaine classe de pièces ou $\pm 60\ \mu\text{m}$ lors de la création d'un nouveau type de géométrie. La précision des pièces dépend de la préparation et du post-traitement appropriés des données.

[2] La stabilité mécanique dépend de la géométrie (hauteur du mur, etc.) et de l'application.

[3] En raison de la structure en couches, la structure de la surface dépend fortement de l'orientation de la surface. Par exemple, les surfaces en pente et courbes présentent un effet d'escalier. Les valeurs dépendent également de la méthode de mesure utilisée. Les valeurs citées ici donnent une indication de ce à quoi on peut s'attendre pour les surfaces verticales.

[4] Le taux de volume est une mesure de la vitesse de construction lors d'une exposition au laser. La vitesse de construction totale dépend du débit moyen, du temps de recouvrement (en fonction du nombre de couches) et d'autres facteurs tels que les paramètres de contour et Up / DownSkin.



Propriétés physiques et chimiques des pièces

EOS StainlessSteel 316L			
Composition du matériau	Element	Min	Max
	Fe	59.50	
	Cr	17.00	19.00
	Ni	13.00	15.00
	Mo	2.25	3.00
	C		0.030
	Mn		2.00
	Cu		0.50
	P		0.025
	S		0.010
	Si		0.75
	N		0.10
Densité relative avec paramètres standard	approx. 100 %		
Densité avec paramètres standard	min. 7.9 g/cm ³		

Propriétés mécaniques des pièces (en température ambiante)

	Brut de fabrication
Résistance à la traction [5]	
- en direction horizontale (XY)	640 ± 50 MPa
- en direction verticale(Z)	540 ± 55 MPa
Limite d'élasticité, Rp0,2% [5]	
- en direction horizontale (XY)	530 ± 60 MPa
- en direction verticale(Z)	470 ± 90 MPa
Module de Young [5]	
- en direction horizontale (XY)	185 GPa
- en direction verticale(Z)	180 GPa
Elongation à la rupture [5]	
- en direction horizontale (XY)	40 ± 15 %
- en direction verticale(Z)	50 ± 20 %
Dureté [6]	85 HRB

5] Usinage et test des éprouvettes selon ISO 6892 / ASTM E8M, éprouvettes proportionnelles, diamètre de la zone du goulot de 5 mm (0,2 pouce), longueur de référence 4D = 20,0 mm (0,79 pouce), taux de contrainte 10 MPa / s. , vitesse de déformation dans la zone plastique 0,375 1 / min.

[6] Mesure de la dureté Rockwell (HRB) selon EN ISO 6508-1 sur une surface polie.

Les valeurs indiquées font référence à l'utilisation de ces matériaux avec les systèmes EOSINT M 280 conformément aux spécifications en vigueur (y compris le dernier logiciel de processus publié, PSW et tout matériel spécifié pour le matériau concerné) et les instructions d'utilisation. Toutes les valeurs sont approximatives. Sauf indication contraire, les propriétés mécaniques et physiques citées se réfèrent aux paramètres de construction standard et aux échantillons de test construits dans une orientation verticale. Ils dépendent des paramètres de construction et des stratégies utilisées, qui peuvent être modifiés par l'utilisateur en fonction de l'application.

Les données sont basées sur nos dernières connaissances et sont sujettes à des modifications sans préavis. Ils sont fournis à titre indicatif et non comme une garantie d'aptitude à une application spécifique. EOS®, EOSINT®, DMLS®, DirectTool® et DirectPart® sont des marques déposées de EOS GmbH

© 2014 EOS GmbH – Electro Optical System. Tous les droits sont réservés.

Traduit de l'anglais par [Cresilas](#).

TDS. 5

Bronze Fibers (BF –UE7)

Bronze shaving - UE7

ALEMO, El Kheroub, Constantine

FICHE PRODUIT UE7

Désignations : **CuSn7Zn4Pb7 (CC493K)**

Bronze à l'étain.

Livré suivant norme EN 1982

Coulée continue – tolérance de livraison : 0/+1mm

Masse volumique : Kg/dm³ : 8.80

Composition chimique

Eléments	% mini	% maxi
Cu Cuivre	81.0	85.0
Ni Nickel		2.0
P Phosphore		0.1
Pb Plomb	5.0	8.0
Sn Etain	6.0	8.0
Zn Zinc	2.0	5.0
Al Aluminium		0.01
Fe Fer		0.20
S Soufre		0.10
Sb Antimoine		0.30
Si Silicium		0.01

Caractéristiques mécaniques des barres à l'état de livraison coulée continue

Rm MPa	260 mini
Rp0.2 MPa	120 mini
A%	12 mini
Dureté HB	70 mini

Ces valeurs sont données à titre indicatif et susceptibles d'être modifiées

TDS. 6

Waste Polyester Fibers (WPF)

Polyester fibers (Cordon fil N° 6)

Cobblers in Skikda, Algeria



Accueil > Produits > Fibres techniques

Polyester

Le polyester est la fibre technique la plus utilisée pour le dépeussierage, du fait de son excellent rapport qualité/prix.

Son aspect thermoplastique autorise tous les traitements de surface imaginables et surtout l'usage de la thermosoudure pour la confection des manches filtrantes.

La fibre est utilisée pour son excellente résistance mécanique jusqu'à des température de 150 °C, mais en présence d'humidité et de SO_x le polyester s'hydrolyse et se fragilise rapidement.

Les fibres polyester sont disponibles dans de nombreuses finesses.

Propriétés de la fibre :

Sigle :	PES
Densité :	1.38 g/cm ³
Absorbtion d'humidité :	0.4 (20°C H.R. 65%)
Tenacité :	4.5-7.5 cN/dtex
Elongation :	11-14 %
Température maximum en continue :	140 °C
Température maximum de pointe :	150 °C
LOI (Limit oxygen index) :	20 %

Résistance de la fibre :

Acide fort :	★ ★ ★ ★
Acide faible :	★ ★ ★ ★
Alcalin fort :	★ ★ ★ ★
Alcalin faible :	★ ★ ★ ★
Oxydants :	★ ★ ★ ★
Hydrolyse :	★ ★ ★ ★
Solvants spécifiques :	H ₂ SO ₄ C ₆ H ₅ NO ₂ C ₆ H ₅ OH

TDS. 7

Water Reducer (SP)

Superplasticizer, "Viscocrete 665"

Sika-El Djazair, Algeria

NOTICE PRODUIT

Sika® ViscoCrete®-665

Superplastifiant/Haut Réducteur d'eau polyvalent pour bétons prêts à l'emploi

INFORMATIONS SUR LE PRODUIT

Sika® ViscoCrete®-665 est un superplastifiant/haut réducteur d'eau polyvalent de nouvelle génération non chloré à base de copolymère acrylique.

Sika® ViscoCrete®-665 est compatible avec tous les ciments même avec un taux C3A faible.

DOMAINES D'APPLICATION

Sika® ViscoCrete®-665 permet la fabrication :

- de bétons plastiques à autoplacants transportés sur de longues distances et pompés.
- de bétons à longs maintiens de rhéologie (>2h30), sans reprise de fluidité dans le temps.

CARACTÉRISTIQUES / AVANTAGES

Sika® ViscoCrete®-665 est un superplastifiant qui confère aux bétons les propriétés suivantes :

- Longue rhéologie (>2h30)
- Evolution rapide des résistances à court et à long terme
- Réduction de la viscosité Amélioration de la stabilité du béton frais et limitation de la ségrégation avec des granulats concassés
- Pas de reprise de fluidité dans le temps
- Qualité de parement
- Diminution du retrait
- Très bonne étanchiété

AGRÉMENTS / NORMES

PV CNERIB : DTEM/171/2021

DESCRIPTION DU PRODUIT

Conditionnement	Fût de 200 kg Cubi de 1000 kg Vrac
Aspect / Couleur	Liquide marron
Durée de Conservation	12 mois dans son emballage d'origine intact
Conditions de Stockage	Dans un local fermé, à l'abri de l'ensoleillement direct et du gel, entre 5 et 30 °C. Sika® ViscoCrete®-665 peut geler, mais, une fois dégelé lentement et réhomogénéisé, il retrouve ses qualités d'origine. En cas de gel prolongé et intense, vérifier qu'il n'a pas été déstabilisé.
Densité	1,085 ± 0,015
Valeur pH	5 ± 1,0
Teneur Totale en Ions Chlorure	≤ 0,1%
Équivalent Oxyde de Sodium	≤ 1,0%

RENSEIGNEMENTS SUR L'APPLICATION

Dosage	0,4 à 2% du poids du liant ou du ciment selon la fluidité et les performances recherchées.
Distribution	Sika® ViscoCrete®-665 est ajouté, soit en même temps que l'eau de gâchage, soit en différé dans le béton préalablement mouillé avec une fraction de l'eau de gâchage.

VALEURS DE BASE

Toutes les valeurs indiquées dans cette Notice Produit sont basées sur des essais effectués en laboratoire. Les valeurs effectives mesurées peuvent varier du fait de circonstances indépendantes de notre contrôle.

ÉCOLOGIE, SANTÉ ET SÉCURITÉ

Pour obtenir des informations et des conseils sur la manipulation, le stockage et l'élimination en toute sécurité des produits chimiques, les utilisateurs doivent consulter la fiche de données de sécurité (FDS) la plus récente contenant les données physiques, écologiques, toxicologiques et autres données relatives à la sécurité.

RESTRICTIONS LOCALES

Veillez noter que du fait de réglementations locales spécifiques, les données déclarées pour ce produit peuvent varier d'un pays à l'autre. Veuillez consulter la Notice Produit locale pour les données exactes sur le produit.

INFORMATIONS LÉGALES

Les informations, et en particulier les recommandations concernant les modalités d'application et d'utilisation finale des produits Sika sont fournies en toute bonne foi et se fondent sur la connaissance et l'expérience que Sika a acquises à ce jour de ses produits lorsqu'ils ont été convenablement stockés, manipulés et appliqués dans des conditions normales, conformément aux recommandations de Sika. En pratique, les différences entre matériaux, substrats et conditions spécifiques sur site sont telles que ces informations ou recommandations écrites, ou autre conseil donné, n'impliquent aucune garantie de qualité marchande autre que la garantie légale contre les vices cachés, ni aucune garantie de conformité à un usage particulier, ni aucune responsabilité découlant de quelque relation juridique que ce soit. L'utilisateur du produit doit vérifier par un essai sur site l'adaptation du produit à l'application et à l'objectif envisagés. Sika se réserve le

droit de modifier les propriétés de ses produits. Notre responsabilité ne saurait d'aucune manière être engagée dans l'hypothèse d'une application non conforme à nos renseignements. Les droits de propriété détenus par des tiers doivent impérativement être respectés. Toutes les commandes sont soumises à nos conditions générales de vente et de livraison en vigueur. Les utilisateurs doivent impérativement consulter la version la plus récente de la Notice Produit correspondant au produit concerné, accessible sur internet ou qui leur sera remise sur demande.

Sika El Djazair SPA
08 route de Larbaa
16111 Les Eucalyptus
ALGERIE
Tél.: 0 21 50 16 92 à 95
Fax: 0 21 50 22 08
dza.sika.com



Notice produit
Sika® ViscoCrete®-665
Décembre 2021, Version 01.03
021301011000002749

SikaViscoCrete-665-fr-DZ-(12-2021)-1-3.pdf